CONTROL OF SERINE RECEPTOR SIGNALING BY THE SENSORY ADAPTATION SYSTEM IN ESCHERICHIA COLI

by

Xuesheng Han

A dissertation submitted to the faculty of
The University of Utah
in partial fulfillment of the requirements for the degree of

Doctor of Philosophy

Department of Biology

The University of Utah

May 2015

Copyright © Xuesheng Han 2015

All Rights Reserved

The University of Utah Graduate School

STATEMENT OF DISSERTATION APPROVAL

The dissertation of Xuesheng Han

has been approved by the following supervisory committee members:

John S. Parkinson	, Chair	2014/12/11 Date Approved
Matthew A. Mulvey	, Member	2014/12/11 Date Approved
Darryl L. Kropf	, Member	2014/12/11 Date Approved
David F. Blair	, Member	2014/12/11 Date Approved
Colin Dale	, Member	2014/12/11 Date Approved

and by Denise M. Dearing , Chair/Dean of

the Department/College/School of Biology

and by David B. Kieda, Dean of The Graduate School.

ABSTRACT

The chemotaxis signaling pathway of *Escherichia coli* is the best studied signal transduction mechanism in biology. Better understanding of this signal-processing machinery at the molecular level will foster new therapies for pathogenic infections and new designs of highly specific and sensitive biosensors. A sensory adaptation system plays a critical role in this chemotactic behavior. Sensory adaptation is regulated by covalent modifications of the chemoreceptors, mediated by CheR and CheB enzymes. This PhD research project explores the sensory adaptation mechanism of the serine receptor (Tsr) in *E. coli.*

In this study, I showed that all adaptation sites of Tsr, including the fifth unorthodox site, worked in a similar way to regulate Tsr signal output. I also found that site 5 (Tsr-E502) and site 3 (Tsr-Q311) have differential signaling effects, mainly due to their different localizations on the methylation helices. Finally, I discovered unexpected signaling effects of CheR and CheB, the two adaptation enzymes. In summary, this thesis provides important insights into the sensory adaptation system and receptor input-output control in bacterial chemotaxis.

This dissertation is dedicated to my father, Zhaoshan Han, and my mother Meiling Chen. Without their care and support in the past many years, I would never have been able to finish such a long journey. I also dedicate this dissertation to my wife, Wei Zhang. Wei has shared all the joys and pains with me, studying and living in USA in the past five years. Last but not least, I want to dedicate it to my one-year-old adorable daughter, Sophia, for allowing me the very first touch of fatherhood and giving me all the best feelings, during the last year of this work.

TABLE OF CONTENTS

LIST OF TABLES

LIST OF ABBREVIATIONS

MCP, methyl-accepting chemotaxis protein;

Tsr, the serine receptor;

CW, clockwise; CCW, counter-clockwise;

MH, methylation helix;

IPTG, isopropyl -D-thio-galactopyranoside;

SDS-PAGE, sodium dodecyl sulfate-containing polyacrylamide gel electrophoresis;

FRET, Förster resonance energy transfer or fluorescence resonance energy transfer.

ACKNOWLEDGEMENTS

I greatly thank my academic supervisor, Dr. John S. Parkinson, who is the best mentor I could have had. When I joined his lab, he always encouraged me to learn how to become a good scientist. His frequent quote “No one was born to be a scientist; you just need to learn how to become one.” gave me enormous courage and confidence in pursuing a science career. I appreciate his patience, financial support, and incredible mentoring for my study and research in the past years.

I also thank my thesis committee, Dr. David F. Blair, Dr. Colin Dale, Dr. Darryl L. Kropf, and Dr. Matthew A. Mulvey. They all helped me achieve my academic goal. I sincerely appreciate their time and patience.

Many thanks go to all these wonderful colleagues in Parkinson laboratory, Dr. Peter Ames, Dr. Runzhi Lai, Dr. German Pinas and Dr. Kika Kitanovic. They all helped me by sharing brilliant ideas with me, supporting me and commenting on this work. Special thanks go to Dr. Peter Ames for his remarkable instruction.

CHAPTER 1

INTRODUCTION

Overview

Chemotaxis allows cells and organisms to move toward or away from chemicals, optimizing their survival and growth environment. Chemotactic behavior influences the environmental distribution of motile microorganisms and plays critical roles in cell survival under nutritional stress or toxic environment. Chemotaxis affects the composition of microbial communities (1–3) and plays key roles in the process of host invasion during the establishment of pathogenic infections (4–9) and beneficial symbioses (10–12). Bacterial chemotactic behavior can also be exploited to remediate environmental pollutants (13, 14), especially in water and soil sources. It can even be utilized to monitor extremely low levels of TNT (trinitrotoluene) and some other toxic chemicals (15).

Although a simple phenomenon, chemotaxis requires a sophisticated signal processing system. The chemotaxis machinery of *Escherichia coli* represents an extensively studied model system for exploring signal transduction and information processing at the molecular level. Better understanding of its signal processing

mechanisms will lead to new therapies for treating pathogenic infections and new designs of highly sensitive and stable biosensors. A full understanding of bacterial chemotaxis should also make major contributions beyond microbiology, in fields like ecology (16), chemistry (17), physics (18), and even astronomy (19).

Bacterial Chemotaxis

Most bacterial cells are too small to detect concentration gradients spatially and instead use temporal sensing to migrate up or down attractant or repellent gradients, respectively (Fig. 1.1). An *E.coli* cell typically contains 4 - 7 bidirectional rotary motors embedded in the inner cytoplasmic membrane and distributed randomly over the cell surface. Powered by proton motive force across the cytoplasmic membrane, these motors drive the rotation of long, helical filaments, called flagella. Bacteria swim by rotating their flagella, at speeds up to 1000 hertz, producing a propulsive force that drives the cell body forward. Counterclockwise (CCW) rotation of the flagella forms a left handed helical bundle that promotes smooth forward swimming (runs) (20). The run speed can be up to 40 μm per second (Fig. 1.1) (21), which is 20 body lengths per second. Clockwise (22) rotation of the motors disrupts the flagellar bundle and randomly reorients the cell's direction (tumbles). The probability of a tumbling event is controlled by the chemotaxis signaling pathway.

In an isotropic medium or environment, cells tend to make short runs (a few seconds) disrupted by brief tumbles (about 0.1 second), resulting in a 3-dimensional random walk.

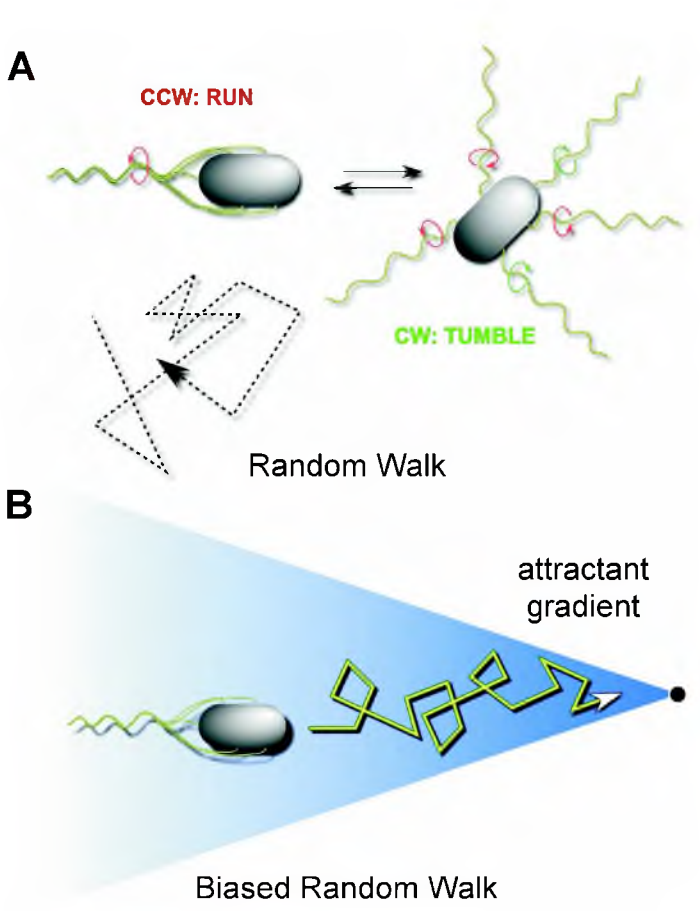

Fig. 1.1 Behaviors of an *E. coli* cell in an isotropic medium (A) and a medium with attractant gradient (B). In both cases, the cell swims in a straight line (run), disrupted by random directional changes (tumbles), yielding a three dimensional random walk. When the cell encounters an attractant, it swims up the gradient by prolonging the averaged duration of runs and suppressing the chance of tumbles. Overall, the cell exhibits a biased random walk and migrates in the up gradient direction. The gradient is sensed in a temporal way by comparing the instantaneous concentration of attractant to the concentration sensed over the past few seconds.

In other words, this movement can be seen as a high-speed version of Brownian motion. When the cell encounters an attractant gradient, it reduces the frequency of tumbling, resulting in an extended period of running toward higher levels of attractant and swimming up the gradient. The migrating path of the cell describes a biased random walk toward the attractant (Fig. 1.1B): prolonged runs (forward swimming) punctuated by very brief tumbles (changing direction). This paradigm of biased random walk can also be applied to many other motile bacterial species. The coupling of various sensory systems to the cellular motors allows bacteria to move toward gradients of light intensity (phototaxis), redox potential (aerotaxis), temperature (thermotaxis), and chemical (chemotaxis) (23–27). Therefore, the chemotactic behaviors enable cells to find new environments that are rich in nutrients and/or low in toxic chemicals.

Chemotaxis Signaling Pathway of Escherichia Coli

The high performance chemotaxis signaling pathway of *Escherichia coli* has a limited number of components but notable sophistication (28–31). Chemical recognition is accomplished in *E. coli* by four closely related canonical Methyl-accepting Chemotaxis Proteins (MCPs) (Tsr, Tar, Tap, and Trg) and a fifth MCP-like receptor (Aer). All these chemoreceptors are localized to the cytoplasmic membrane. Tsr mediates attractant responses to L-serine, as does Tar to L-aspartate and maltose. Tap senses dipeptides and pyrimidines; Trg senses ribose, glucose, and galactose; and Aer is responsible for aerotactic responses. Chemical ligands bind to the periplasmic domain of the

homodimeric chemoreceptors, causing conformational changes that modulate their cytoplasmic signaling domains.

The chemoreceptors, the receptor-coupled autokinase CheA, and coupling adaptor protein CheW form noncovalent but highly stable ternary signaling complexes at the membrane-distal cytoplasmic tip of receptor molecules (Fig. 1.2) (32). Active CheA (default state is ON) phosphorylates itself on a histidine residue that is highly conserved in all Histidine Protein Kinase (HPKs) (Fig. 1.2). It then donates the phosphoryl group to an aspartyl residue of the CheY protein, which is the response regulator for the CheA-CheY two-component signaling pathway. Phospho-CheY regulates the CCW-to-CW and CW-to-CCW switches of a flagellar motor by directly binding to and dissociating from the motor, respectively (33). High levels of phospho-CheY promote CW rotation, while low levels of phospho-CheY favor CCW rotation. The binding of 13 ± 7 phospho-CheY molecules to a motor is sufficient to induce CW rotation, and the binding and dissociation both occurred in about 0.1 second during a switch (33). Phospho-CheY can be dephosphorylated by the CheZ phosphatase, lowering the intracellular level of phospho-CheY in a few seconds (34, 35). Attractant binding to the receptor inhibits CheA activity, lowers the level of phospho-CheY, and increases the chance of CCW rotation.

Besides this motor control signaling pathway, *E. coli* chemotaxis also has a robust sensory adaptation system, which is accomplished by regulating the methylation level of the receptor. Phoshpo-CheA can donate phosphoryl groups to CheB, a methylesterase.

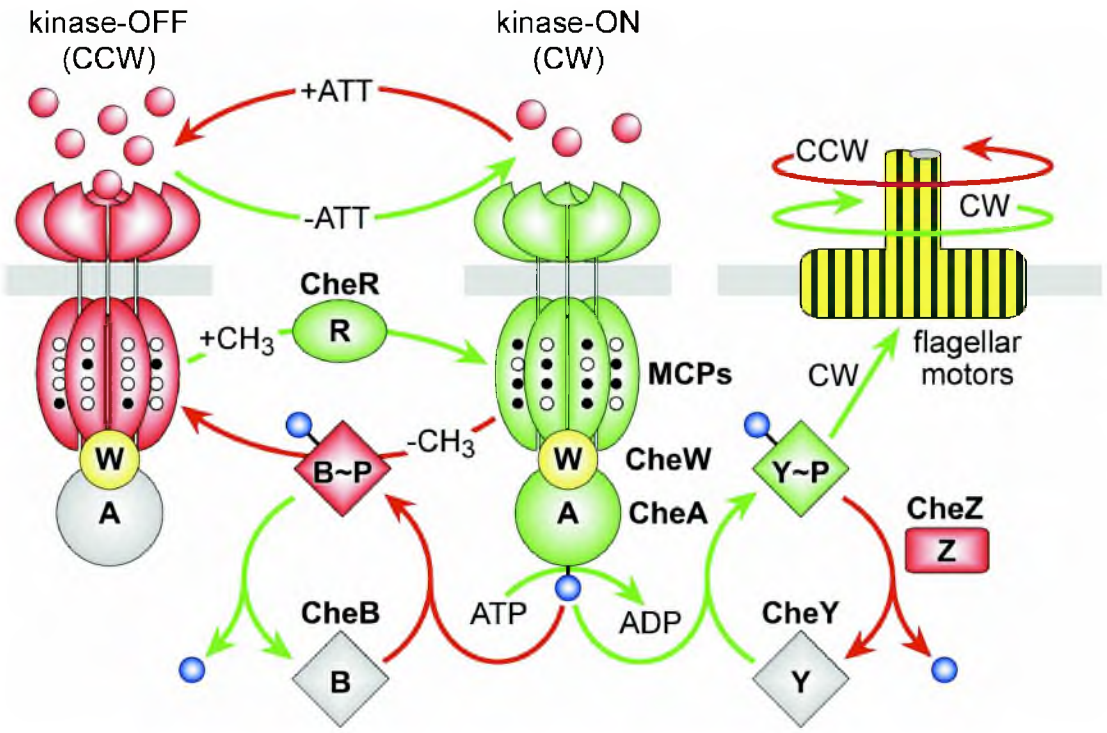

Fig. 1.2 The chemotaxis signaling pathway of *E. coli*. Components and reactions colored in green promote CW rotation of the flagellar motor, while red ones promote CCW rotation. Chemoreceptors work as trimers of homodimers, forming a ternary complex with CheA and CheW. Activated CheA transfers phosphoryl groups to the CheY protein and the CheB methylesterase. Phosphorylated CheY binds to the switch/motor complex and promotes CW rotation of the flagellar motor. Phosphorylated CheB removes methyl groups from the receptors, while methyltransferase CheR adds methyl groups. Attractant binding to the receptor inhibits CheA activity, decreasing the levels of phosphorylated CheY and phosphorylated CheB. CheZ phosphatase also lowers the level of phosphorylated CheY, promoting CCW rotation. Increased methylation level of the receptor enhances CheA activity and compensates for the effect of attractant binding on CheA activity.

Phospho-CheB becomes active in removing methyl groups from the receptor, while the methyltransferase CheR is responsible for adding methyl groups (Fig. 1.2). Attractant-bound receptors undergo methylation increases through two effects: (1) the inhibition of CheA activity leads to lower levels of phospho-CheB and reduced CheB activity; (2) attractant-bound receptor becomes a better substrate for CheR methylation. The increased methylation level restores the original ground state CheA activity, thereby bringing phospho-CheY and phospho-CheB back to prestimulus levels and resetting the original ratio of CW and CCW rotations. The needed increase in MCP methylation occurs several seconds slower than the inhibition of CheA activity and the drop of phospho-CheY level (less than 0.2 second) (37, 38). This difference in the timescales of CheA inhibition and sensory adaptation functions as a "memory" mechanism for temporal sensing. The cell uses temporal sensing to compare the current concentration of attractant, measured by the extent of receptor occupancy, with the concentration in the recent past, recorded as the methylation level. This precise sensory adaptation system allows the cell to adjust its detection sensitivity to a wide range of chemoeffector concentrations.

Signal Gain and Chemoreceptor Clusters

Transmembrane signal transduction and kinase regulation in chemotaxis can be performed by small receptor-kinase complexes that only consist of 2–3 receptor dimers, several CheWs, and one CheA (39, 40). However, chemotaxis signaling complexes are

organized in the cell into much larger macromolecular clusters (Fig. 1.3) that contain thousands of receptors and associated chemotaxis proteins. Chemoreceptors work as homodimers, which can interact to form trimer of dimers (41). These trimers of dimers form roughly hexagonal arrays (42–45) by incorporating CheA and CheW proteins at the cytoplasmic tip of the receptors (Fig. 1.3) (46, 47). Some of the CheR, CheB, CheY, and CheZ proteins localize to the clusters through interactions with either receptor or CheA (48–56), but none of them is required for cluster formation.

Interaction within clusters is thought to contribute to some significant features of the chemotaxis signaling pathway: high signal gain, extensive cooperativity, wide dynamic range, and robust adaptation. The chemoreceptor clusters can sense very small stimuli and amplify them up to ~100-fold. *In vivo* measurements of CheA kinase activity using fluorescence resonance energy transfer (FRET) showed that much of this amplification occurs at the signaling complexes (52), rather than in the interaction of phosphor-CheY with flagellar motors (57), suggesting a functional network that couples each receptor to multiple CheA kinase molecules. Both *in vitro* and *in vivo* studies (58–61) have confirmed cooperative interactions between receptors and their role in amplifying chemotactic signals (34, 59).

Chemoreceptor clusters also exhibit a wide dynamic response range, sensing gradients over five orders of magnitude (62, 63), presumably owing to the allosteric interactions between receptors in the cluster. Another advantage of clustering for chemotaxis signaling is to enhance the efficiency of signaling reactions by increasing the

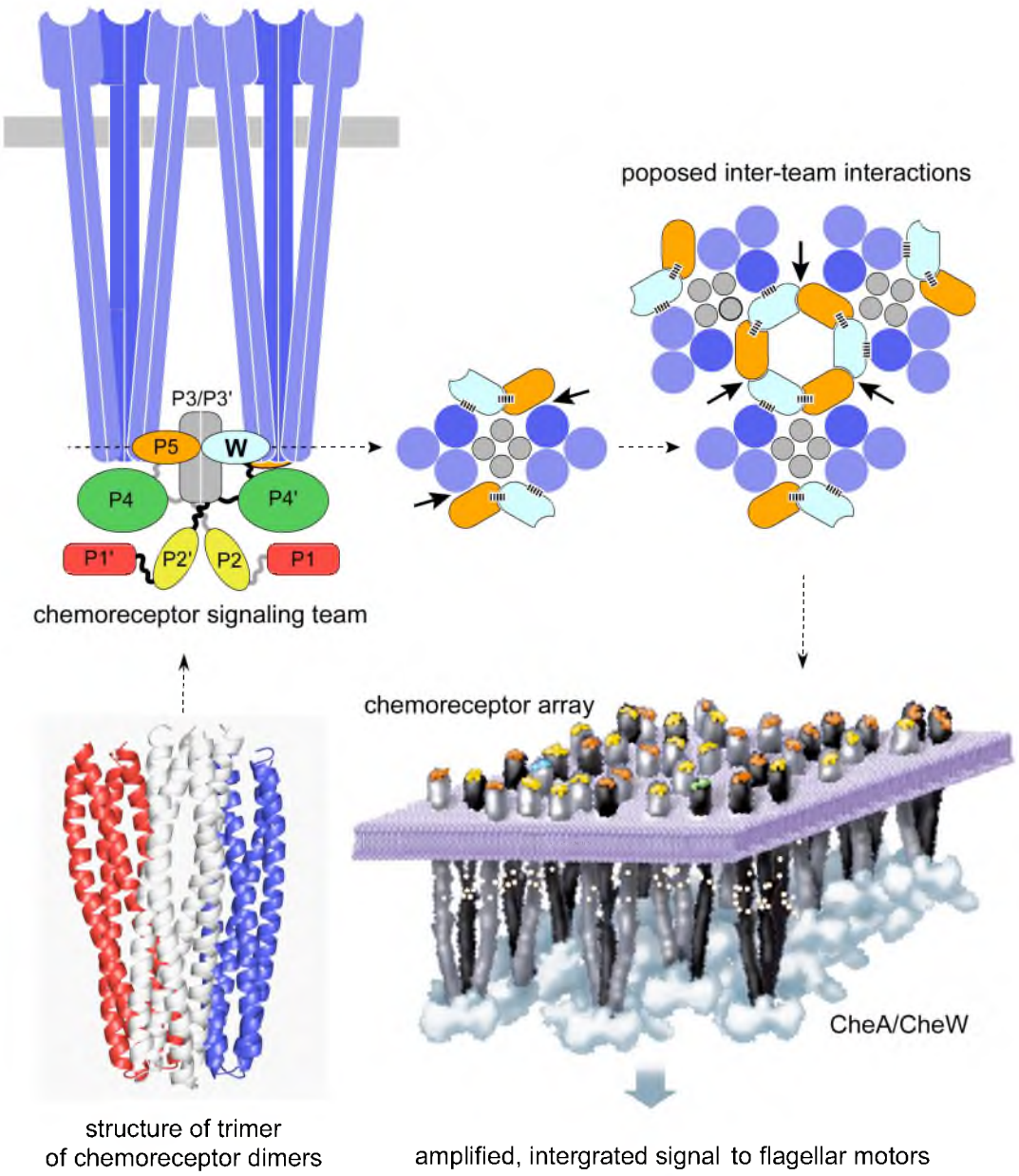

Fig. 1.3 Assembly of the chemoreceptor cluster (64). W, CheW protein; P1, P2, P3, P4, and P5 are the domains of one CheA subunit of the dimer; P1', P2', P3', P4', and P5' are the domains of the other CheA subunit. Short black lines between receptor and CheW protein, and between P5 of CheA and CheW, indicate known interactions that contribute to receptor cluster formation, whereas solid black arrows point to some proposed interactions important for cluster formation.

local concentration of signaling proteins. The receptor cluster localizes chemotaxis proteins in positions favorable for their catalytic activities, and defects in protein localization can be compensated by overexpression of the affected proteins (65). Localization seems to be especially important for the function of adaptation enzymes. Precise adaptation, which is the accurate resetting of signaling and behavior to the prestimulus state after stimulation, requires interactive cooperation between neighboring receptors (66–68). Both CheB and CheR bind to a C-terminal pentapeptide (NWETF) tether end, which is connected to the rest of the receptor by a flexible linker. Once bound to a tether end, both CheR and CheB are able to act on several adjacent receptors (69), creating adaptational assistance neighbourhoods with about six receptor dimers (66). Assistance neighbourhoods provide each adaptation enzyme with ~48 methylation sites instead of ~8 for one receptor, thereby allowing a more gradual adjustment of overall receptor activity and preventing enzyme saturation. Thus, chemoreceptor clusters seem to play a key role in maintaining precise adaptation to a wide dynamic range of stimuli (67).

Structural and Functional Features of Chemoreceptors

E.coli chemoreceptor homodimers are elongated needle-like structures of helical bundles and coiled coils oriented approximately perpendicular to the membrane. It spanned about 300 Å in length from tip to tip. Starting from the periplasmic region, each receptor homodimer contains several functional modules: lignad binding, transmembrane

sensing, signal conversion, sensory adaptation, and kinase control, each with distinct structural and functional features (Fig. 1.4). The ligand binding site is located at the interface between subunits. The "transmembrane sensing module" is a dimer of two antiparallel, membrane spanning, four-helix bundles (70, 71). Attractant binding causes a piston-like sliding of one helix downward along the long axes of the receptor dimer (72). This signaling helix extends from the ligand-binding domain across the membrane and connects to the N-terminal helix (AS1) of the "signal conversion" module via a short unstructured control cable (Fig. 1.4).

The "signal conversion" module is a HAMP domain, found in histidine kinases, adenylyl cyclases, methyl-accepting chemotaxis proteins, and some phosphatases, which consisits of two amphipathic helices (AS1 and AS2) (Fig. 1.4). A high-resolution structure of HAMP is not available for any *E.coli* chemoreceptor. However, a solution structure of a HAMP fragment from an archaeal, hyperthermophilic, transmembrane protein describes a homodimeric, parallel, four-helix, coiled coil domain with a knob-to-knob interhelical packing arrangement (73). Further analyses of the HAMP domain in different intact *E. coli* chemoreceptors (74–77) are consistent with this parallel four-helix bundle structure. The HAMP AS2 helix connects to the adaptation region of the receptor by a 4-residue phase stutter.

The "kinase control module" is an extended, antiparallel four-helix coiled-coil structure (41, 47, 78) (Fig. 1.4) and widely conserved in all MCPs (79). Each subunit has two helices, with a hairpin turn at its membrane distal end. The adaptation region, which is

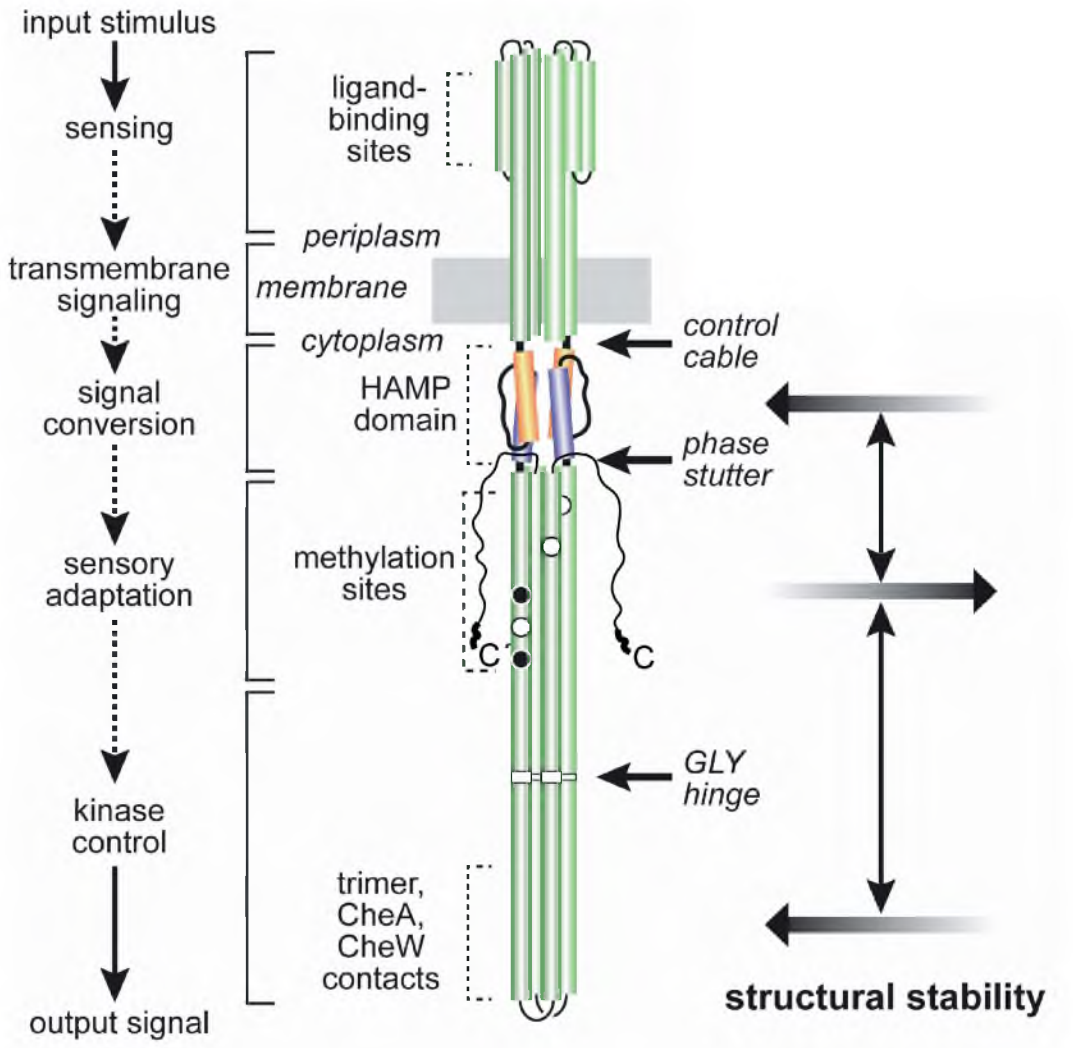

Fig. 1.4 Structural and functional features of the Tsr chemoreceptor. Shown is a Tsr homodimer, and cylindrical segments represent α-helices, drawn approximately to scale. From top to bottom, each dimer has several functional domains: inter-subunit ligand binding domain, transmembrane signaling domain, HAMP domain, methylation region (MH bundle), flexible region, and kinase control domain. The dynamic-static model proposes that the structural stabilities of adjacent bundles are coupled in opposition. Shaded arrows on the right indicate the structural stabilities of HAMP bundle, MH bundle, and kinase control bundle: the darker, the more stable. See details in text.

roughly 8–10 paired heptads adjacent to the HAMP module, contains several methylation sites (5 sites for each Tsr monomer) (Fig. 1.4). These sites are either glutamates or glutamines. The consensus 9 residue sequence of the methylation sites is [A/S]-X-X-E-[E/Q]-X-[A/S/T]-A-[A/S/T] (80, 81), in which the residues of the methylation site are underlined. Given that the first three sites of Tsr are 7 residues apart on the coiled coil helix, the spacing places them on the same face of the helix, forming an adaptation surface that provides access for adaptation enzymes (Fig. 1.4). The flexible region, located between the adaptation and protein interaction regions, contains a conserved glycine hinge that allows the four helix bundle to bend ~10° (41, 82). The glycine hinge is suggested to be important for on-off signaling and perhaps also for kinase docking.

The protein interaction region, which is typically 4-paired, highly conserved heptads bracketing the membrane distal hairpin turn, directly binds and regulates CheA kinase. Conformational changes at the inter-subunit interface (rather than at the intra-subunit interface) within the kinase control module, are probably responsible for signal transduction (83–85). The protein interaction region is also important for trimer formation, CheW binding, and interaction with some other chemotaxis proteins. The C-terminal pentapeptide tether end NWETF serves as the binding motif for both CheR and CheB (49, 64, 86).

The exact mechanisms of signal transduction from ligand input to receptor output are not clear yet. A dynamic-static mechanism has been proposed for signal transmission

through adjacent structural regions along the cytoplasmic signaling modules (75, 77, 85, 87–90). The model proposes that the four-residue phase stutter segment between the AS2 and MH1 helices couples the structural stabilities of the HAMP and MH bundles in opposition (Fig. 1.4). The glycine hinge containing flexible region also seems to couple the structural stabilities of the MH bundle and protein interaction region antisymmetrically (85, 89, 91). Thus, tight packing of the helices in the HAMP bundle forces the adjoining methylation site helices to a looser packing arrangement in the MH bundle, in turn driving the protein interaction region to a tighter packing state, leading to kinase off output. Conversely, looser packing of the HAMP bundle stabilizes the MH bundle, destabilizes the protein interaction region, and produces kinase on output. This mechanistic view also predicts that the sensory adaptation system modulates receptor signaling by adjusting the packing stability of the MH bundle: CheR mediated methylation should enhance stability; CheB mediated demethylation and deamidation should reduce stability.

Specific Research Aims

Characterize the signaling role of Tsr-E502: the unorthodox fifth methylation site. The sensory adaptation system plays a very important role in the receptor signaling process. The serine receptor Tsr has a fifth methyaltion site, E502, which deviates from the consensus sequence. This site may play a different signaling role than the orthodox methylation sites, owing to its unique features: E502 is localized in a more buried position near the intrasubunit packing interface of the methylation helices; it

lies closest to the HAMP domain, which mediates input-output control in Tsr through its interaction with the adjacent MH bundle.

To explore the signaling properties of Tsr-E502, I constructed a series of mutant receptors with amino acid replacements at various Tsr methylation sites and tested their methylation, demethylation, and deamidation behaviors. I then tested their serine dose-response signaling properties with an *in vivo* FRET kinase assay. I also constructed amino acid replacements at Tsr-E502 and characterized their effects on Tsr signaling behavior *in vivo.*

Characterize the signaling role of Tsr-Q311: the most reactive methylation site. Tsr-Q311 is probably the most important of the five methylation sites. It is located farthest from the HAMP domain and closest to the kinase control domain, which binds and regulates CheA kinase. Q311 is the first site to be deamidated by CheB and the one that undergoes CheR-mediated methylation fastest. I hypothesized that Q311 might have a more potent effect on regulating CheA kinase activity than the other sites. To explore this possibility, I constructed a series of single amino acid replacements at Tse-Q311 and characterized their signaling effects in hosts with different combinations of adaptation enzymes using an *in vivo* FRET kinase assay. I also tested their methylation, deamidation, and demethylation patterns *in vivo.*

Study the signaling effects of CheR on Tsr. Normally, CheR preferentially methylates receptors in the kinase-off output state, and the subsequent methylation increase probably stabilizies the MH bundle, shifting output toward the kinase-on state.

CheB preferentially deamidates or demethylates on-state receptors and thereby probably destabilizes the MH bundle. Thus, CheR increases the response threshold of wild type Tsr to serine, and CheB decreases that threshold. However, I observed that many Tsr mutant receptors showed a different effect of CheR: CheR lowered their response thresholds to serine in the FRET assay.

To explore the mechanistic basis for this counterintuitive signaling effect of CheR, I constructed different Tsr variants (wild type Tsr and Tsr mutants with no available methylation sites) with or without the C-terminal pentapeptide tether. I then tested their signaling behaviors in different FRET hosts to determine the dependence of the CheR signaling effect on the tether NWETF. I also constructed new FRET hosts that have wild-type or noncatalytic mutant CheR under inducible xylose control. I used these strains to assess the effects of CheR catalysis and CheR expression levels on the CheR threshold-lowering action with the FRET assay.

References

1. Fenchel T. 2002. Microbial behavior in a heterogeneous world. Science **296**:1068–1071.

2. Overmann J, Schubert K. 2002. Phototrophic consortia: model systems for symbiotic interrelations between prokaryotes. Arch Microbiol **177**:201–208.

3. Chaparro AP, Ali SK, Klose KE. 2010. The ToxT-dependent methyl-accepting chemoreceptors AcfB and TcpI contribute to Vibrio cholerae intestinal colonization. FEMS Microbiology Letters **302**:99–105.

4. Yao J, Allen C. 2006. Chemotaxis is required for virulence and competitive fitness of the bacterial wilt pathogen Ralstonia solanacearum. J Bacteriol **188**:3697–3708.

5. Stecher B, Barthel M, Schlumberger MC, Haberli L, Rabsch W, Kremer M, Hardt WD. 2008. Motility allows S. Typhimurium to benefit from the mucosal defence. Cellular Microbiology **10**:1166–1180.

6. Lux R, Shi W. 2004. Chemotaxis-guided movements in bacteria. Crit Rev Oral Biol Med **15**:207–220.

7. Butler SM, Camilli A. 2004. Both chemotaxis and net motility greatly influence the infectivity of Vibrio cholerae. Proc Natl Acad Sci USA **101**:5018–5023.

8. Butler SM, Camilli A. 2005. Going against the grain: chemotaxis and infection in Vibrio cholerae. Nat Rev Microbiol **3**:611–620.

9. Grim CJ, Kotewicz MK, Power KA, Gopinath G, Franco AA, Jarvis KG, Yan QQ, Jackson SA, Sathyamoorthy V, Hu L, Pagotto F, Iversen C, Lehner A, Stephan R, Fanning S, Tall BD. 2013. Pan-genome analysis of the emerging foodborne pathogen Cronobacter spp. suggests a species-level bidirectional divergence driven by niche adaptation. BMC Genomics **14**.

10. Caetano-Anolles G, Wall LG, De Micheli AT, Macchi EM, Bauer WD, Favelukes G. 1988. Role of motility and chemotaxis in efficiency of nodulation by Rhizobium meliloti. Plant Physiol **86**:1228–1235.

11. Miller RM, Tomaras AP, Barker AP, Voelker DR, Chan ED, Vasil AI, Vasil ML. 2008. Pseudomonas aeruginosa twitching motility-mediated chemotaxis towards phospholipids and fatty acids: specificity and metabolic requirements. J Bacteriol **190**:4038–4049.

12. Nilsson M, Rasmussen U, Bergman B. 2006. Cyanobacterial chemotaxis to extracts of host and nonhost plants. FEMS Microbiol Ecol **55**:382–390.

13. Pandey G, Rakesh K. Jain. 2002. Bacterial Chemotaxis toward Environmental Pollutants: Role in Bioremediation. Appl Environ Microbiol **68**:5789–5795.

14. Joy Sinha SJR, Justin P Galllivan. 2010. Reprogramming bacteria to seek and destroy an herbicide. Nat Chem Biol **6**:464–470.

15. Leungsakul T, Keenan BG, Smets BF, Wood TK. 2005. TNT and nitroaromatic compounds are chemoattractants for Burkholderia cepacia R34 and Burkholderia sp. strain DNT. Appl Microbiol Biotechnol **69**:321–325.

16. Mazzag BC, Zhulin IB, Mogilner A. 2003. Model of bacterial band formation in aerotaxis. Biophys J **85**:3558–3574.

17. Hirota N, Imae Y. 1983. Na+-driven flagellar motors of an alkalophilic Bacillus strain YN-1. J Biol Chem **258**:10577–10581.

18. Berg HC. 1996. Touring machines. Curr Biol **6**:624.

19. Wisdom J. 2003. Swimming in spacetime: motion by cyclic changes in body shape. Science **299**:1865–1869.

20. Berg HC, Anderson RA. 1973. Bacteria swim by rotating their flagellar filaments. Nature **245**:380–382.

21. M. Meister GL, H.C. Berg. 1987. The proton flux through the bacterial flagellar motor. Cell **49**:643–650.

22. de Pina K, Navarro C, McWalter L, Boxer DH, Price NC, Kelly SM, Mandrand-Berthelot MA, Wu LF. 1995. Purification and characterization of the periplasmic nickel-binding protein NikA of Escherichia coli K12. Eur J Biochem **227**:857–865.

23. Adler J, Tso W-W. 1974. "Decision"-making in bacteria: chemotactic response of Escherichia coli to conflicting stimuli. Science **184**:1292–1294.

24. Maeda K, Imae Y, Shioi JI, Oosawa F. 1976. Effect of temperature on motility and chemotaxis of Escherichia coli. J Bacteriol **127**:1039–1046.

25. Bibikov SI, Biran R, Rudd KE, Parkinson JS. 1997. A signal transducer for aerotaxis in Escherichia coli. J Bacteriol **179**:4075–4079.

26. Adler J, Hazelbauer GL, Dahl MM. 1973. Chemotaxis toward sugars in Escherichia coli. J Bacteriol **115**:824–847.

27. Manson MD, Blank V, Brade G, Higgins CF. 1986. Peptide chemotaxis in E. coli involves the Tap signal transducer and the dipeptide permease. Nature **321**:253–256.

28. Bourret RB, Stock AM. 2002. Molecular information processing: Lessons from bacterial chemotaxis. J Biol Chem **277**:9625–9628.

29. Sourjik V. 2004. Receptor clustering and signal processing in E. coli chemotaxis. Trends Microbiol **12**:569–576.

30. Parkinson JS, Ames P, Studdert CA. 2005. Collaborative signaling by bacterial chemoreceptors. Curr Opin Microbiol **8**:116–121.

31. Baker MD, Wolanin PM, Stock JB. 2006. Signal transduction in bacterial chemotaxis. Bioessays **28**:9–22.

32. Erbse AH, Falke JJ. 2009. The core signaling proteins of bacterial chemotaxis assemble to form an ultrastable complex. Biochemistry **48**:6975–6987.

33. Fukuoka H, Sagawa T, Inoue Y, Takahashi H, Ishijima A. 2014. Direct imaging of intracellular signaling components that regulate bacterial chemotaxis. Sci Signal **7**:32.

34. Sourjik V, Berg HC. 2002. Binding of the Escherichia coli response regulator CheY to its target measured in vivo by fluorescence resonance energy transfer. Proc Natl Acad Sci USA **99**:12669–12674.

35. David Kentner, Sourjik V. 2009. Dynamic map of protein interactions in the Escherichia coli chemotaxis pathway. Mol Syst Biol **5**:77.

36. Bergman K, Gulash HM, Hovestadt RE, Larosiliere RC, Ronco Pd, Su L. 1988. Physiology of behavioral mutants of Rhizobium meliloti: evidence for a dual chemotaxis pathway. J Bacteriol **170**:3249–3254.

37. Segall JE, Manson MD, Berg HC. 1982. Signal processing times in bacterial chemotaxis. Nature **296**:855–857.

38. Springer MS, Goy MF, Adler J. 1979. Protein methylation in behavioural control mechanisms and in signal transduction. Nature **280**:279–284.

39. Boldog T, Grimme S, Li M, Sligar SG, Hazelbauer GL. 2006. Nanodiscs separate chemoreceptor oligomeric states and reveal their signaling properties. Proc Natl Acad Sci USA **103**:11509–11514.

40. Divya N. Amin, Hazelbauer GL. 2010. Chemoreceptors in signaling complexes: shifted conformation and asymmetric coupling. Mol Microbiol **78**:1313–1323.

41. Kim KK, Yokota H, Kim SH. 1999. Four-helical-bundle structure of the cytoplasmic domain of a serine chemotaxis receptor. Nature **400**:787–792.

42. Briegel A, Ding HJ, Li Z, Werner J, Gitai Z, Dias DP, Jensen RB, Jensen GJ. 2008. Location and architecture of the Caulobacter crescentus chemoreceptor array. Mol Microbiol **69**:30–41.

43. Briegel A, Li X, Bilwes AM, Hughes KT, Jensen GJ, Crane BR. 2012. Bacterial chemoreceptor arrays are hexagonally packed trimers of receptor dimers networked by rings of kinase and coupling proteins. Proc Natl Acad Sci USA **109**:3766–3771.

44. Briegel A, Ortega DR, Tocheva EI, Wuichet K, Li Z, Chen S, Muller A, Iancu CV, Murphy GE, Dobro MJ, Zhulin IB, Jensen GJ. 2009. Universal architecture of bacterial chemoreceptor arrays. Proc Natl Acad Sci USA **106**:17181–17186.

45. Liu J, Hu B, Morado DR, Jani S, Manson MD, Margolin W. 2012. Molecular architecture of chemoreceptor arrays revealed by cryoelectron tomography of Escherichia coli minicells. Proc Natl Acad Sci USA **109**:E1481–1488.

46. Miller AS, Kohout SC, Gilman KA, Falke JJ. 2006. CheA kinase of bacterial chemotaxis: chemical mapping of four essential docking sites. Biochemistry **45**:8699–8711.

47. Park SY, Borbat PP, Gonzalez-Bonet G, Bhatnagar J, Pollard AM, Freed JH, Bilwes AM, Crane BR. 2006. Reconstruction of the chemotaxis receptor-kinase assembly. Nat Struct Mol Biol **13**:400–407.

48. Wu J, Li J, Li G, Long DG, Weis RM. 1996. The receptor binding site for the methyltransferase of bacterial chemotaxis is distinct from the sites of methylation. Biochemistry **35**:4984–4993.

49. Barnakov AN, Barnakova LA, Hazelbauer GL. 1999. Efficient adaptational demethylation of chemoreceptors requires the same enzyme-docking site as efficient methylation. Proc Natl Acad Sci USA **96**:10667–10672.

50. Shiomi D, Zhulin IB, Homma M, Kawagishi I. 2002. Dual recognition of the bacterial chemoreceptor by chemotaxis-specific domains of the CheR methyltransferase. J Biol Chem **277**:42325–42333.

51. Banno S, Shiomi D, Homma M, Kawagishi I. 2004. Targeting of the chemotaxis methylesterase/deamidase CheB to the polar receptor-kinase cluster in an Escherichia coli cell. Mol Microbiol **53**:1051–1063.

52. Sourjik V, Berg HC. 2002. Receptor sensitivity in bacterial chemotaxis. Proc Natl Acad Sci USA **99**:123–127.

53. Cantwell BJ, Manson MD. 2009. Protein domains and residues involved in the CheZ/CheAS interaction. J Bacteriol **191**:5838–5841.

54. O'Connor C, Matsumura P, Campos A. 2009. The CheZ binding interface of CheAS is located in alpha-helix E. J Bacteriol **191**:5845–5848.

55. Cantwell BJ, Draheim RR, Weart RB, Nguyen C, Stewart RC, Manson MD. 2003. CheZ phosphatase localizes to chemoreceptor patches via CheA-short. J Bacteriol **185**:2354–361.

56. Thakor H, Nicholas S, Porter IM, Hand N, Stewart RC. 2011. Identification of an anchor residue for CheA-CheY interactions in the chemotaxis system of Escherichia coli. J Bacteriol **193**:3894–3903.

57. Cluzel P, Surette M, Leibler S. 2000. An ultrasensitive bacterial motor revealed by monitoring signaling proteins in single cells. Science **287**:1652–1655.

58. Li G, Weis RM. 2000. Covalent modification regulates ligand binding to receptor complexes in the chemosensory system of Escherichia coli. Cell **100**:357–365.

59. Sourjik V, Berg HC. 2004. Functional interactions between receptors in bacterial chemotaxis. Nature **428**:437–441.

60. Lai RZ, Manson JM, Bormans AF, Draheim RR, Nguyen NT, Manson MD. 2005. Cooperative signaling among bacterial chemoreceptors. Biochemistry **44**:14298–14307.

61. Vaknin A, Berg HC. 2008. Direct evidence for coupling between bacterial chemoreceptors. J Mol Biol **382**:573–577.

62. Berg HC, Tedesco PM. 1975. Transient response to chemotactic stimuli in Escherichia coli. Proc Natl Acad Sci USA **72**:3235–3239.

63. Mesibov R, Ordal GW, Adler J. 1973. The range of attractant concentrations for bacterial chemotaxis and the threshold and size of response over this range. Weber law and related phenomena. J Gen Physiol **62**:203–223.

64. Bray D. 2003. Molecular prodigality. Science **299**:1189–1190.

65. Jahreis K, Morrison TB, Garzon A, Parkinson JS. 2004. Chemotactic signaling by an Escherichia coli CheA mutant that lacks the binding domain for phosphoacceptor partners. J Bacteriol **186**:2664–2672.

66. Li M, Hazelbauer GL. 2005. Adaptational assistance in clusters of bacterial chemoreceptors. Mol Microbiol **56**:1617–1626.

67. Endres RG, Wingreen NS. 2006. Precise adaptation in bacterial chemotaxis through "assistance neighborhoods." Proc Natl Acad Sci USA **103**:13040–13044.

68. Endres RG, Falke JJ, Wingreen NS. 2007. Chemotaxis receptor complexes: from signaling to assembly. PLoS Comput Biol **3**:e150.

69. Li M, Hazelbauer GL. 2006. The carboxyl-terminal linker is important for chemoreceptor function. Mol Microbiol **60**:469–479.

70. Miller AS, Falke JJ. 2004. Side chains at the membrane-water interface modulate the signaling state of a transmembrane receptor. Biochemistry **43**:1763–1770.

71. Boldog T, Hazelbauer GL. 2004. Accessibility of introduced cysteines in chemoreceptor transmembrane helices reveals boundaries interior to bracketing charged residues. Protein Science **13**:1466–1475.

72. Falke JJ, Hazelbauer GL. 2001. Transmembrane signaling in bacterial chemoreceptors. Trends Biochem Sci **26**:257–265.

73. Hulko M, Berndt F, Gruber M, Linder JU, Truffault V, Schultz A, Martin J, Schultz JE, Lupas AN, Coles M. 2006. The HAMP domain structure implies helix rotation in transmembrane signaling. Cell **126**:929–940.

74. Swain KE, Falke JJ. 2007. Structure of the conserved HAMP domain in an intact, membrane-bound chemoreceptor: a disulfide mapping study. Biochemistry **46**:13684–13695.

75. Ames P, Zhou Q, Parkinson JS. 2008. Mutational analysis of the connector segment in the HAMP domain of Tsr, the Escherichia coli serine chemoreceptor. J Bacteriol **190**:6676–6685.

76. Watts KJ, Johnson MS, Taylor BL. 2008. Structure-function relationships in the HAMP and proximal signaling domains of the aerotaxis receptor Aer. J Bacteriol **190**:2118–127.

77. Zhou Q, Ames P, Parkinson JS. 2011. Biphasic control logic of HAMP domain signalling in the Escherichia coli serine chemoreceptor. Mol Microbiol **80**:596–611.

78. Pollard AM, Bilwes AM, Crane BR. 2009. The structure of a soluble chemoreceptor suggests a mechanism for propagating conformational signals. Biochemistry **48**:1936–1944.

79. Alexander RP, Zhulin IB. 2007. Evolutionary genomics reveals conserved structural determinants of signaling and adaptation in microbial chemoreceptors. Proc Natl Acad Sci USA **104**:2885–2890.

80. Terwilliger TC, Wang JY, Koshland DE, Jr. 1986. Surface structure recognized for covalent modification of the aspartate receptor in chemotaxis. Proc Natl Acad Sci USA **83**:6707–6710.

81. Nowlin DM, Bollinger J, Hazelbauer GL. 1987. Sites of covalent modification in Trg, a sensory transducer of Escherichia coli. J Biol Chem **262**:6039–6045.

82. Coleman MD, Bass RB, Mehan RS, Falke JJ. 2005. Conserved glycine residues in the cytoplasmic domain of the aspartate receptor play essential roles in kinase coupling and on-off switching. Biochemistry **44**:7687–7695.

83. Freeman JA, Bassler BL. 1999. Sequence and function of LuxU: a two-component phosphorelay protein that regulates quorum sensing in Vibrio harveyi. J Bacteriol **181**:899–906.

84. Winston SE, Mehan R, Falke JJ. 2005. Evidence that the adaptation region of the aspartate receptor is a dynamic four-helix bundle: cysteine and disulfide scanning studies. Biochemistry **44**:12655–12666.

85. Starrett DJ, Falke JJ. 2005. Adaptation mechanism of the aspartate receptor: electrostatics of the adaptation subdomain play a key role in modulating kinase activity. Biochemistry **44**:1550–1560.

86. Djordjevic S, Stock AM. 1998. Chemotaxis receptor recognition by protein methyltransferase CheR. Nat Struct Biol **5**:446–450.

87. Zhou Q, Ames P, Parkinson JS. 2009. Mutational analyses of HAMP helices suggest a dynamic bundle model of input-output signalling in chemoreceptors. Mol Microbiol **73**:801–814.

88. Ames P, Zhou Q, Parkinson JS. 2014. HAMP domain structural determinants for signalling and sensory adaptation in Tsr, the Escherichia coli serine chemoreceptor. Mol Microbiol **91**:875–886.

89. Swain KE, Gonzalez MA, Falke JJ. 2009. Engineered socket study of signaling through a four-helix bundle: evidence for a yin-yang mechanism in the kinase control module of the aspartate receptor. Biochemistry **48**:9266–9277.

90. Airola MV, Sukomon N, Samanta D, Borbat PP, Freed JH, Watts KJ, Crane BR. 2013. HAMP domain conformers that propagate opposite signals in bacterial chemoreceptors. PLoS Biol **11**:e1001479.

91. Falke JJ, Piasta KN. 2014. Architecture and signal transduction mechanism of the bacterial chemosensory array: progress, controversies, and challenges. Curr Opin Struct Biol **29**:85–94.

CHAPTER 2

AN UNORTHODOX SENSORY ADAPTATION SITE IN THE ESCHERICHIA COLI SERINE CHEMORECEPTOR

Reprinted with permission from Han, X. S. & J. S. Parkinson, (2014) An unorthodox sensory adaptation site in the *Escherichia coli* serine chemoreceptor. *J. Bacteriol.* **196(3)**: 641 - 649.

An Unorthodox Sensory Adaptation Site in the *Escherichia coli* Serine Chemoreceptor

Xue-Sheng Han, John S. Parkinson

Biology Department, University of Utah, Salt Lake City, Utah, USA

The serine chemoreceptor of *Escherichia coli* contains four canonical methylation sites for sensory adaptation that lie near intersubunit helix interfaces of the Tsr homodimer. An unexplored fifth methylation site, E502, lies at an intrasubunit helix interface closest to the HAMP domain that controls input-output signaling in methyl-accepting chemotaxis proteins. We analyzed, with *in vivo* Förster resonance energy transfer (FRET) kinase assays, the serine thresholds and response cooperativities of Tsr receptors with different mutationally imposed modifications at sites 1 to 4 and/or at site 5. Tsr variants carrying E or Q at residue 502, in combination with unmodifiable D and N replacements at adaptation sites 1 to 4, underwent both methylation and demethylation/deamidation, although detection of the latter modifications required elevated intracellular levels of CheB. These Tsr variants could not mediate a chemotactic response to serine spatial gradients, demonstrating that adaptational modifications at E502 alone are not sufficient for Tsr function. Moreover, E502 is not critical for Tsr function, because only two amino acid replacements at this residue abrogated serine chemotaxis: Tsr-E502P had extreme kinase-off output and Tsr-E502I had extreme kinase-on output. These large threshold shifts are probably due to the unique HAMP-proximal location of methylation site 5. However, a methylation-mimicking glutamine at any Tsr modification site raised the serine response threshold, suggesting that all sites influence signaling by the same general mechanism, presumably through changes in packing stability of the methylation helix bundle. These findings are consistent with control of input-output signaling in Tsr through dynamic interplay of the structural stabilities of the HAMP and methylation bundles.

Motile bacteria detect and follow gradients of attractant and repellent chemicals through chemotaxis signaling pathways (recently reviewed in references 1, 2, and 3). The well-studied chemotaxis machinery of *Escherichia coli* employs chemoreceptors known as methyl-accepting chemotaxis proteins (MCPs) to regulate the autophosphorylation activity of a cytoplasmic histidine kinase, CheA. A small cytoplasmic protein, CheW, couples CheA to receptor control. Ternary receptor signaling complexes form arrays at the cell poles that produce large changes in CheA activity in response to small changes in chemoeffector concentration. CheA in turn donates its phosphoryl groups to two cytoplasmic response regulators, CheY and CheB, to control rotation of the cell's flagellar motors and a sensory adaptation process, respectively. Phosphorylation of CheY promotes clockwise (CW) motor rotation; phosphorylation of CheB augments its receptor-modifying enzymatic activity, demethylation or deamidation of specific MCP residues. Another cytoplasmic enzyme, CheR, is responsible for methylating receptor modification sites. The interplay of CheR and CheB activities regulates the receptor methylation state to offset signaling responses to ambient chemoeffector levels, thereby adjusting sensitivity and extending the detection range of the receptor array.

E. coli has four homodimeric, transmembrane MCPs (Fig. 1A) that detect various attractant compounds: Tsr (serine), Tar (aspartate and maltose), Tap (dipeptides and pyrimidines), and Trg (ribose and galactose). A fifth MCP-related receptor, Aer, has no periplasmic domain, but it monitors cellular redox status through a cytoplasmic FAD-binding domain to mediate aerotactic behavior. All five of these MCP family receptors have highly similar cytoplasmic domains that form ternary signaling complexes with CheA and CheW. The Aer signaling domain contains no methylation sites, and its mechanism of sensory adaptation remains unclear. In contrast, the other MCPs contain four canonical methylation sites per subunit. Each site resides in a 9-residue primary structure motif [(A/S)-X-X-E-(E/Q)-X-(A/S/T)-A-(A/S/T)] thought to represent the consensus substrate site for CheB and CheR action (Fig. 1A) (4, 5). Both glutamate (E) and glutamine (Q) at the target residue (boldface in the consensus sequence) can serve as sites for adaptational modifications. CheB irreversibly deamidates Q's to E's; CheR methylates E's, forming glutamyl-methyl esters (Em); CheB demethylates Em sites by hydrolysis back to E. These four canonical sites are always the second residue of an E-E or E-Q pair and reside on the solvent-exposed faces of the cytoplasmic methylation helices (MH), where they most likely influence intersubunit interactions in the four-helix MH bundle through electrostatic effects. Methylation should enhance MH packing stability; demethylation and deamidation should reduce MH packing stability (6, 7).

The serine receptor Tsr contains a fifth methylation site, E502, that does not conform to the consensus motif (Fig. 1A) (8). It is the first of an E-E pair and resides in a more buried location near the intrasubunit packing interface of the MH bundle (Fig. 1). Moreover, of the five Tsr methylation sites, E502 lies closest to the HAMP domain, which mediates input-output signaling transactions in chemoreceptors through its structural interplay with the MH bundle (9). These unique features could mean that E502 plays

Received 30 September 2013 Accepted 14 November 2013

Published ahead of print 22 November 2013

Address correspondence to John S. Parkinson, parkinson@biology.utah.edu.

Supplemental material for this article may be found at http://dx.doi.org/10.1128/JB.01164-13.

Copyright © 2014, American Society for Microbiology. All Rights Reserved.

doi:10.1128/JB.01164-13

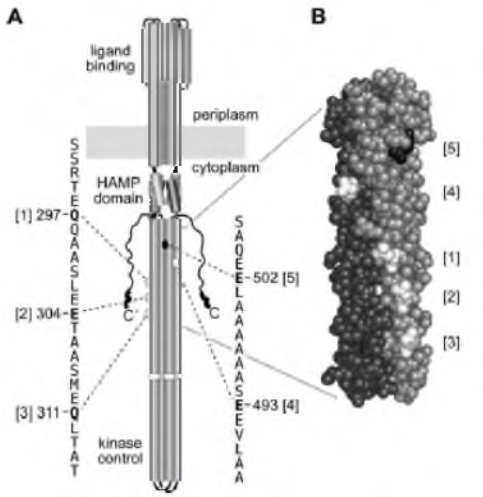

FIG 1 Structural features of Tsr and its methylation sites. (A) The Tsr homodimer. Cylindrical segments represent α-helices, drawn approximately to scale. Each Tsr subunit has five methylation sites (boldfaced residues in the primary sequence; sites 1 to 4 are in white, site 5 is in black). (B) Structure of the native methylation helix (MH) bundle. Shown are residues R271 to A320 and A462 to V512 in each subunit of the Tsr dimer. One subunit is shaded gray, the other dark gray. Methylation sites 1 to 4 (white atoms) lie near the intersubunit interface; methylation site 5 (black atoms) lies near the intrasubunit interface. The atomic coordinates were modeled and extrapolated from the crystal structure of the kinase control region of Tsr (38).

a different signaling role than do the canonical Tsr methylation sites. To explore that possibility, we constructed a series of mutant receptors with amino acid replacements at Tsr methylation sites and measured their methylation, demethylation, and deamidation properties and their serine dose-response signaling behaviors. Our results show that Tsr site 5 influences receptor signaling in the same way as do sites 1 to 4, but it has a much more potent effect on stimulus sensitivity, most likely owing to its proximity to the HAMP domain. These findings provide additional insights into the mechanisms of input-output signaling and sensory adaptation control in MCP molecules.

MATERIALS AND METHODS

Bacterial strains. Strains used in this study were isogenic derivatives of *E. coli* K-12 strain RP437 (10). Their designations and relevant genotypes were the following: UU1250, *Δaer-1 Δtsr-7028* Δ(*tar-tap*)*5201 Δtrg-100* (11); UU2610, *Δaer-1* Δ(*tar-cheB*)*4346 Δtsr-5547 Δtrg-4543* (12); UU2611, *Δaer-1* Δ(*tar-cheR*)*4283 Δtsr-5547 Δtrg-4543* (12); UU2612, *Δaer-1* Δ(*tar-tap*)*4530 Δtsr-5547 Δtrg-4543* (12); UU2632, *Δaer-1* Δ(*tar-tap*)*4530* Δ(*cheB*)*4345 Δtsr-5547 Δtrg-4543* (12); UU2567, Δ(*tar-cheZ*)*4211* Δ(*tsr*)*-5547* Δ(*aer*)*-1 Δtrg-4543* (R. Z. Lai and J. S. Parkinson, unpublished data); UU2697, Δ(*cheY-cheZ*)*1215* Δ(*cheB*)*4345* Δ(*tar-tap*)*4530 Δtsr-5547 Δaer-1 Δtrg-4543* (Lai and Parkinson, unpublished); UU2699, Δ(*cheY-cheZ*)*1215* Δ(*tar-cheR*)*4283 Δtsr-5547 Δaer-1 Δtrg-4543* (Lai and Parkinson, unpublished); and UU2700, Δ(*cheY-cheZ*)*1215* Δ(*tar-tap*)*4530 Δtsr-5547 Δaer-1 Δtrg-4543* (Lai and Parkinson, unpublished).

CheR/CheB phenotype notation. A shorthand notation is used throughout to indicate strain phenotypes with respect to the CheR (R^-, R^+) and CheB (B^-, B^+) proteins.

Plasmids. Plasmids used in the study were the following: pKG116, a derivative of pACYC184 (13) that confers chloramphenicol resistance and has a sodium salicylate-inducible expression/cloning site (14); pPA114, a relative of pKG116 that carries wild-type (wt) *tsr* under salicylate control (11); pRZ30, a derivative of pKG116 that carries *cheY-YFP* and *cheZ-CFP* fusions under salicylate control (Lai and Parkinson, unpublished); pPA827, a derivative of pKG116 that carries wild-type *cheB* under salicylate control; pRR48, a derivative of pBR322 (15) that confers ampicillin resistance and has an expression/cloning site with a *tac* promoter and an ideal (perfectly palindromic) *lac* operator under the control of a plasmid-encoded *lacI* repressor, inducible by isopropyl-β-D-thiogalactopyranoside (IPTG) (16); pRR53, a derivative of pRR48 that carries wild-type *tsr* under IPTG control (16); and pVS88, a plasmid that carries *cheY-YFP* and *cheZ-CFP* fusions under IPTG control (17).

Chemotaxis assays. Host strains carrying *tsr* plasmids were assessed for chemotactic ability on tryptone or minimal glycerol plus serine soft-agar plates (18) containing the appropriate antibiotics (ampicillin [50 μg/ml] or chloramphenicol [12.5 μg/ml]) and inducer (100 μM IPTG or 0.6 μM sodium salicylate). Tryptone plates were incubated at 30 to 32.5°C for 7 to 10 h or at 24°C for 15 to 20 h. Minimal plates were incubated at 30 to 32.5°C for 15 to 20 h.

Mutant construction. Mutations in the *tsr* gene of plasmid pPA114 or pRR53 were generated by QuikChange PCR mutagenesis, using either degenerate-codon or site-specific primers, as previously described (11). QuikChange products were introduced into UU1250 by $CaCl_2$ transformation and tested for the ability to support Tsr function on tryptone and minimal serine soft-agar plates. Candidate plasmids were verified by sequencing the entire *tsr* coding region.

Expression levels and modification patterns of mutant Tsr proteins. Cells harboring pRR53 derivatives were grown in tryptone broth containing 50 μg/ml ampicillin and 100 μM IPTG; cells harboring pPA114 derivatives were grown in tryptone broth containing 12.5 μg/ml chloramphenicol and 0.6 μM sodium salicylate. Strain UU2610 (R^-B^-) was used for measuring expression levels of mutant proteins to avoid receptor molecules in multiple modification states. Strains UU2611 (R^-B^+), UU2632 (R^+B^-), and UU2612 (R^+B^-) were used to assess the CheR and CheB substrate properties of mutant Tsr proteins. Cells were grown at 30°C to mid-exponential phase, and 1-ml samples were pelleted by centrifugation, washed twice with KEP (10 mM KPO_4, 0.1 mM K-EDTA, pH 7.0), and lysed by boiling in sample buffer (19). Tsr bands were resolved by electrophoresis in 11% polyacrylamide gels containing sodium dodecyl sulfate and visualized by immunoblotting with a polyclonal rabbit antiserum raised against Tsr residues 290 to 470 (20). Gel band intensities were quantified with ImageJ software (http://imagej.nih.gov/ij).

Flagellar rotation assays. Flagellar rotation patterns of plasmid-containing cells were analyzed by antibody tethering as described previously (21). Cells were classified into five rotation patterns, and the fraction of CW rotation time for a population of tethered cells was computed by a weighted sum of these rotation classes, as described previously (11).

***In vivo* FRET CheA kinase assay.** The experimental system, cell sample chamber, stimulus protocol, and data analysis closely followed the hardware, software, and methods described by Sourjik et al. (17). Cells containing a Förster resonance energy transfer (FRET) reporter plasmid (pRZ30 or pVS88) and a compatible *tsr* expression plasmid (pRR53 or pPA114 derivative) were grown to mid-exponential phase in tryptone broth, washed, attached to a round coverslip with polylysine, and mounted in a flow cell (22). The flow cell and all motility buffer test solutions (KEP containing 10 mM Na lactate, 100 μM methionine, and various concentrations of serine) were maintained at 30°C throughout each experiment. Cells were illuminated at the cyan fluorescent protein (CFP) excitation wavelength, and light emission was detected at the CFP (FRET donor) and yellow fluorescent protein (YFP; FRET acceptor) wavelengths with photomultipliers. The ratio of YFP to CFP photon counts accurately reflects CheA kinase activity and changes in response to serine stimuli (23, 24). Fractional changes in kinase activity versus applied

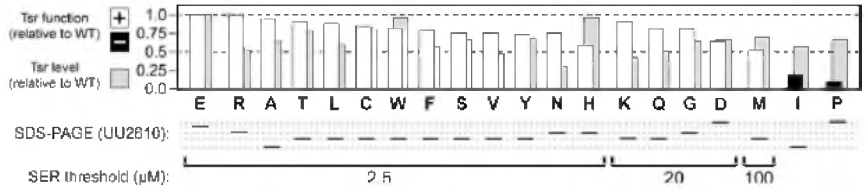

FIG 2 Mutational survey of Tsr-E502. Boldface letters below the histogram indicate the amino acid at residue 502 of Tsr (E, Tsr wild type). White and black bars indicate the relative colony size on tryptone soft agar produced by strain UU1250 carrying a plasmid expressing each Tsr variant. White bars denote wild-type colony morphology; black bars denote colonies with no evident ring of chemotactic cells at their periphery. Gray bars indicate the relative expression levels of the mutant Tsr proteins. Black horizontal bars beneath the mutant amino acid indicate the relative positions of the mutant subunits in SDS-PAGE analyses (see Fig. S1 in the supplemental material). Dashed horizontal gray lines are simply intended to facilitate comparison of band positions. Serine thresholds of the Tsr-E502 mutants were defined by chemotactic ring formation on minimal soft-agar plates containing 2.5, 20, or 100 μM serine. Amino acid replacement mutants are arranged left to right within each threshold group in order of decreasing colony size on tryptone soft agar.

serine concentrations were fitted to a multisite Hill equation, yielding two parameter values: $K_{1/2}$, the attractant concentration that inhibits 50% of the kinase activity, and the Hill coefficient, reflecting the extent of cooperativity of the response (17, 25).

Protein modeling and structural display. Structure images were prepared with MacPyMOL software (http://www.pymol.org). Atomic coordinates for the modeled Tsr methylation helix bundle were obtained from Sung-Hou Kim (UC-Berkeley).

RESULTS

Mutational survey of Tsr-E502. To determine whether residue E502 is critical for Tsr function, we constructed derivatives of *tsr* expression plasmid pPA114 that encoded Tsr proteins with all possible amino acid replacements at the 502 position. On tryptone soft-agar plates at an optimal inducer concentration of 0.6 μM sodium salicylate, the parental pPA114 plasmid confers robust serine chemotaxis to host strain UU1250, which carries deletions of all five *E. coli* MCP family genes (*tsr*, *tar*, *trg*, *tap*, and *aer*) (11). All but two of the resulting E502 amino acid replacement mutant proteins (here designated Tsr-E502*) conferred at least 50% of the wild-type colony size to the receptor-less host on tryptone soft agar (Fig. 2). This finding indicates that Tsr function tolerates a variety of amino acids at residue 502. However, subsequent chemotaxis tests on minimal soft-agar plates containing 2.5, 20, or 100 μM serine showed that five of the functional Tsr mutants had elevated serine-sensing thresholds (Fig. 2). Overall, 12 Tsr-E502 amino acid replacements (R, A, T, L, C, W, F, S, V, Y, N, and H) supported chemotaxis at 2.5 μM serine, as did wild-type Tsr (Tsr-wt); four (K, D, G, and Q) produced chemotaxis at 20 μM serine; one (M) showed function at 100 μM serine; and two (I and P) could not mediate a chemotactic response at any serine concentration tested, including on tryptone medium, which contains ~670 μM serine (26).

SDS-PAGE analysis of Tsr-E502* proteins. The E502* mutants with impaired Tsr function might make a misfolded or unstable protein. To test this possibility, we measured the steady-state intracellular levels of all plasmid-expressed E502* proteins in the receptor-less host strain UU2610, which lacks the sensory adaptation enzymes CheR and CheB (R^-B^-). Tsr subunits synthesized in this host strain lack adaptational modifications; therefore, they migrate as a single band on SDS-PAGE (11). Nearly all of the E502* proteins, including six of the seven impaired-function mutants (D, G, Q, M, I, and P), had intracellular levels of 50% or more of the wild type (Fig. 2, gray bars). Moreover, the mutant protein with the lowest expression level (E502N; 31% of Tsr-wt) had nearly full function (76% of Tsr-wt). We conclude that the E502* proteins have essentially normal expression levels and intracellular stabilities and that even those with functional defects probably have near-native structures.

Adaptational modifications can shift the SDS-PAGE mobility of MCP subunits. Methylated (or Q-bearing) forms migrate faster than do demethylated and deamidated (i.e., E-bearing) forms. The mechanistic basis for those effects is unknown, but one possibility is that Tsr subunits retain residual secondary structures in SDS that influence electrophoretic mobility. Remarkably, every E502* mutant protein exhibited a different SDS-PAGE mobility than the wild-type protein (Fig. 2; also see Fig. S1 in the supplemental material). Tsr-E502P and Tsr-E502D migrated slower than Tsr-wt; all other mutant forms, regardless of their functional properties or side chain chemical character, migrated faster than Tsr-wt. We consider implications of this phenomenon in Discussion.

Measurement and interpretation of mutant Tsr signaling patterns. To assess the signaling properties of mutant Tsr receptors, we adopted a FRET-based kinase assay, developed by Sourjik and Berg (23), to monitor *in vivo* Tsr control of CheA activity in response to serine stimuli. This assay measures interaction of YFP-tagged phospho-CheY (the FRET acceptor) and its CFP-tagged phosphatase CheZ (the FRET donor). The FRET signal reflects the receptor-coupled autophosphorylation activity of CheA, the rate-limiting step in CheY phosphorylation. The FRET dose-response data were fitted to a multisite Hill equation to obtain a $K_{1/2}$ value, the attractant concentration that inhibits 50% of CheA activity, and a Hill coefficient, which reflects the extent of response cooperativity.

We interpret shifts in the serine response sensitivity of Tsr mutants in terms of a two-state signaling model in which receptor ternary complexes can adopt CheA-activating (kinase-on [ON], or CW) and CheA-deactivating (kinase-off [OFF], or counterclockwise [CCW]) output states. Accordingly, a cell's overall kinase activity and stimulus sensitivity reflect the proportions of receptor signaling complexes in the ON and OFF states. The OFF state is assumed to have higher affinity for attractant ligands than the ON state. Thus, chemoattractants elicit CCW flagellar responses by driving receptor signaling complexes to the OFF state. According to this two-state view, mutant receptors that show enhanced serine sensitivity (i.e., lower $K_{1/2}$ values than the wild type) should have equilibrium shifts toward the OFF state (OFF biased). Conversely, mutant receptors with reduced serine sensitivity (i.e.,

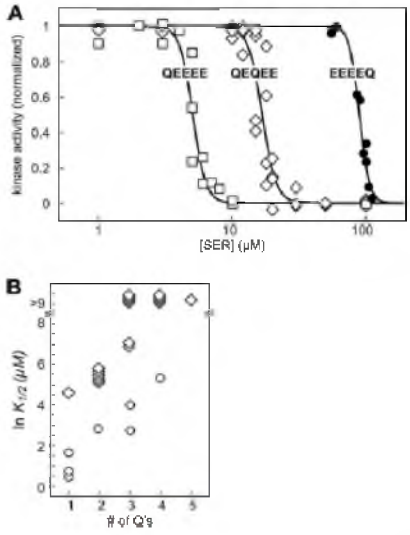

FIG 3 Dose-response behaviors of Tsr-Q/E variants. Plasmid pRR53 and pPA114 derivatives encoding Tsr variants with different combinations of E and Q residues at methylation sites 1 to 5 were tested for serine responses in strain UU2567 (R^- B^-) carrying the pRZ30 or pVS88 FRET reporter plasmid, respectively. (A) Hill fits for three Tsr-Q/E variants. Individual fits were done to aggregate data from several independent experiments (see Table S1 in the supplemental material) to illustrate the extent of variability in the FRET-derived data. $K_{1/2}$, Hill coefficient, and number of experiments were the following: Tsr-QEEEE (5.1 μM; 8.9; 2), Tsr-QEQEE (16.9 μM; 8.3; 4), and Tsr-EEEEQ (90 μM;11.7; 2). (B) Summary of average $K_{1/2}$ values for all Tsr-Q/E variants tested (see Table S1). ○, Tsr variants with E at site 5; ◇, Tsr variants with Q at site 5. Receptors with ln $K_{1/2}$ values of >9 showed no kinase inhibition response to a 10 mM serine stimulus.

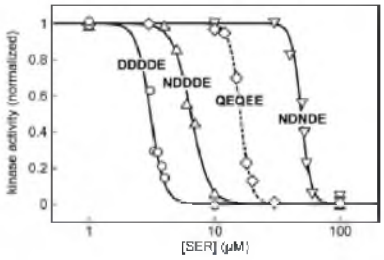

FIG 4 Dose-response behaviors of Tsr-N/D variants. Plasmid pRR53 derivatives encoding Tsr variants with different combinations of D and N residues at methylation sites 1 to 4 were tested for serine responses in strain UU2567 (R^- B^-) carrying the pRZ30 FRET reporter plasmid. Solid-line fits were to unaveraged data from one or more independent experiments (see Table S2 in the supplemental material). The fit for Tsr-wt (QEQEE; dashed line) was obtained by averaging data points from four independent experiments (Fig. 3A; also see Table S1). $K_{1/2}$ and Hill coefficient values in these experiments were the following: Tsr-DDDDE (3.1 μM; 7.9), Tsr-NDDDE (6.5 μM; 6.0), Tsr-NDNDE (50 μM; 11.3), and Tsr-QEQEE (16.2 μM; 10.2).

elevated $K_{1/2}$ values) should have equilibrium shifts toward the ON state (ON biased).

Signaling effects of adaptational modifications at E502. In the context of a two-state model, the sensory adaptation system shifts receptor signaling complexes to the ON or OFF state to cancel ligand-induced responses. CheR-mediated methylation at sites 1 to 4 favors the ON state; CheB-mediated demethylation or deamidation at sites 1 to 4 drives receptors toward the OFF state (1). To determine whether adaptational modifications at Tsr-E502 produce output effects similar to those at sites 1 to 4, we constructed a series of variant receptors with different combinations of E and Q residues at sites 1 to 5 and measured their serine thresholds and response cooperativities with *in vivo* FRET kinase assays. E residues represent the unmethylated state, whereas Q residues are closest in structure to glutamyl-methyl-esters and approximate the signaling effects of the methylated state (27). Mutant *tsr* plasmids were tested in a $CheR^-$ $CheB^-$ strain (UU2567) to preclude modification of the Q and E residues by the sensory adaptation system. The dose-response parameters are summarized in Table S1 in the supplemental material. Representative curves are shown in Fig. 3A, and the relationship between the number of Q sites and serine sensitivity is presented in Fig. 3B. These experiments showed, consistent with previous *in vivo* (24) and *in vitro* (27, 28) studies, that at sites 1 to 4 each Q residue progressively shifts Tsr to a higher serine threshold, i.e., toward the ON state. A glutamine at site 5 also elevated the serine response threshold, suggesting that methylation at E502 affects Tsr output in the same way as does methylation at sites 1 to 4 (Fig. 3B). However, a Q at site 5 produced a much larger threshold increase than did a single Q at any other site (Fig. 3B). For example, a single Q at site 1, 2, 3, or 4 produced $K_{1/2}$ values ranging from ~2 μM (EEEQE) to ~5 μM (QEEEE) (see Table S1), whereas the EEEEQ receptor had a $K_{1/2}$ value of ~100 μM (see Table S1), substantially higher than even that of wild-type Tsr (QEQEE; $K_{1/2}$, ~17 μM), which has glutamines at both sites 1 and 3 (Fig. 3). These results imply that methylation at E502 produces a much larger shift toward the ON state than does methylation at sites 1 to 4.

To determine whether Tsr methylation site 5 alone could support serine chemotaxis, we used combinations of D and N replacements at sites 1 to 4 to approximate the signaling properties of the wild-type E and Q residues at those positions. Aspartate and asparagine closely resemble glutamate and glutamine, respectively, except that their side chains are one methyl group shorter. Neither D nor N is an effective substrate for CheR and CheB modification reactions (see below). FRET kinase assays in the R^- B^- strain showed that Tsr variants with combinations of D and N residues at sites 1 to 4 had signaling properties similar to those of their E and Q counterparts (Fig. 4; also see Table S2 in the supplemental material). For example, Tsr-NDDDE (Fig. 4) and Tsr-QEEEE (Fig. 3A) had comparable serine sensitivities; Tsr-NDNDE and wild-type Tsr (QEQEE) had similar sensitivities (Fig. 4; also see Table S2). Despite these normal dose-response behaviors in FRET assays, all Tsr variants with combinations of D and N residues at sites 1 to 4 failed to support serine chemotaxis of an R^- B^- strain (UU2612) on tryptone or minimal serine soft-agar plates (see Table S2). These findings indicate that E502 alone cannot support full Tsr function in cells that contain the sensory adaptation enzymes. Either Tsr residue E502 cannot undergo reversible methylation-demethylation reactions or those modifications are not sufficient for tracking spatial serine gradients.

CheR-dependent methylation of Tsr-E502. CheR promotes methylation of Tsr residue E502 (8), but how extensive and reversible those modifications are *in vivo* remains an open issue. To look for *in vivo* methylation at site 5, we examined the SDS-PAGE band

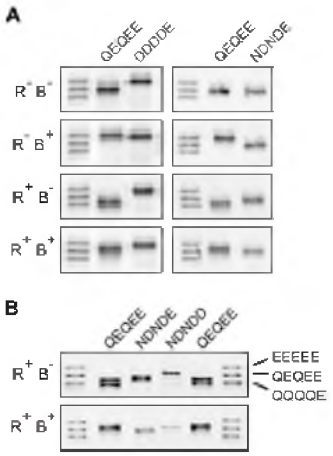

FIG 5 Methylation of Tsr residue E502. Panels show SDS-PAGE migration patterns of Tsr subunits (see Materials and Methods). Triplet bands are modification variant standards. Their ranking, from slowest to fastest, is the following: Tsr-EEEEE, Tsr-QEQEE (wild type), Tsr-QQQQE. (A) Band profiles of Tsr variants in host strains expressing different combinations of the CheR and CheB enzymes: R^-B^- (UU2610), R^-B^+ (UU2611), R^+B^- (UU2632), and R^+B^+ (UU2612). In Tsr-DDDDE and Tsr-NDNDE, only E502 is available for methylation, whereas in wild-type Tsr (QEQEE), multiple sites are available for deamidation, methylation, and demethylation. (B) CheR-dependent band shift of Tsr-NDNDE compared to Tsr-NDNDD.

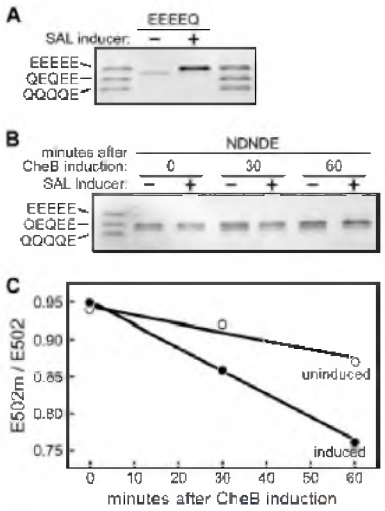

FIG 6 Deamidation and demethylation at Tsr residue 502. (A) SDS-PAGE profile of Tsr-EEEEQ subunits expressed from pRR53 in strain UU2611 (R^-B^+) carrying a salicylate (SAL)-inducible CheB expression plasmid (pPA827): −, no salicylate induction; +, 2 μM salicylate. (B) Demethylation time course of Tsr-NDNDE expressed from pRR53 in strain UU2612 (R^+B^+) carrying plasmid pPA827: −, no salicylate induction; +, 2 μM salicylate. Protein samples taken at 30-min intervals after addition of the CheB inducer were analyzed by SDS-PAGE. (C) Quantitation of demethylation time course shown in panel B. The relative intensities of methylated (E502m) and unmethylated (E502) Tsr subunits were determined by area integration of the corresponding gel bands using ImageJ software.

patterns of Tsr-DDDDE and Tsr-NDNDE molecules expressed in strains with different combinations of the CheR and CheB enzymes (Fig. 5). In hosts lacking CheR function (R^-B^-; R^-B^+), both receptors migrated as a single species, whereas in hosts containing CheR (R^+B^-; R^+B^+), Tsr-DDDDE and Tsr-NDNDE subunits migrated as two species, the faster of which was unique to the hosts that had CheR function (Fig. 5A). These results suggest that residue E502 in both receptors can undergo CheR-mediated methylation. To determine whether that CheR-dependent modification required a glutamate residue at site 5, we compared the band profiles of Tsr-NDNDE and Tsr-NDNDD in the R^+ hosts (Fig. 5B). The subunits bearing the E502D replacement exhibited only one band, demonstrating that an aspartate residue could not support the modification. These findings indicate, consistent with a prior study of Tar methylation sites (29), that D residues at any of the Tsr modification sites are poor substrates for CheR-mediated methylation. Moreover, it appears that an N residue, at least at Tsr sites 1 and 3, is refractory to deamidation by physiological levels of CheB (Fig. 5A). We conclude, consistent with the original study of Rice and Dahlquist (8), that Tsr-E502 is subject to CheR-mediated methylation *in vivo*.

CheB-dependent deamidation of Tsr-E502. A glutamine at Tsr methylation site 1 or 3 can undergo *in vivo* CheB-mediated deamidation to glutamate (30). To determine whether this is also the case for a glutamine at Tsr residue 502, we compared the signal outputs and SDS-PAGE profiles of Tsr-EEEEQ and Tsr-EEEEE receptors in various host strains. In an R^-B^- strain (UU2610), Tsr-EEEEQ produced more CW flagellar rotation than did Tsr-EEEEE (see Table S3 in the supplemental material), consistent with their different dose-response behaviors in FRET assays (Fig. 3A). If E502Q can be deamidated to glutamate by CheB, then the signal output of Tsr-EEEEQ in an R^-B^+ strain (UU2611) should approach that of Tsr-EEEEE. However, the flagellar rotation pattern produced by Tsr-EEEEQ showed no CheB-dependent change (see Table S3), suggesting that physiological levels of CheB cannot appreciably deamidate E502Q. In support of this conclusion, Tsr-EEEEQ subunits expressed in the R^-B^+ strain also showed no CheB-dependent bandshifts upon SDS-PAGE analysis (see Fig. S2A). However, high-level expression of CheB from an inducible plasmid shifted Tsr-EEEEQ to the EEEEE state (Fig. 6A), demonstrating that deamidation can occur at site 5, but less efficiently than it does at sites 1 to 4.

CheB-dependent demethylation at Tsr-E502. If CheB-dependent deamidation at E502Q occurs inefficiently, is CheB-mediated demethylation of methylated E502 (E502m) also inefficient? To answer this question, we expressed Tsr-NDNDE in an R^+B^- host (UU2612). At the mid-exponential growth phase, the culture was treated with chloramphenicol to stop further protein synthesis and cell samples were taken at 15-min intervals and analyzed by SDS-PAGE (see Fig. S2 in the supplemental material). Under these conditions, any band shifts that occur must be due to modifications at residue E502 (Fig. 5). At time zero, two Tsr bands were evident, corresponding to the unmethylated (NDNDE) and methylated (NDNDEm) forms of Tsr. With continued incubation in the absence of new protein synthesis, the unmethylated (NDNDE) form of Tsr became less prominent, indicating net conversion of Tsr to the methylated form (see Fig. S2). Thus, at physiological levels of CheR and CheB, methylation at residue E502 is evident but E502m demethylation is not.

As a more stringent test for whether E502m demethylation can occur, we expressed plasmid-encoded Tsr-NDNDE in an R^+ B^- strain (UU2612) that also carried a compatible, salicylate-inducible CheB expression plasmid (pPA827). At the mid-exponential growth stage, we induced CheB overexpression and monitored the Tsr modification state over a 60-min time course by SDS-PAGE (Fig. 6B). In this experiment, the methylated band (E502m) diminished over time and the unmethylated band (E502) increased in intensity (Fig. 6B). The ratio of the two band intensities (E502m:E502) decreased linearly over the 60-min time course in both the uninduced and induced cultures, but the rate of demethylation was faster in the induced culture (Fig. 6C). Thus, CheB-mediated demethylation occurs at site 5 but requires high levels of CheB to be detected. The demethylation efficiency of E502m is evidently lower than it is for other Tsr adaptation sites.

Signaling effects of amino acid replacements at E502. The E502I and E502P mutant receptors were the only ones in the Tsr-E502* set that could not support serine chemotaxis in tryptone soft-agar assays (Fig. 2). To explore the functional defect(s) caused by these particular amino acid replacements at E502, we examined the signaling properties of the mutant receptors with *in vivo* FRET kinase assays in host strains that had various combinations of the CheR and CheB adaptation enzymes (Fig. 7; also see Table S4 in the supplemental material). For comparison we also tested Tsr-E502Q, which mediated reduced-sensitivity serine chemotaxis in an adaptation-proficient host (Fig. 2). In an R^- B^- strain (UU2567) lacking both adaptation enzymes, Tsr-wt (QEQEE) produced a sensitive, highly cooperative response to serine ($K_{1/2}$, ~17 μM; Hill coefficient, ~15), whereas the E502I, E502P, and E502Q receptors failed to respond even to 10 mM serine (Fig. 7; also see Table S4). In an R^- B^+ strain (UU2700) containing both adaptation enzymes, Tsr-wt showed more sensitive but less cooperative signaling behavior ($K_{1/2}$, ~0.4 μM; Hill coefficient, ~2.4). All three mutant receptors also showed serine responses in the adaptation-proficient host, implying that they can undergo CheR and/or CheB modifications that improve their signaling properties. In that background, Tsr-E502Q ($K_{1/2}$, ~8.6 μM) was somewhat less sensitive than Tsr-wt, consistent with its higher serine threshold in plate assays (Fig. 2) and an ON-biased signaling change. E502I was much less sensitive and more cooperative ($K_{1/2}$, ~133 μM; Hill coefficient, ~5.4), whereas E502P showed nearly wild-type sensitivity and cooperativity (Fig. 7; also see Table S4).

To determine the nature of the output shifts caused by the E502I and E502P lesions, we examined their signaling responses in hosts containing only one of the two adaptation enzymes. CheR-mediated methylation should shift Tsr output to the ON state, thereby reducing response sensitivity to serine, whereas CheB-mediated deamidation and demethylation should shift output toward the OFF state to enhance serine sensitivity (Fig. 3). Indeed, Tsr-wt had an elevated serine threshold in an R^- B^- strain (UU2697) and failed to respond in an R^- B^+ strain (UU2699) (Fig. 7; also see Table S4 in the supplemental material), which probably deamidated the wild-type receptor molecules to the unresponsive EEEEE state (see Table S1). Tsr-E502I produced a serine response in the R^- B^+ strain but not in the R^+ B^- strain, consistent with an intrinsic ON-biased output (Fig. 7; also see Table S4). In contrast, CheR function alone restored E502P responsiveness whereas CheB did not, suggesting that Tsr-E502P has an intrinsic OFF-biased output (Fig. 7; also see Table S4).

These tests also revealed some unexpected dose-response behaviors. (i) The E502Q receptor became more sensitive to serine in both the R^+ B^- and R^- B^+ strains. (ii) The E502Q and E502I receptors were most sensitive to serine in the host with both adaptation enzymes (Fig. 7; also see Table S4 in the supplemental material). (iii) The E502P receptor was more sensitive in the R^+ B^- host than it was in the R^+ B^+ host. We interpret these paradoxical behaviors as evidence of a direct influence of the CheR protein on receptor signaling complexes (31). Whereas CheB can enhance receptor sensitivity through its enzymatic activities (23, 31), CheR might promote attractant responses by preferentially binding to receptors in the OFF signaling state (31). This model predicts that the catalytic activity of CheR plays no role in shifting receptors to the OFF state and may even compete with that signaling effect. Experiments that test these ideas will be the subject of a follow-up study.

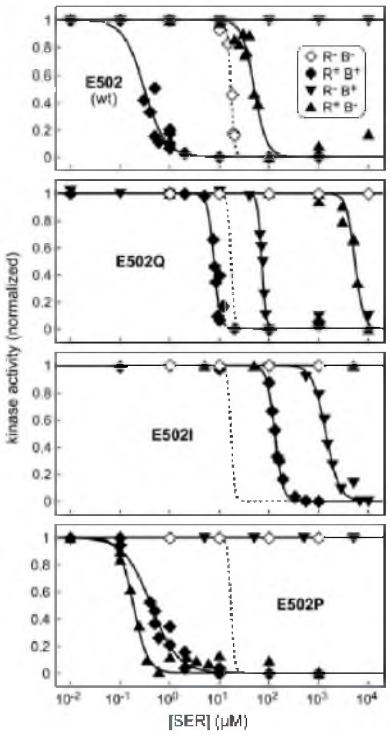

FIG 7 Dose-response behaviors of Tsr-E502Q, Tsr-E502I, and Tsr-E502P. Plasmid pPA114 derivatives encoding Tsr-E502 mutant proteins were tested for serine responses in four different hosts carrying the pVS88 FRET reporter plasmid: UU2567 (R^- B^-, ◇), UU2700 (R^+ B^+, ◆), UU2697 (R^+ B^-, ▲), and UU2699 (R^- B^+, ▼). Note that the UU2697 and UU2699 data can be less precise because subsaturating stimuli may elicit Tsr modification state changes (methylation in UU2697; deamidation in UU2699) that affect subsequent responses. Solid lines indicate Hill fits to data from one or more independent experiments (see Table S4 in the supplemental material). Dashed lines indicate the Hill fit to Tsr-wt (QEQEE) data averaged from two independent experiments (see Table S4).

DISCUSSION

HAMP signaling models. HAMP domains mediate input-output transactions in many bacterial signaling proteins. Two types of

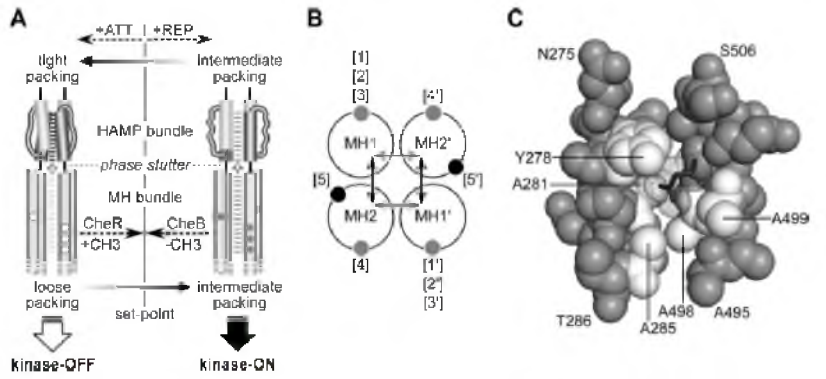

FIG 8 Mechanistic interpretation of Tsr-E502 signaling effects. (A) Dynamic bundle model of HAMP domain signal control in Tsr (33). The phase stutter connection at the HAMP-MH bundle junction is proposed to produce an oppositional stability relationship between packing of the HAMP and MH bundles. Open arrows between the bundles indicate the direction of structure-destabilizing forces. Tight packing of HAMP (horizontal black lines) destabilizes MH bundle packing (light gray lines), leading (by an unspecified mechanism) to deactivation of CheA. A second kinase-OFF state (not shown because it did not arise in the experiments of this study) results when MH packing is tight and HAMP packing is loose (9). CheA activation occurs (by an unspecified mechanism) when the MH and HAMP bundles have intermediate packing stabilities (dark gray lines). Attractants and repellents produce stimulus responses by acting on HAMP stability; subsequent methylation (sites 1 to 4, gray; site 5, black) and demethylation (sites 1 to 5, white) changes produce sensory adaptation by shifting the packing stability of the MH bundle to counterbalance HAMP input effects, driving the system back to an intermediate set-point stability. (B) Proposed structure-stabilizing effects of receptor methylation. The four helices of the MH bundle are shown in cross-section, as viewed from the membrane toward the cytoplasmic tip. Adaptation sites 1 to 4 (gray) probably modulate MH bundle stability by influencing intersubunit interactions (gray arrows); site 5 (black) probably modulates MH bundle stability by influencing intrasubunit interactions (black arrows). Unmethylated, negatively charged E residues should lower MH bundle stability; methylation (or uncharged amino acid replacements, such as Q) should stabilize MH bundle packing interactions. (C) Local structural environment of Tsr-E502. Segments of the MH1 (N275-T286) and MH2 (A495-S506) helices from one subunit of the Tsr dimer are shown. All C, N, and O atoms are shown as spheres, except for E502, whose main-chain atoms are not shown and whose side chain is shown as black sticks and space-filling dots. Hydrophobic amino acids whose side chains are within 5 Å of E502 side chain atoms are shown in white; other residues are gray. The Y278 label line points to the oxygen atom of the side chain hydroxyl group on the aromatic ring. Label lines for A281, A285, A498, and A499 point to the carbon atom of their side chain methyl group.

mechanistic models have been proposed for HAMP signaling. Two-state mechanisms, such as the gearbox model (32), postulate discrete, alternative HAMP conformations that elicit different output signals, for example, low versus high kinase activity. The proposed gearbox signaling states correspond to different packing arrangements of the four-helix HAMP bundle. In contrast, the dynamic bundle model proposes that overall HAMP packing stability, defined by ensembles of isoenergetic conformations, controls output activity (33).

HAMP function has been most intensively investigated in sensor histidine kinases and in MCP-family chemoreceptors. In the chemoreceptor models, a sensory adaptation system modulates HAMP operation, allowing for experimental manipulation of the structural interplay between HAMP and adjoining methylation sites. This study focused on Tsr-E502, a methylation site seemingly unique to the serine chemoreceptor of *E. coli*. Amino acid replacements at this Tsr residue produced a variety of mutant signaling behaviors that are most readily explained by the dynamic bundle model of HAMP output control (33).

Structural interplay of the HAMP and MH bundles. The dynamic bundle model proposes that a four-residue phase stutter segment between the AS2 and MH1 helices couples the structural stabilities of the HAMP and MH bundles in opposition (Fig. 8A). Thus, optimal packing of the helices in the HAMP bundle forces the adjoining methylation site helices away from their optimal packing arrangement in the MH bundle, leading to kinase-off output. Conversely, tighter packing of the MH bundle destabilizes the HAMP bundle and produces kinase-on output. This model predicts that chemoeffector stimuli elicit signaling responses by influencing HAMP stability and that the sensory adaptation system terminates those responses by adjusting the opposed packing stability of the MH bundle: methylation enhances stability; demethylation and deamidation reduce stability.

Extensive studies of methylation sites 1 to 4 in the aspartate receptor Tar, which are structurally analogous to Tsr sites 1 to 4, suggest that adaptational modifications regulate receptor output by controlling the packing stability of the four-helix methylation bundle (6, 7, 34). Unmethylated adaptation sites that contain negatively charged glutamic acid (E) residues could destabilize the MH bundle through localized electrostatic effects on helix structure and coiled-coil packing interactions. Methylation of E residues forms glutamyl methyl-esters (Em), which are uncharged and should enhance MH packing. Indeed, mutational replacement of a methyl-accepting E site with a variety of uncharged amino acids can mimic the signaling effects of methylation (Fig. 4; also see Tables S2 and S3 in the supplemental material) (35–37). Glutamine (Q), which is closest in structure to a glutamyl methyl-ester, is the best methylation mimic, but it is less effective than methylation in its signaling effects (24).

Tsr methylation sites 1 to 4 lie at the subunit interface in receptor dimers (Fig. 1B and 8B) and should influence MH bundle stability most directly by modulating the strength of intersubunit packing interactions. In contrast, Tsr-E502 lies close to the interface between N and C helices from the same subunit of the receptor dimer. Accordingly, we suggest that Tsr site 5 influences over-

all MH bundle stability by modulating the strength of intrasubunit packing interactions (Fig. 8B).

Signaling consequences of adaptational modifications at Tsr-E502. Tsr-E502 undergoes CheR-mediated methylation (Fig. 5) (8) and, less efficiently, CheB-dependent demethylation (Fig. 6B and C). Using Q residues as a proxy for methylated E sites in hosts lacking CheR function, we found that Tsr-EEEEQ receptors produced high levels of CW rotation, whereas Tsr-EEEEE did not (see Table S3 in the supplemental material). Moreover, Tsr-EEEEE did not generate enough kinase activity to detect a signaling response to serine, whereas Tsr-EEEEQ responded well but with a substantially higher threshold than wild-type (QEQEE) Tsr (see Table S1). Other single-Q Tsr variants (e.g., QEEEE) detected serine with thresholds lower than that of wild-type Tsr (see Table S1).

Although a Q at residue 502 shifts Tsr output toward the kinase-on state, as do Q residues at Tsr adaptation sites 1 to 4, the E502Q receptor exhibited a very large increase in serine detection threshold (see Table S1 in the supplemental material). We ascribe the signaling potency of Tsr-E502 to two structural factors: (i) the unique ability of this modification site to modulate intrasubunit, rather than intersubunit, packing stability of the MH bundle (Fig. 8B) and (ii) the close proximity of Tsr site 5 to the AS2 output helices of HAMP (Fig. 8A). Although Tsr-E502 does not have a direct covalent connection to the AS2 helix, the dynamic bundle model predicts that methylation at site 5 exerts a strong destabilizing effect on the HAMP bundle through its stabilizing effects on MH bundle packing. Conceivably, the intensity of the structural clash between the HAMP and MH bundles declines with distance from the phase stutter connection.

Signaling consequences of amino acid replacements at Tsr-E502. The wild-type E502 residue of Tsr is likely to have a destabilizing effect on local MH bundle packing near the HAMP junction (Fig. 8C). In the modeled bundle structure, extrapolated from the X-ray structure of the Tsr hairpin tip (38), the negatively charged side chain of E502 resides in a moderately hydrophobic cavity lined with alanine residues from both the C and N helices in each subunit. In addition, Y278 from the N helix caps the cavity (Fig. 8C). Although the polar E502 carboxyl group might H-bond to the tyrosine hydroxyl group, this interaction alone is unlikely to stabilize the E side chain in the cavity. We suggest that E502 is a good substrate for CheR-mediated methylation because its acidic side chain adopts a less buried, more exposed location. Additionally, looser packing of the MH helices in the vicinity of E502 might promote CheR recognition and docking.

Neutralization of the E502 carboxyl group through CheR-mediated methylation should enhance intrasubunit packing forces and make the Em side chain less solvent accessible. A more buried side chain would explain why receptors methylated at E502 are not readily demethylated by CheB (Fig. 6B and C). Similar reasoning applies to Tsr-E502Q, which is a poor substrate for CheB-mediated deamidation (Fig. 6A; also see Fig. S2 in the supplemental material). In the context of the dynamic bundle model, tighter packing of the MH bundle would also make it more difficult for serine binding to drive HAMP to its stable, kinase-off signaling state (Fig. 8A), thereby accounting for the high response threshold of the Tsr-E502Q receptor (Fig. 7).

Only two amino acid replacements at E502 fully abrogated Tsr function. Tsr-E502P exhibited signaling properties consistent with a large shift to the kinase-off output state. CheR function (i.e., conversion of E to Em) shifted the mutant receptors to a serine-responsive condition, whereas CheB function alone did not (Fig. 7). In contrast, Tsr-E502I exhibited signaling properties characteristic of a large shift to the kinase-on output state. CheB function (i.e., conversion of Q to E) shifted Tsr-E502I to a responsive range, whereas CheR function alone did not (Fig. 7).

The signaling behavior of Tsr-E502P probably reflects local destabilization of the proline-containing helix and a consequent drop in MH bundle packing stability comparable to that of an unmethylated receptor, which generates little kinase activity (e.g., Tsr-EEEEE; see Tables S1 and S3 in the supplemental material). An isoleucine side chain at residue 502 might instead prefer the hydrophobic environment of the 502 cavity, thereby enhancing intrasubunit and MH bundle packing interactions, perhaps approximating the structural stability of highly modified receptors (e.g., Tsr-QQQQQ) whose kinase activity cannot be downregulated (see Tables S1 and S3).

Structural insights from SDS-PAGE bandshifts. Every amino acid replacement at residue E502 shifted Tsr subunit mobility in denaturing gel electrophoresis (Fig. 2; also see Fig. S1 in the supplemental material). Perhaps receptor subunits retain some native secondary and tertiary structures in the presence of SDS. If so, then interactions between those structural elements could influence gel migration rates. For example, pairing interactions between the N and C helices that are subject to E502 control in native Tsr might accelerate subunit migration, whereas extended, noninteracting helices might cause slower gel mobility. This interpretation is consistent with the proposed structural consequences of amino acid replacements at E502: P (and the wild-type E) most likely reduce intrasubunit and MH bundle packing interactions, whereas Q and I probably enhance those interactions. E502P subunits had the slowest SDS-PAGE mobility, while E502I had the fastest (Fig. 2; also see Fig. S1). Conceivably, the relative mobilities of other mutant subunits reflect similar structural and signaling changes.

Chemotactic signaling role of Tsr-E502. The fifth methylation site of Tsr is not critical for chemotaxis, because most mutant receptors with an E502 amino acid replacement mediated normal chemotactic behavior on tryptone soft agar (Fig. 2). A few changes (K, Q, G, D, and M) caused demonstrably reduced detection sensitivity, but even so, the remaining sensory adaption sites compensated effectively for the on-shifted outputs of these mutant receptors.

Tsr residue E502 also is not sufficient for chemotaxis. It failed to support Tsr function when adaptation sites 1 to 4 were rendered nonfunctional. The disparity in CheR and CheB modification rates at site 5 probably contributes to this functional deficit. CheR-mediated methylation occurs more readily at E502 than does CheB-mediated deamidation or demethylation. Considering the small number of CheB molecules that operate in a normal receptor array (39), methylation at E502 might be effectively irreversible. Perhaps methylation of Tsr-E502 is an adaptational modification of last resort that only comes into play at very high serine levels. Perhaps other *E. coli* MCPs lack a corresponding adaptation site, because the cells seldom encounter, or prefer to ignore, high levels of their cognate ligands.

In summary, our study of Tsr-E502 has provided new insights into how the structural interplay between HAMP and adjoining sensory adaptation elements controls the signaling behavior of a chemoreceptor.

ACKNOWLEDGMENTS

This work was supported by research grant GM19559 from the National Institute of General Medical Sciences.

We thank Germán Piñas (University of Utah) and Runzhi Lai (University of Utah) for comments on the manuscript, Sung-Hou Kim (UC-Berkeley) for Tsr atomic coordinates, and Victor Sourjik (U. Heidelberg) for plasmid pVS88 and for advice on setting up the FRET kinase assay.

The Protein-DNA Core Facility at the University of Utah receives support from National Cancer Institute grant CA42014 to the Huntsman Cancer Institute.

REFERENCES

1. **Hazelbauer GL, Falke JJ, Parkinson JS.** 2008. Bacterial chemoreceptors: high-performance signaling in networked arrays. Trends Biochem. Sci. 33:9–19. http://dx.doi.org/10.1016/j.tibs.2007.09.014.
2. **Sourjik V, Armitage JP.** 2010. Spatial organization in bacterial chemotaxis. EMBO J. 29:2724–2733. http://dx.doi.org/10.1038/emboj.2010.178.
3. **Porter SL, Wadhams GH, Armitage JP.** 2011. Signal processing in complex chemotaxis pathways. Nat. Rev. Microbiol. 9:153–165. http://dx.doi.org/10.1038/nrmicro2505.
4. **Terwilliger TC, Wang JY, Koshland DE, Jr.** 1986. Surface structure recognized for covalent modification of the aspartate receptor in chemotaxis. Proc. Natl. Acad. Sci. U. S. A. 83:6707–6710. http://dx.doi.org/10.1073/pnas.83.18.6707.
5. **Nowlin DM, Bollinger J, Hazelbauer GL.** 1987. Sites of covalent modification in Trg, a sensory transducer of Escherichia coli. J. Biol. Chem. 262:6039–6045.
6. **Starrett DJ, Falke JJ.** 2005. Adaptation mechanism of the aspartate receptor: electrostatics of the adaptation subdomain play a key role in modulating kinase activity. Biochemistry 44:1550–1560. http://dx.doi.org/10.1021/bi048089z.
7. **Winston SE, Mehan R, Falke JJ.** 2005. Evidence that the adaptation region of the aspartate receptor is a dynamic four-helix bundle: cysteine and disulfide scanning studies. Biochemistry 44:12655–12666. http://dx.doi.org/10.1021/bi0507884.
8. **Rice MS, Dahlquist FW.** 1991. Sites of deamidation and methylation in Tsr, a bacterial chemotaxis sensory transducer. J. Biol. Chem. 266:9746–9753.
9. **Parkinson JS.** 2010. Signaling mechanisms of HAMP domains in chemoreceptors and sensor kinases. Annu. Rev. Microbiol. 64:101–122. http://dx.doi.org/10.1146/annurev.micro.112408.134215.
10. **Parkinson JS, Houts SE.** 1982. Isolation and behavior of *Escherichia coli* deletion mutants lacking chemotaxis functions. J. Bacteriol. 151:106–113.
11. **Ames P, Studdert CA, Reiser RH, Parkinson JS.** 2002. Collaborative signaling by mixed chemoreceptor teams in *Escherichia coli*. Proc. Natl. Acad. Sci. U. S. A. 99:7060–7065. http://dx.doi.org/10.1073/pnas.092071899.
12. **Zhou Q, Ames P, Parkinson JS.** 2011. Biphasic control logic of HAMP domain signalling in the *Escherichia coli* serine chemoreceptor. Mol. Microbiol. 80:596–611. http://dx.doi.org/10.1111/j.1365-2958.2011.07577.x.
13. **Chang ACY, Cohen SN.** 1978. Construction and characterization of amplifiable multicopy DNA cloning vehicles derived from the p15A cryptic miniplasmid. J. Bacteriol. 134:1141–1156.
14. **Gosink KK, Buron-Barral M, Parkinson JS.** 2006. Signaling interactions between the aerotaxis transducer Aer and heterologous chemoreceptors in *Escherichia coli*. J. Bacteriol. 188:3487–3493. http://dx.doi.org/10.1128/JB.188.10.3487-3493.2006.
15. **Bolivar F, Rodriguez R, Greene PJ, Betlach MC, Heyneker HL, Boyer HW.** 1977. Construction and characterization of new cloning vehicles. Gene 2:95–113. http://dx.doi.org/10.1016/0378-1119(77)90000-2.
16. **Studdert CA, Parkinson JS.** 2005. Insights into the organization and dynamics of bacterial chemoreceptor clusters through *in vivo* crosslinking studies. Proc. Natl. Acad. Sci. U. S. A. 102:15623–15628. http://dx.doi.org/10.1073/pnas.0506040102.
17. **Sourjik V, Vaknin A, Shimizu TS, Berg HC.** 2007. In vivo measurement by FRET of pathway activity in bacterial chemotaxis. Methods Enzymol. 423:363–391. http://dx.doi.org/10.1016/S0076-6879(07)23017-4.
18. **Parkinson JS.** 1976. *cheA*, *cheB*, and *cheC* genes of *Escherichia coli* and their role in chemotaxis. J. Bacteriol. 126:758–770.
19. **Laemmli UK.** 1970. Cleavage of structural proteins during assembly of the head of bacteriophage T4. Nature 227:680–685. http://dx.doi.org/10.1038/227680a0.
20. **Ames P, Parkinson JS.** 1994. Constitutively signaling fragments of Tsr, the *Escherichia coli* serine chemoreceptor. J. Bacteriol. 176:6340–6348.
21. **Slocum MK, Parkinson JS.** 1985. Genetics of methyl-accepting chemotaxis proteins in *Escherichia coli*: null phenotypes of the *tar* and *tap* genes. J. Bacteriol. 163:586–594.
22. **Berg HC, Block SM.** 1984. A miniature flow cell designed for rapid exchange of media under high-power microscope objectives. J. Gen. Microbiol. 130:2915–2920.
23. **Sourjik V, Berg HC.** 2002. Receptor sensitivity in bacterial chemotaxis. Proc. Natl. Acad. Sci. U. S. A. 99:123–127. http://dx.doi.org/10.1073/pnas.011589998.
24. **Shimizu TS, Tu Y, Berg HC.** 2010. A modular gradient-sensing network for chemotaxis in Escherichia coli revealed by responses to time-varying stimuli. Mol. Syst. Biol. 6:382.
25. **Sourjik V, Berg HC.** 2004. Functional interactions between receptors in bacterial chemotaxis. Nature 428:437–441. http://dx.doi.org/10.1038/nature02406.
26. **BD.** 2006. Bionutrients technical manual, 3rd ed, revised. BD, Franklin Lakes, NJ.
27. **Bornhorst JA, Falke JJ.** 2001. Evidence that both ligand binding and covalent adaptation drive a two-state equilibrium in the aspartate receptor signaling complex. J. Gen. Physiol. 118:693–710. http://dx.doi.org/10.1085/jgp.118.6.693.
28. **Li G, Weis RM.** 2000. Covalent modification regulates ligand binding to receptor complexes in the chemosensory system of *Escherichia coli*. Cell 100:357–365. http://dx.doi.org/10.1016/S0092-8674(00)80671-6.
29. **Shapiro MJ, Koshland DE, Jr.** 1994. Mutagenic studies of the interaction between the aspartate receptor and methyltransferase from *Escherichia coli*. J. Biol. Chem. 269:11054–11059.
30. **Kehry MR, Bond MW, Hunkapiller MW, Dahlquist FW.** 1983. Enzymatic deamidation of methyl-accepting chemotaxis proteins in *Escherichia coli* catalyzed by the *cheB* gene product. Proc. Natl. Acad. Sci. U. S. A. 80:3599–3603. http://dx.doi.org/10.1073/pnas.80.12.3599.
31. **Kim C, Jackson M, Lux R, Khan S.** 2001. Determinants of chemotactic signal amplification in *Escherichia coli*. J. Mol. Biol. 307:119–135. http://dx.doi.org/10.1006/jmbi.2000.4389.
32. **Hulko M, Berndt F, Gruber M, Linder JU, Truffault V, Schultz A, Martin J, Schultz JE, Lupas AN, Coles M.** 2006. The HAMP domain structure implies helix rotation in transmembrane signaling. Cell 126:929–940. http://dx.doi.org/10.1016/j.cell.2006.06.058.
33. **Zhou Q, Ames P, Parkinson JS.** 2009. Mutational analyses of HAMP helices suggest a dynamic bundle model of input-output signalling in chemoreceptors. Mol. Microbiol. 73:801–814. http://dx.doi.org/10.1111/j.1365-2958.2009.06819.x.
34. **Swain KE, Gonzalez MA, Falke JJ.** 2009. Engineered socket study of signaling through a four-helix bundle: evidence for a yin-yang mechanism in the kinase control module of the aspartate receptor. Biochemistry 48:9266–9277. http://dx.doi.org/10.1021/bi901020d.
35. **Shapiro MJ, Chakrabarti I, Koshland DE, Jr.** 1995. Contributions made by individual methylation sites of the *Escherichia coli* aspartate receptor to chemotactic behavior. Proc. Natl. Acad. Sci. U. S. A. 92:1053–1056. http://dx.doi.org/10.1073/pnas.92.4.1053.
36. **Nowlin DM, Bollinger J, Hazelbauer GL.** 1988. Site-directed mutations altering methyl-accepting residues of a sensory transducer protein. Proteins 3:102–112. http://dx.doi.org/10.1002/prot.340030205.
37. **Nishiyama S, Nara T, Homma M, Imae Y, Kawagishi I.** 1997. Thermosensing properties of mutant aspartate chemoreceptors with methyl-accepting sites replaced singly or multiply by alanine. J. Bacteriol. 179:6573–6580.
38. **Kim KK, Yokota H, Kim SH.** 1999. Four-helical-bundle structure of the cytoplasmic domain of a serine chemotaxis receptor. Nature 400:787–792. http://dx.doi.org/10.1038/23512.
39. **Li M, Hazelbauer GL.** 2004. Cellular stoichiometry of the components of the chemotaxis signaling complex. J. Bacteriol. 186:3687–3694. http://dx.doi.org/10.1128/JB.186.12.3687-3694.2004.

Table S1. Serine dose-response parameters for Tsr-Q/E variants in strain UU2567.

# Q's	modification site residues	receptor & FRET reporter plasmids	$K_{1/2}$ (μM) [a]	Hill coefficient [a]	number of experiments
E at fifth site:					
0	E E E E E	pRR53 & pRZ30	NR	NR	5
1	E E Q E E	pRR53 & pRZ30	2.2 ± 0.5	5.5 ± 1.0	5
1	E E E Q E	pRR53 & pRZ30	1.9 ± 0.7	3.7 ± 0.3	3
1	Q E E E E	pRR53 & pRZ30	5.3 ± 0.4	27 ± 3.7	3
2 (wt)	**Q E Q E E**	**pRR53 & pRZ30**	**17 ± 1.2**	**18 ± 5.0**	**4**
2 (wt)	**Q E Q E E**	**pPA114 & pVS88**	**17 ± 1.1**	**15 ± 7.5**	**2**
3	Q E Q Q E	pRR53 & pRZ30	15 ± 2.4	16 ± 6.7	3
3	Q Q Q E E	pRR53 & pRZ30	53 ± 1.5	14 ± 3.5	2
4	Q Q Q Q E	pRR53 & pRZ30	203 ± 7.0	8.5 ± 2.5	2
Q at fifth site:					
1	E E E E Q	pRR53 & pRZ30	104 ± 14	8.0 ± 4.0	2
2	E E E Q Q	pRR53 & pRZ30	202	7	1
2	E E E Q Q	pPA114 & pVS88	232 ± 52	14 ± 4.0	2
2	E Q E E Q	pPA114 & pVS88	216	16.0	1
2	Q E E E Q	pPA114 & pVS88	235	7.2	1
2	E E Q E Q	pPA114 & pVS88	284	16	1
3	E Q Q E Q	pPA114 & pVS88	1030	16	1
3	E E Q Q Q	pPA114 & pVS88	1138 ± 180	7.0 ± 1.0	2
3	E Q E Q Q	pPA114 & pVS88	NR	NR	1
3	Q E Q E Q	pPA114 & pVS88	NR	NR	1
3	Q Q E E Q	pPA114 & pVS88	NR	NR	1
3	Q E E Q Q	pPA114 & pVS88	NR	NR	1
4	E Q Q Q Q	pPA114 & pVS88	NR	NR	1
4	Q Q Q E Q	pPA114 & pVS88	NR	NR	1
4	Q E Q Q Q	pPA114 & pVS88	NR	NR	1
4	Q Q E Q Q	pPA114 & pVS88	NR	NR	1
5	Q Q Q Q Q	pRR53 & pRZ30	NR	NR	7

[a] For multiple experiments, means and standard errors were determined from the best-fit parameter values for each independent experiment. NR: no response to 10 mM serine.

Table S2. Serine dose-response parameters for Tsr-N/D variants in strain UU2567.

modification site residues	$K_{1/2}$ (μM) [a]	Hill coefficient [a]	number of experiments
D D D D E	3.5 ± 0.4	6.4 ± 1.5	2
N D D D E	6.5	6.0	1
D N D D E	5.2 ± 0.5	14 ± 1.9	2
N D N D E	43 ± 7.1	8.9 ± 2.3	2
N D N D D	NR	NR	4

Tsr variants were expressed from plasmid pRR53 derivatives in strain UU2567 containing the pRZ30 FRET reporter plasmid.

[a] For multiple experiments, means and standard errors were determined from the best-fit parameter values for each independent experiment. NR: no response to 10 mM serine.

Table S3. Flagellar rotation patterns produced by Tsr-Q/E and Tsr-N/D variants.

modification site residues [a]		%CW rotation time in UU2610	%CW rotation time in UU2611	%CW rotation time in UU2632	%CW rotation time in UU2612
E E E E E		18 ± 3 [2]	20 ± 0.5 [2]	nd	28
E E E E Q		72 ± 10 [2]	65 ± 5 [2]	nd	nd
Q Q Q Q E		61 ± 3 [3]	58 ± 8 [3]	57 ± 8 [3]	52 ± 16 [2]
Q Q Q Q Q		62 ± 3 [4]	61 ± 2 [2]	68 ± 13 [2]	87 ± 8 [2]
Q E Q E E	**(wt)**	**68 ± 3 [5]**	**40 ± 9 [3]**	**70**	**25 ± 2 [3]**
D D D D E		70 ± 10 [2]	65	48 ± 9 [3]	32
N D D D E		69	61	48	46
D N D D E		63	66	47	70
N D N D E		59 ± 9 [3]	77	31 ± 8 [3]	77
N D N D D		62	48	48	49

[a] Derivatives of plasmid pRR53 were transferred to rotation host strains; induction with 50 μM IPTG.

Table S4. Serine dose-response parameters for Tsr-E502Q, Tsr-E502I, and Tsr-E502P.

Tsr mutant [a]	FRET host strain [b]	$K_{1/2}$ (μM) [c]	Hill coefficient [c]	number of experiments
wild-type				
	UU2567	17 ± 1.1	15 ± 7.5	2
	UU2699	NR	NR	1
	UU2697	49 ± 6.6	8.5 ± 4.8	3
	UU2700	0.4 ± 0.1	2.4 ± 0.2	2
E502Q				
	UU2567	NR	NR	2
	UU2699	73	10	1
	UU2697	5243 ± 100	13 ± 9.3	2
	UU2700	8.6 ± 0.75	9.2 ± 2.8	2
E502I				
	UU2567	NR	NR	5
	UU2699	1424	3	1
	UU2697	NR	NR	2
	UU2700	133	5.4	1
E502P				
	UU2567	NR	NR	5
	UU2699	NR	NR	2
	UU2697	0.2	3.0	1
	UU2700	0.5 ± 0.1	1.6 ± 0.05	2

[a] Derivatives of plasmid pPA114 were transferred to FRET host strains; induction with 0.6 pM sodium salicylate.

[b] Strains also carried the FRET reporter pVS88; induction with 50 μM IPTG.

[c] For multiple experiments, means and standard errors were determined from the best-fit parameter values for each independent experiment. NR: no response to 10 mM serine.

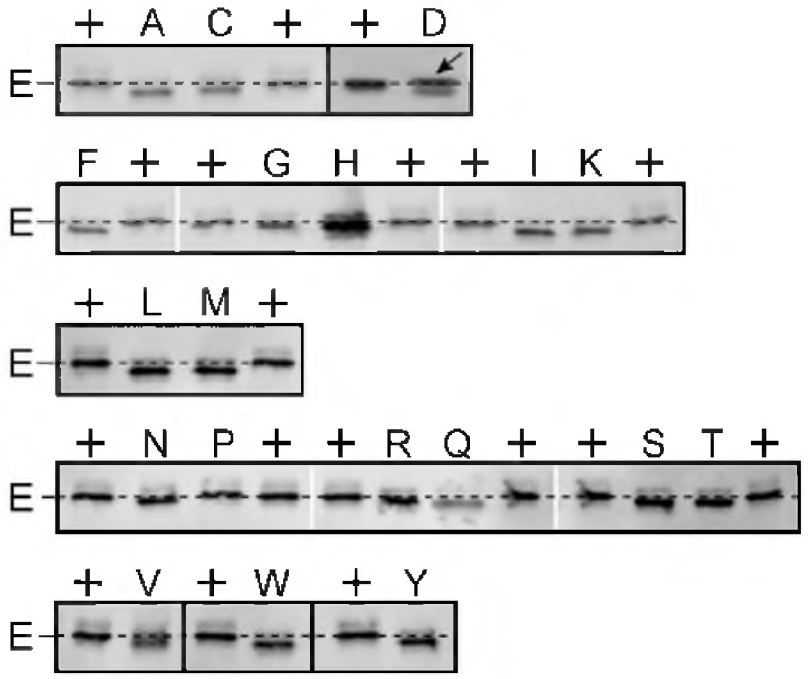

Fig. S1. Mobility of Tsr-E502* proteins in SDS-PAGE

Plasmid pPA114 Tsr-E502* derivatives were expressed in host strain UU2610, as detailed in Methods. Cell extracts were subjected to electrophoresis in denaturing 11% polyacrylamide gels and Tsr bands were visualized by immunoblotting. Lanes labeled + contain wild-type Tsr; letters above lanes indicate Tsr-E502 amino acid replacement proteins. Dashed horizontal lines indicate the positions of the wild-type bands (E) in each gel segment. Segments from the same gel that were individually adjusted to align the wild-type markers are separated by white vertical lines. Note that the wild-type lanes immediately adjacent to the white separators are the same. Individually ajusted segments of different gels or noncontiguous segments of the same gel are separated by a black vertical line. Samples of the Tsr-E502D protein contained variable amounts of a Tsr proteolysis product just below the uncleaved upper band (indicated with an arrow).

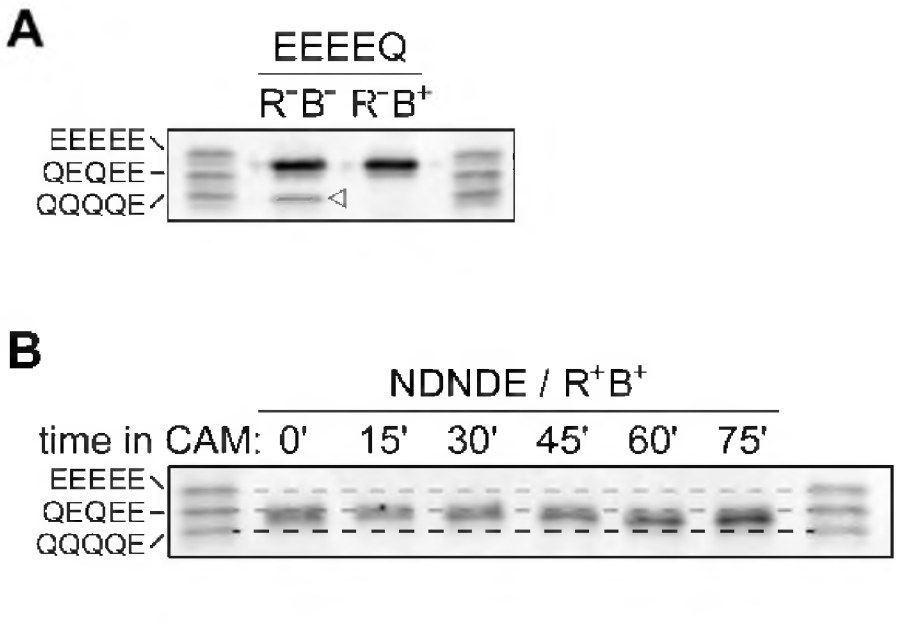

Fig. S2. Inefficient deamidation and demethylation at Tsr adaptation site 5 under physiological conditions.

A. Comparison of SDS-PAGE band profiles of Tsr-EEEEQ subunits produced in strain UU2610 (R^- B^-) and in strain UU2611 (R^- B^+). The minor band indicated with an open triangle is a Tsr proteolytic product that arises in some cell extracts.

B. Timecourse of methylation at Tsr-E502. Tsr-NDNDE was expressed in strain UU2612 (R^+ B^+). At time zero, chloramphenicol (CAM) was added to the culture to block further protein synthesis and samples were removed at the indicated times for SDS-PAGE analysis.

CHAPTER 3

SIGNALING ROLES OF TWO ADAPTATION SITES Q311 AND E502 IN THE SERINE CHEMORECEPTOR

Abstract

Tsr, the serine chemoreceptor of *Escherichia coli,* has five methylation sites per subunit, denoted as QEQEE. I studied the signaling roles of two adaptation sites: Q311 and E502. The Q311 site had been shown to be the most readily-modified site. Moreover, Q311 is located farthest from the HAMP domain but closest to the kinase control domain and therefore might have the most potent effect receptor-coupled CheA kinase activity. To test this working hypothesis, I constructed a series of mutant receptors with single amino acid replacements at Q311 and tested their modification by adaptation enzymes. I also tested their serine dose-response signaling behaviors. All Tsr-Q311* mutants had reduced kinase activity, suggesting an important role of Q311 in kinase control. Most Tsr-Q311* mutants showed modification and signaling properties similar to WT, indicating Q311 alone is not critical for Tsr function. Two mutants showed unusual behaviors：Q311D was shifted toward the kinase-off output but could not be modified by CheR; Q311R was shifted toward the kinase-on output but could

not be modified by CheB. The E502 site is located closest to the HAMP domain that mediates the receptor output through its interactions with the adjacent MH bundle. To explore the signaling properties of E502, I analyzed all single amino acid replacements at this position with an *in vivo* FRET assay. Most Tsr-E502* mutants showed altered response sensitivities to serine, implying a critical role of E502 in modifying packing interactions of the methylation helices.

Introduction

The high-efficiency chemotaxis signaling pathway of *Escherichia coli* is composed of chemoreceptors (methyl-accepting chemotaxis proteins [MCPs]), a histidine kinase CheA and coupling protein CheW, downstream CheY and CheZ proteins, and sensory adaptation enzymes CheR and CheB (1–3). MCPs direct cell movements by regulating the autophosphorylation activity of a coupled histidine autokinase, CheA, whose default state is kinase-on. Phosphorylated CheA donates its phoshporyl group to the response regulater CheY. Phosphorylated CheY promotes clockwise rotation of the flagellar motors, causing cell tumbling (randomly changing swimming direction). Attractants inhibit CheA kinase activity, lowering phophorylated CheY levels and promoting counterclockwise (CCW) rotation, which produces forward swimming runs. Chemoreceptors sense chemoeffector gradients temporally, utilizing a sensory adaptation system (i.e., reversible methylation) composed of two modification enzymes, CheB and CheR. CheA also donates phosphoryl groups to CheB. Phosphorylated

CheB deamidates or demethylates MCP adaptation sites to glutamates (E). Another cytoplasmic enzyme, CheR, methylates those E sites. The interplay of CheB and CheR enzyme activities modulates receptor methylation state to match the ever-changing chemoeffector levels, thereby adjusting chemotactic sensitivity and extending the range of signal detection.

MCPs are homodimeric transmembrane proteins defined by highly conserved cytoplasmic domains (Fig. 3.1A). *E. coli* contains four canonical MCPs: Tsr (serine), Tar (aspartate and maltose), Trg (ribose and galactose), and Tap (dipeptides and pyrimidines). It also has a fifth MCP-like oxygen sensing transducer (4), which has no periplasmic domain, but mediates aerotactic behavior through a cytoplasmic FAD-binding domain. The Aer signaling domain lacks methylation sites, and its sensory adaptation mechanism is still unknown. The other four MCPs contain 4 to 6 methylation sites per subunit (5-7). Tsr and Tar are the most abundant chemoreceptor molecules in *E. coli* and the most extensively studied. Both glutamine (Q) and glutamate (E) residues can serve as sites for adaptational modification. Each Tsr monomer has five methylation sites: Q297, E304, Q311, E493, and E502 (Fig. 3.1). Glutamines first need to be deamidated by CheB to glutamates for CheR methylation; CheR methylates glutamates, forming glutamyl-methyl esters (Em); CheB demethylates Em sites back to glutamates. Methylation is thought to enhance MH packing stability; demethylation and deamidation are thought to reduce MH packing stability (8–10). It had been proposed that the oppositional structural interplay of HAMP domain, adaptation region (MH bundle), and

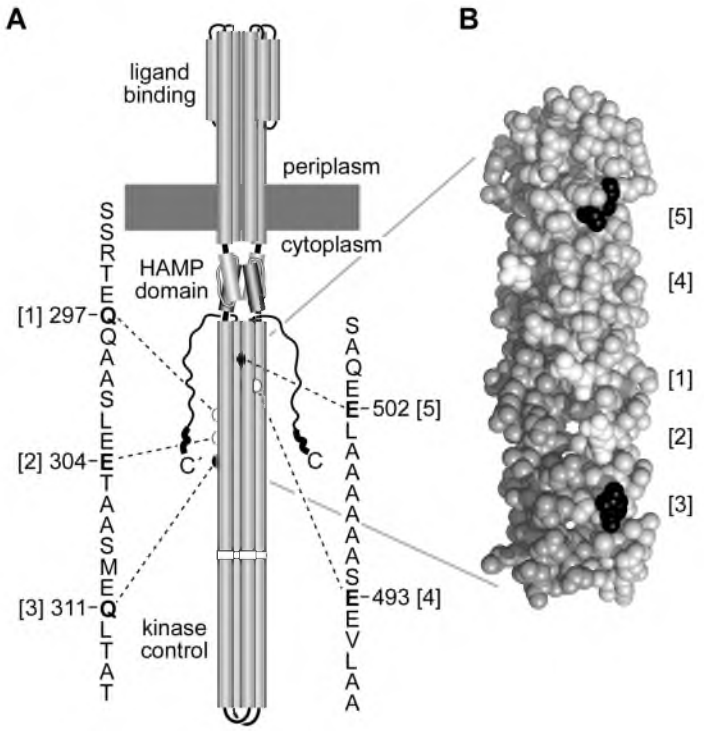

Fig. 3.1 Structural features of Tsr and its methylation sites. A. The Tsr homodimer. Cylindrical segments represent α-helices, drawn approximately to scale. Each Tsr subunit has five methylation sites (bolded residues in the primary sequence: sites 1, 2, and 4 are labeled in white, sites 3 and 5 are labeled in black. B. Structure of the native methylation helix (MH) bundle. Shown are residues R271-A320 and A462-V512 in each subunit of the Tsr dimer. One subunit is shaded gray, the other light gray. Methylation sites 1 - 4 lie near the inter-subunit interface; methylation site 5 lies near the intra-subunit interface. Both sites 3 and 5 are labeled as black, and other sites white. Site 3 is localized closest to the kinase control domain of the receptor, and site 5 is localized closest to the adjacent HAMP domain. The atomic coordinates were modeled and extrapolated from the crystal structure of the kinase control region of Tsr.

protein interaction region modulates the input-output signal control in MCPs: tighter packing of MH bundle causes reduced packing stabilities of HAMP bundle and protein interaction region and shifts receptor to the kinase-on state, whereas looser packing of MH bundle forces HAMP bundle and protein interaction region to less stable packing arrangements and shifts receptor to the kinase-off state (8, 10–15).

Tsr-Q311 the preferred site for CheR-mediated methylation (7, 16–18), and also probably the fastest deamidation site (7). Moreover, the inter-subunit location and the proximity of Tsr-Q311 to the downstream kinase control module (Fig. 3.1A) may enable it to exert the strongest control over receptor-coupled CheA kinase activity (8, 9, 19). Tsr-E502 is closest to the HAMP domain that mediates receptor output and probably modulates intra-subunit packing interactions of the methylation helices (Chapter 2). These unique features of Q311 and E502 could mean that these two adaptation sites may play different signaling roles than the other three sites: Q311 site may have the largest effect on CheA activity; the E502 site may have the most effect on MH and HAMP stabilities.

To test these possibilities, I constructed variant receptors with single amino acid replacements at residues Q311 and E502 and measured their signaling properties with various *in vivo* approaches. I also constructed amino acid replacements at all methylation sites and tested their modification and signaling behaviors. I found that both sites Q311 and E502 influence Tsr signaling in a similar way, as do the other methylation sites, presumably by modulating the overall packing interactions of the MH bundle.

However, the results also suggested that Q311 probably has a more potent effect on modulating kinase activity, whereas E502 has a more significant effect on the packing stability of MH and thereby the interaction with HAMP. This study provides additional knowledge of the mechanisms of sensory adaptation and input-output signal control in Tsr receptor signaling.

Materials and Methods

Bacterial Strains. Strains used in this study were isogenic derivatives of *E. coli* K-12 strain RP437 (20). Their designations and relevant genotypes were UU1250 [*Δaer-1 Δtsr-7028 Δ(tar-tap)5201 Δtrg-100*] (20); UU2610 [*Δaer-1 Δ(tar-cheB)4346 Δtsr-5547 Δtrg-4543*] (20); UU2611[*Δaer-1 Δ(tar-cheR)4283 Δtsr-5547 Δtrg-4543*] (20); UU2612 [*Δaer-1 Δ(tar-tap)4530 Δtsr-5547 Δtrg-4543*] (20); UU2632 [*Δaer-1 Δ(tar-tap)4530 Δ(cheB)4345 Δtsr-5547 Δtrg-4543*] (20); UU2567 [*Δ(tar-cheZ)4211 Δ(tsr)-5547 Δ(aer)-1 Δtrg-4543*] (20); UU2697 [*Δ(cheY-cheZ)1215 Δ(cheB)4345 Δ(tar-tap)4530 Δtsr-5547 Δaer-1 Δtrg-4543*] (20); UU2699 [*Δ(cheY-cheZ)1215 Δ(tar-cheR)4283 Δtsr-5547 Δaer-1 Δtrg-4543*] (20); UU2700 [*Δ(cheY-cheZ)1215 Δ(tar-tap)4530 Δtsr-5547 Δaer-1 Δtrg-4543*] (20).

CheR/CheB phenotype notation. A shorthand notation is used throughout to indicate strain phenotypes with respect to the CheR (R^-, R^+) and CheB (B^-, B^+) proteins.

Plasmids. Plasmids used in the study were pKG116, a derivative of pACYC184 (20) that confers chloramphenicol resistance and has a sodium salicylate-inducible

expression/cloning site (20); pPA114, a relative of pKG116 that carries wild-type *tsr* under salicylate control (20); pRZ30, a derivative of pKG116 that carries *cheY-YFP* and *cheZ-CFP* fusions under salicylate control (20); pPA810, a derivative of pKG116 that carries wild-type *cheR* under salicylate control; pRR48, a derivative of pBR322 (20) that confers ampicillin resistance and has an expression/cloning site with a *tac* promoter and an ideal (perfectly palindromic) *lac* operator under the control of a plasmid-encoded *lacI* repressor, inducible by IPTG (20); pRR53, a derivative of pRR48 that carries wild-type *tsr* under IPTG control (20); and pVS88, a plasmid that carries *cheY-YFP* and *cheZ-CFP* fusions under IPTG control (20).

Chemotaxis assays. Host strains carrying *tsr* plasmids were assessed for chemotactic ability on tryptone or minimal glycerol plus serine soft agar plates (20) containing the appropriate antibiotics (ampicillin [50 μg/ml] or chloramphenicol [12.5 μg/ml]) and inducers [100 μM IPTG or 0.6 μM sodium salicylate]. Tryptone plates were incubated at 30 - 32.5 °C for 7 - 10 h or at 24 °C for 15 - 20 h. Minimal plates were incubated at 30 - 32.5 °C for 15 - 20 h.

Mutant construction. Mutations in the *tsr* gene of plasmids pPA114 or pRR53 were generated by QuikChange PCR mutagenesis, using either degenerate-codon or site-specific primers, as previously described (20). QuikChange products were introduced into UU1250 by $CaCl_2$ transformation and tested for the ability to support Tsr function on tryptone and minimal serine soft agar plates. Candidate plasmids were verified by sequencing the entire *tsr* coding region.

Expression levels and modification patterns of mutant Tsr proteins. Cells harboring pRR53 derivatives were grown in tryptone broth containing 50 μg/ml ampicillin and 100 μM IPTG; cells harboring pPA114 derivatives were grown in tryptone broth containing 12.5 μg/ml chloramphenicol and 0.6 μM sodium salicylate. Strain UU2610 (R^- B^-) was used for measuring expression levels of mutant proteins to avoid receptor molecules in multiple modification states. Strains UU2611 (R^- B^+), UU2632 (R^+ B^-), and UU2612 (R^+ B^+) were used to assess the CheR and CheB substrate properties of mutant Tsr proteins. Cells were grown at 30 °C to midexponential phase, and 1-ml samples were pelleted by centrifugation, washed twice with KEP (10 mM K-PO_4, 0.1 mM K-EDTA, pH 7.0), and lysed by boiling in sample buffer (20). Tsr bands were resolved by electrophoresis in 11% polyacrylamide gels containing sodium dodecyl sulfate and visualized by immunoblotting with a polyclonal rabbit antiserum raised against Tsr residues 290 - 470 (20). Gel band intensities were quantified with ImageJ software (*http://imagej.nih.gov/ij*).

Flagellar rotation assays. Flagellar rotation patterns of plasmid-containing cells were analyzed by antibody tethering as described previously (20). Cells were classified into five rotation patterns, and the fraction of CW rotation time for a population of tethered cells was computed by a weighted sum of these rotation classes, as described (20).

***In vivo* FRET CheA kinase assay.** The experimental system, cell sample chamber, stimulus protocol, and data analysis closely followed the hardware, software, and methods described by Lai and Parkinson (20). Cells containing a FRET reporter

plasmid (pRZ30 or pVS88) and a compatible *tsr* expression plasmid (pRR53 or pPA114 derivative) were grown to midexponential phase in tryptone broth, washed, attached to a round coverslip with polylysine, and mounted in a flow cell (20). The flow cell and all motility buffer test solutions [KEP containing 10 mM Na lactate, 100 μM methionine, and various concentrations of serine] were maintained at 30 °C throughout each experiment. Cells were illuminated at the CFP excitation wavelength and light emission detected at the CFP (FRET donor) and YFP (FRET acceptor) wavelengths with photomultipliers. The ratio of YFP to CFP photon counts accurately reflects CheA kinase activity and changes in response to serine stimuli (20). Fractional changes in kinase activity versus applied serine concentrations were fitted to a multisite Hill equation, yielding two parameter values: $K_{1/2}$, the attractant concentration that inhibits 50% of the kinase activity, and the Hill coefficient, reflecting the extent of cooperativity of the response (20) . The maximum amount of receptor-regulated CheA kinase activity was also obtained by using either saturating serine stimuli or 3 mM KCN.

Protein modeling and structural display. Structure images were prepared with MacPyMOL software (*http://www.pymol.org*). Atomic coordinates for the modeled Tsr methylation helix bundle were obtained from Professor Sung-Hou Kim (UC-Berkeley).

Results

Mutational survey of Tsr-Q311*. To assess whether residue Q311 is critical for Tsr function, I constructed and characterized variants of *tsr* expression plasmid pRR53

that encoded Tsr proteins with all possible amino acid replacements at the Q311 position. On tryptone soft-agar plates at an optimal inducer concentration of 100 μM IPTG, the parental pRR53 plasmid confers robust serine chemotaxis to host strain UU1250, which carries deletions of all five *E. coli* MCP family genes (*tsr, tar, trg, tap, and aer*) (21). The majority of the resulting Q311 single amino acid replacement mutant proteins (here designated Tsr-Q311*) still produced at least 50% colony size in host UU1250 on soft agar plate (Fig. 3.2). This observation shows that Tsr function can tolerate a variety of amino acids at residue Q311. However, subsequent chemotactic response assays on minimal soft agar plates containing 4, 20, or 100 μM serine indicated that five of the functional Tsr mutants had increased serine-sensing thresholds (Fig. 3.2). In summary, 12 Tsr-Q311 amino acid replacements (I, L, E, C, M, V, T, Y, H, N, F, and A) produced chemotaxis at 4 μM serine, as did wild-type Tsr (Tsr-wt); three (G, W, and P) supported chemotaxis at 20 μM serine; two (S, and D) showed function at 100 μM serine; and two (R and K) could not produce any chemotactic response at any serine concentration tested, including on tryptone medium, which contains about 670 μM serine (Chapter 2).

SDS-PAGE analysis of Tsr-Q311* molecules. It is reasonable to suspect that the Tsr-Q311* receptors with impaired Tsr function might make an unstable or misfolded protein. To test this possibility, I measured the steady-state intracellular levels of all plasmid-expressed Q311* proteins in the receptor-less host strain UU2610, which lacks the adaptation enzymes CheR and CheB ($R^- B^-$). Tsr molecules synthesized in this host are in an unmodified uniform state and thus migrate as a single band on SDS-PAGE (21).

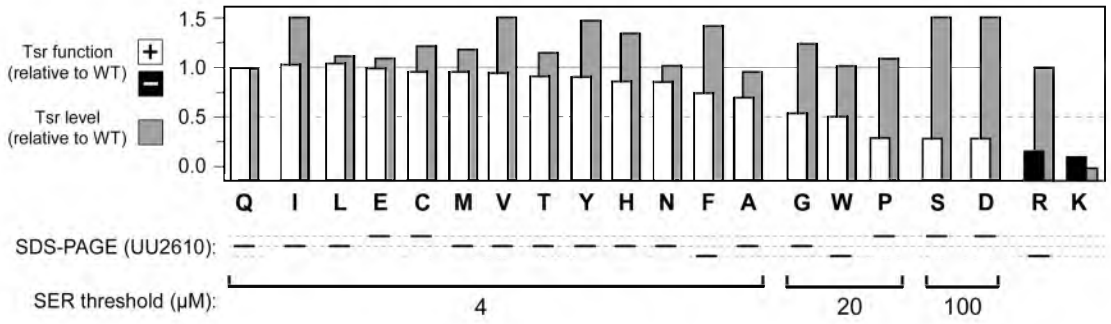

Fig. 3.2 Mutational survey of Tsr-Q311. Bold letters below the histogram indicate the amino acid at residue Q311 of Tsr (Q = Tsr wild type). White or black bars indicate the relative colony size on tryptone soft agar produced by strain UU1250 carrying a plasmid expressing each Tsr variant. White bars denote wild-type colony morphology; black bars denote colonies with no evident ring of chemotactic cells at their periphery. Gray bars indicate the relative expression levels of the mutant Tsr proteins. Black horizontal bars beneath the mutant amino acid indicate the relative positions of the mutant subunits in SDS-PAGE analyses. Dashed horizontal gray lines are simply intended to facilitate comparison of band positions. Serine thresholds of the Tsr-Q311 mutants were also defined by chemotactic ring formation on minimal soft agar plates containing 4, 20, or 100 μM serine.

All Q311* receptors, except Q311K, had intracellular levels comparable to that of the wild type (Fig. 3.2). Moreover, the mutant receptors with reduced function (R, D, S, and P) showed normal or even better expression than Tsr-wt. The Tsr-Q311K plasmid did not show any band on SDS-PAGE, suggesting that The Q311K molecule is misfolded and unstable (The Q311K mutant will not be discussed in the following part of Results). In conclusion, the Q311* receptors have essentially normal expression levels and intracellular stabilities. Even those with functional defects probably have near-native structure.

Adaptation enzymes can shift the SDS-PAGE mobility of receptor molecules. Methylated (or Q-bearing) forms migrate faster than do demethylated and deamidated (i.e., E-bearing) forms. The exact mechanism for those effects is unknown, but one possible explanation is that Tsr subunits retain residual secondary structures in SDS that influence electrophoretic mobility. Most of the Q311* proteins showed SDS-PAGE mobility similar to the wild-type protein (Fig. 3.2). Five mutant proteins (Q311E, C, P, S, and D) with differential functional features and side chain chemical properties migrated slower than Tsr-wt. Tsr-Q311F, Q311W, and Q311R migrated faster than Tsr-wt. These findings suggest that site Q311 may affect the structural stability of Tsr, but in a less significant manner, compared to site E502 (Chapter 2).

Modification of Tsr-Q311* receptors by the sensory adaptation enzymes. To assess their propensities for adaptational modifications, Tsr-Q311* mutant receptors were expressed in host strains with different combinations of CheR and CheB enzymes

[UU2611 (R^- B^+), UU2632 (R^+ B^-) and UU2612 (R^+ B^+)], and their SDS-PAGE band profiles were examined (Table 3.1). Most Tsr-Q311* mutant receptors underwent extensive CheR-mediated methylation, as did wild type Tsr in both R^+ B^- and R^+ B^+ hosts (Table 3.1). The majority of Q311 mutant receptors underwent little or no CheB-mediated deamidation in the R^- B^+ host (Table 3.1), suggesting that these receptors had kinase off-shifted character. Two mutant receptors (Q311L, Q311W) underwent extensive CheR methylation, but were not be modified by CheB (Table 3.1). Another mutants (Q311D) underwent significant modification by CheB, but were not be modified by CheR, even in response to a large serine stimulus (10 mM) (Table 3.1). Tsr-Q311R was the only mutant receptor that can not be modified by either CheB or CheR, even after a large serine stimulus.

Signaling properties of Tsr-Q311* receptors in the absence of sensory adaptation. To explore the signaling properties of the Q311* mutant receptors, a FRET kinase assay was used to monitor *in vivo* receptor-regulated CheA activity in response to serine stimuli (22). The dose-response data were fitted to a multisite Hill equation to obtain a $K_{1/2}$ value, the attractant concentration that inhibits half of the CheA activity, and a Hill coefficient, which reflects the extent of response cooperativity. I also measured the maximum amount of the Tsr-controlled CheA activity by using saturating serine stimulus or 3 mM KCN (20).

In UU2567, a FRET reporter strain lacking both CheR and CheB sensory adaptation enzymes, receptor molecules remain unmodified, undergoing neither methylation nor

Table 3.1 Modification patterns of Tsr-Q311* mutant receptors.

Q311 replacement	Modification by CheB?	Modification by CheR?	Modification in R^+ B^+? [a]
E	+	++	++
D	++	-	-
Q (wt)	++	++	++
S	+	++	++
T	+	++	+
A	+	++	++
C	+	++	++
G	+	++	++
N	+	++	++
P	+	+	+
H	+	++	++
V	+	++	++
Y	+	++	++
W	-	++	+
L	-	++	++
I	+	+	+
F	+	++	++
M	+	++	++
R	-	-	-

[a] modification patterns of Tsr variants were tested in R^+ B^+ strain in response to 100 mM serine. ++: modification is comparable to that of WT; +: modification but not as significant as that of wild type; - : no measurable modification.

demethylation/deamidation reactions. Under these conditions, wild-type Tsr molecules have a QEQEE residue pattern at adaptation sites 1-5. To explore the signaling effects of amino acid replacements at Q311, I first tested their FRET behaviors in UU2567. The dose-response parameters are summarized in Fig. 3.3. Tsr-Q311* mutants showed a wide variety of response thresholds to serine (Fig. 3.3A), suggesting the signaling role of methylation sites in regulating packing stability of the MH bundle.

In the $R^- B^-$ strain, Tsr-wt (Q311) produced a sensitive, highly cooperative response to serine ($K_{1/2}$ ~19 μM; Hill coefficient ~20). Tsr-Q311E and Q311D mutants were the only ones that showed lower serine thresholds than Tsr-wt in $R^- B^-$ strain, with $K_{1/2}$ ~5 μM and ~9 μM, respectively (Fig. 3.3A). A group of Tsr-Q311* mutants (S, T, A, C, G, N, P, and H) showed slightly higher serine thresholds than Tsr-wt in $R^- B^-$ strain (Fig. 3.3A). Another group of Tsr-Q311* mutants (V, Y, W, L, I, and F) had significantly higher serine thresholds than Tsr-wt in the $R^- B^-$ strain (Fig. 3.3A). Tsr-Q311M and Q311R failed to respond even to 10 mM serine (Fig. 3.3A). All responsive Tsr-Q311* mutants had Hill coefficients in the wild type range in the $R^- B^-$ strain. However, all Tsr-Q311* mutants had lower CheA activity than Tsr wt (data not shown). In conclusion, site Q311 is not critical for serine sensing, but is important for normal CheA kinase activity.

Effects of adaptation enzymes on the signaling properties of Tsr-Q311* receptors. In a two-state model, the sensory adaptation system cancels serine-induced responses by shifting receptor signaling complexes toward the ON state. CheR-mediated methylation at adaptation sites favors the ON state, thereby increasing

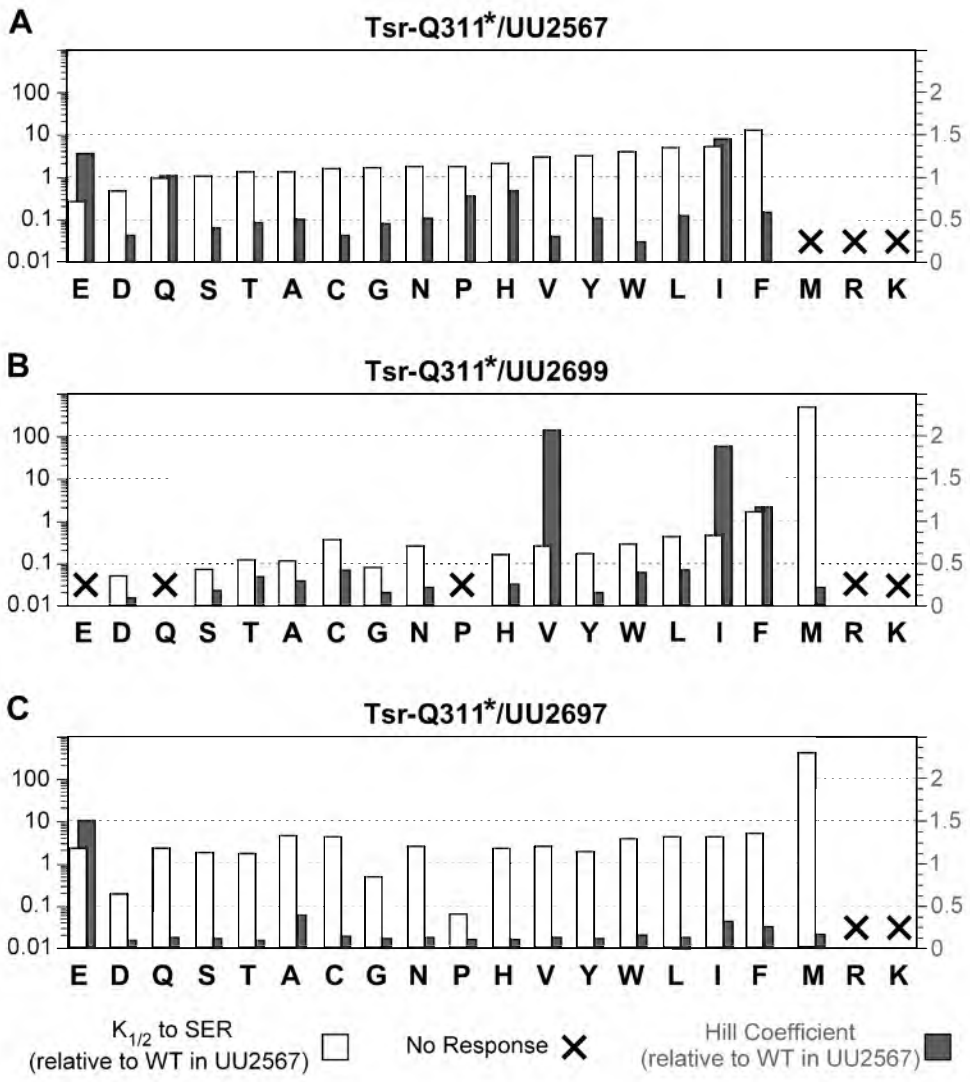

Fig. 3.3 Serine dose-response parameters of Tsr-Q311* variants. Bold letters below the histogram indicate the amino acid at residue Q311 of Tsr (Q = Tsr wild type). White bars denote the relative fold of $K_{1/2}$ of indicated mutant receptor in that host, compared to that of wild type in host UU2567 (R^-B^-). White bars were measured by the left Y-axis in log scale. Gray bars denote the relative fold of *Hill coefficient* indicated mutant receptor in that host, compared to that of wild type in host UU2567 (R^-B^-). Gray bars were measured by the gray-font right Y-axis in linear scale. No response means the receptor failed to respond even to 10mM serine. A, UU2567 (R^-B^-); B, UU2699 (R^-B^+); C, UU2697 (R^+B^-).

the serine threshold ($K_{1/2}$); CheB-mediated demethylation or deamidation favors the OFF state, thereby decreasing the serine threshold ($K_{1/2}$). Tsr-wt had an elevated serine threshold in an $R^+ B^-$ strain ($K_{1/2}$ ~ 49 μM) and failed to respond even to 10 mM serine in an $R^- B^+$ strain. These signaling effects demonstrate that CheR-mediated methylation shifts wild type Tsr toward the ON state and that CheB-mediated deamidation and/or demethylation shifts wild type Tsr toward the OFF state. Tsr-wt produced a much more sensitive response to serine in $R^+ B^+$ host ($K_{1/2}$ ~0.4 μM) than it did in $R^- B^-$ host. This behavior indicates that the combined activities of CheR and CheB, which create a mixture of receptor molecules in different modification states (22), bring wild type Tsr into a state with much higher sensitivity.

To determine the effects of adaptation enzymes on the signaling properties of Tsr-Q311* mutant receptors, I examined their response behaviors in hosts containing only one of the two enzymes ($R^+ B^-$ and $R^- B^+$). The dose-response parameters are summarized in Fig. 3.3. One group of Tsr-Q311* mutants (E, S, T, A, C, N, and H) showed reduced serine thresholds in $R^- B^+$ strain (Fig. 3.3B) and increased serine thresholds in $R^+ B^-$ strain compared to the $R^- B^-$ strain (Fig. 3.3C). This group of mutants exhibited signaling behaviors similar to wild type Tsr did in these three host strains, consistent with the known effects of catalytic activities of CheB and CheR.

Another group of Tsr-Q311* mutants (D, G, V, Y, W, L, I, F, and M) showed decreased serine thresholds in $R^- B^+$ strain (Fig. 3.3B), but also slightly decreased serine thresholds in $R^+ B^-$ strain, compared to the $R^- B^-$ strain (Fig. 3.3C). More significantly,

Q311P failed to respond even to 10 mM serine in $R^- B^+$ host, but showed a much more sensitive response in $R^+ B^-$ host ($K_{1/2}$ ~ 1.3 μM) than it did in $R^- B^-$ host ($K_{1/2}$ ~ 34 μM). Tsr-Q311R is the only mutant receptor that failed to respond even to 10 mM serine in any of the three host strains ($R^- B^-$, $R^+ B^-$, and $R^- B^+$), consistent with that Q311R cannot be modified by neither CheR nor CheB (Table 3.1). Also, its relatively high kinase activities in these hosts are consistent with an intrinsic ON-biased output. Similar to wild type Tsr, most Tsr-Q311* mutant receptors showed lower Hill coefficients in $R^+ B^-$ and $R^- B^+$ host strains than in the $R^- B^-$ host strain. Consistent with the SDS-PAGE analyses (Table 3.1), these results demonstrate that most Q311* mutant receptors can be modified by CheR and CheB.

Signaling properties of Tsr-E502* receptors in the absence of sensory adaptation. To explore the functional defects caused by amino acid replacements at E502, I first examined the signaling properties of these mutant receptors with the *in vivo* FRET kinase assay in the $R^- B^-$ host. The dose-response results are summarized in Fig. 3.4A. The signaling patterns of Tsr-E502I, E502P, and E502Q had been discussed earlier in detail (Chapter 2). Most other Tsr-E502* mutant receptors showed a certain response to serine in the $R^- B^-$ host strain (Fig. 3.4A). Several Tsr-E502* mutants (F, Y, and A) produced lower serine thresholds than Tsr-wt did in $R^- B^-$ host. Tsr-E502W and E502V showed slightly higher serine thresholds, whereas other Tsr mutants (L, H, D, R, S, T, N, and K) had significantly higher serine thresholds than did wild type Tsr in the $R^- B^-$ host strain. Finally, some Tsr-E502* mutants (C, G, M, I, P, and Q) failed to respond

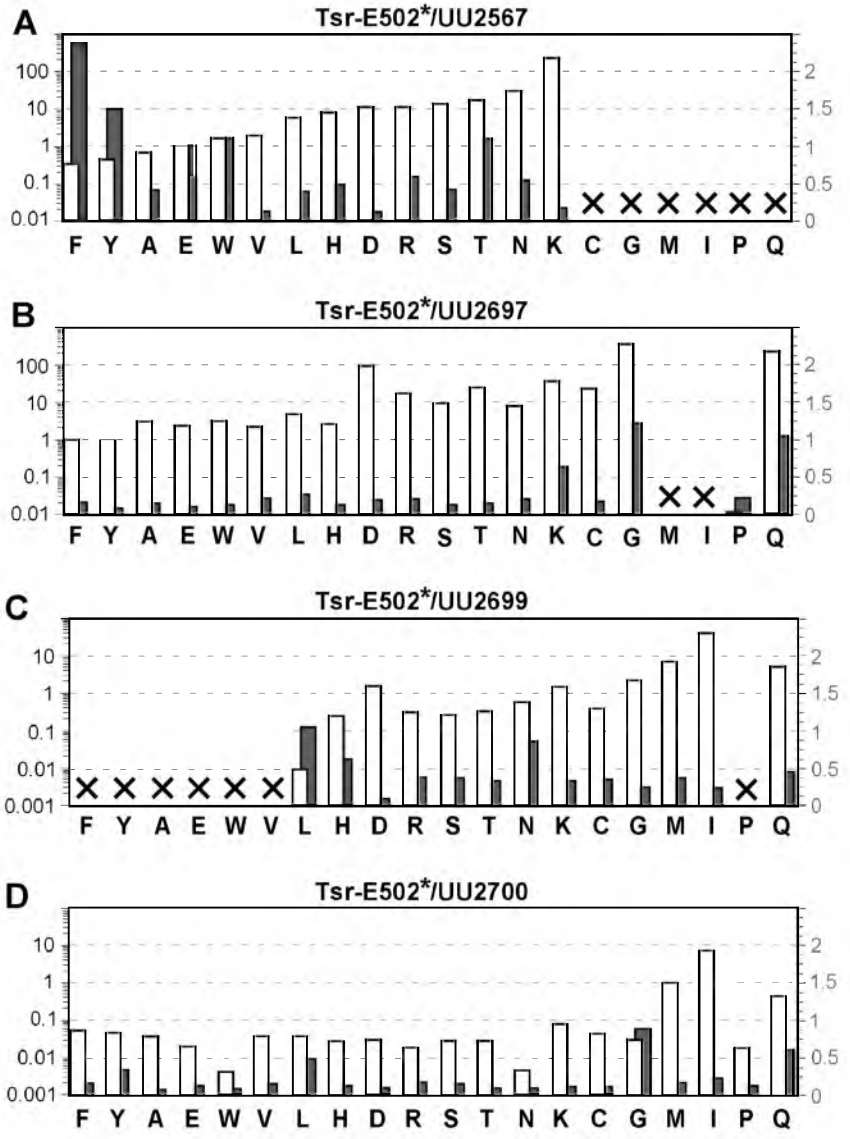

Fig. 3.4 Serine dose-response parameters of Tsr-E502* variants. Bold letters below the histogram indicate the amino acid at residue E502 of Tsr (E = Tsr wild type). White bars denote the relative fold of $K_{1/2}$ of indicated mutant receptor in that host, compared to that of wild type in host UU2567 ($R^- B^-$). White bars were measured by the left Y-axis in log scale. Gray bars denote the relative fold of *Hill coefficient* indicated mutant receptor in that host, compared to that of wild type in host UU2567 ($R^- B^-$). Gray bars were measured by the gray-font right Y-axis in linear scale. No response means the receptor failed to respond even to 10 mM serine.

even to 10 mM serine, suggesting intrinsic ON-biased or OFF-biased output. Tsr-E502V, D and K mutants showed a lower Hill coefficient than that of wild type Tsr. All other responsive E502* receptors showed a Hill coefficient in the wild type range. The diverse variety of response sensitivities (Fig. 3.4A) suggests that site E502 may play an important role in regulating the packing stability of the MH bundle.

Effects of adaptation enzymes on the signaling properties of Tsr-E502* receptors. To determine the effects of adaptation enzymes on the signaling properties of Tsr-E502* mutant receptors, I tested their response behaviors in hosts containing one or two of the adaptation enzymes ($R^+ B^-$, $R^- B^+$, and $R^+ B^+$). The dose-response data are summarized in Fig. 3.4. Many Tsr-E502* receptors (F, Y, A, W, V, D, R, and T) produced similar signaling patterns to that of Tsr-wt in these host strains (Fig. 3.4): increased response thresholds in the $R^+ B^-$ host, decreased thresholds or no response in the $R^- B^+$ host, and more sensitive response in the $R^+ B^+$ host. These results are consistent with the effects of CheR mediated methylation and CheB mediated deamidation and/or demethylation.

Another group of Tsr-E502* mutant receptors (L, H, S, N, and K) showed decreased serine thresholds in the $R^- B^+$ host and also slightly decreased thresholds in the $R^+ B^-$ host compared to the $R^- B^-$ host (Fig. 3.4), consistent with earlier observation of the threshold-lowering effect of CheR. Taking E502K for example, the threshold-lowering effect of CheR is probably not dependent on methylation reactions because the E502K molecule cannot be modified by CheR (data not shown). In the $R^- B^-$ host, mutants

E502C, G, M, I, P, and Q failed to respond even to 10 mM serine. But all six mutants showed certain serine response in the adaptation proficient host, suggesting that they can undergo CheR and/or CheB modifications that enhance their signaling behaviors. Tsr-E502C, G, M, and Q were somewhat less sensitive than wild type in both the $R^+ B^-$ and the $R^+ B^+$ background (Fig. 3.4), consistent with their ON-biased signaling changes. Tsr-E502I and E502M did not respond even to 10 mM serine in either the $R^- B^-$ or the $R^+ B^-$ host, but did respond to serine in both the $R^- B^+$ and the $R^+ B^-$ hosts (Fig. 3.4). These findings suggest that both E502M and E502I have intrinsic ON-biased output, consistent with their relatively high kinase activity measured *in vivo* (data not shown). All Tsr-E502* mutant receptors responded to serine in the $R^+ B^+$ host. Responsive mutant receptors also showed a Hill coefficient in wild type range in all hosts.

How many adaptation sites are sufficient for chemotaxis? As the first and major site for adaptation modification, is site Q311 alone sufficient for performing chemotaxis to serine? To answer this question, I used combinations of D and N replacements at the other three canonical sites to approximate the signaling features of the wild type E and Q residues at those positions. Aspartate and asparagine had been shown to produce signaling properties similar to glutamate and glutamine, respectively (Chapter 2). A, F, Y, and V replacements at the unorthodox site 5 are amino acid residues that give the most sensitive responses to serine (Fig. 3.4). FRET kinase assays in $R^- B^-$ strain showed that Tsr variants NDQDF, NDQDV, and NDQDY all had comparable signaling features to those of the wild type Tsr, and only Tsr-NDQDA had

response threshold considerably higher than wild type (Table 3.2). Despite these normal dose-response behaviors in FRET assays and their normal intracellular expression levels and stabilities (Table 3.3), all these mutant receptors failed to support serine chemotaxis in an R^+ B^+ strain (Table 3.3). These findings show that the Q311 site alone cannot support Tsr function in cells that contain the sensory adaptation enzymes, suggesting that it takes more than one site for effective sensory adaptation. Evidently, adaptational modifications at Q311 alone are not sufficient for tracking spatial serine gradients.

I next determined the minimum number of methylation sites the receptor needs for chemotaxis function. I constructed a variety of mutants with a different number of intact methylation sites, with other sites being replaced by signal-approximating amino acid residues. FRET kinase assays with these mutants in the R^- B^- strain showed that all these receptors had signaling properties comparable to those of wild type Tsr (Table 3.2). But their chemotactic behaviors were quite variable: mutants with only one intact site obviously had no function, neither did mutants with two intact sites (Tsr-NDDEE, NENDE, NDNEE, NDQDE, and ADQDE); Tsr-NENEE (three intact sites) supported ~50% of wild type chemotaxis function; Tsr-DEEEE, NEEEE, EENEE, NEQEE, and QENEE (four intact sites) produced essentially full wild-type function. These results indicate that it probably requires at least three of the five methylation sites to support good chemotaxis function for Tsr.

Table 3.2 Serine dose-response parameters of Tsr variants in strain UU2567.

modification site residues	$K_{1/2}$ (μM) [a]	Hill coefficient [a]	number of experiments
Q E Q E E[b]	17 ± 1.1	15 ± 7.5	2
E E N E E	6.6	14	1
E E D E E	NR	NR	3
N E E E E	1.5	4.8	1
D E E E E	0.7	2	1
N D D E E	6.0	8.5 ± 1.5	2
N D N E E	12 ± 0.4	12 ± 3.5	2
N E N D E	22 ± 1.3	11± 1.0	2
N E N E E	8.2	3.5	1
N E Q E E	4.8	11	1
Q E N E E	31	9.7	1
Q E D E E	9.3 ± 1.1	7.3 ± 2.4	2
N D A D E	25	17	1
A D N D E	20	14	1
D D D D E[b]	3.5 ± 0.4	6.4 ± 1.5	2
N D D D E[b]	6.5	6.0	1
D N D D E[b]	5.2 ± 0.5	14 ± 1.9	2
N D N D E[b]	43 ± 7.1	8.9 ± 2.3	2
N D N D D[b]	NR	NR	4
N D Q D A	117	23	1
N D Q D F	22	7.6	1
N D Q D V	16	9.2	1
N D Q D Y	19	13	1
N D Q D E	34	8.0 ± 3.0	2
A D Q D E	27	14	1

Tsr variants were expressed from plasmid pRR53 derivatives in strain UU2567 containing the pRZ30 FRET reporter plasmid. [a] For multiple experiments, means and standard errors were determined from the best-fit parameter values for each independent experiment. NR: no response to 10 mM serine. [b] indicates data from Chapter 2, for comparison.

Table 3.3 Chemotaxis function and expression levels of Tsr variants.

modification site residues	Tsr Function [a]	protein expression [b]
Q E Q E E	1.0	1.0
E E N E E	0.7	0.9
E E D E E	0.3	1.0
N E E E E	0.7	0.9
D E E E E	0.8	1.1
N D D E E	0.2	0.9
N D N E E	0.3	1.1
N E N D E	0.2	0.8
N E N E E	0.5	0.9
N E Q E E	0.9	0.9
Q E N E E	0.7	1.0
Q E D E E	0.3	1.6
N D A D E	0.2	0.8
A D N D E	0.2	0.5
D D D D E	0.2	0.8
N D D D E	0.2	0.7
D N D D E	0.2	0.6
N D N D E	0.2	0.6
N D N D D	0.2	0.6
N D Q D A	0.3	1.0
N D Q D F	0.3	1.0
N D Q D V	0.3	0.9
N D Q D Y	0.2	0.8
N D Q D E	0.3	0.8
A D Q D E	0.3	0.7

Tsr variants were expressed from plasmid pRR53 derivatives in strain UU1250 or UU2610. [a] Tsr function, measured as chemotaxis ring size, was normalized to that of wild type Tsr. Mutant with value 0.3 or smaller is considered as nonfunction. [b] Protein expression level was normalized to that of wild type. Mutant with value between 0.5 and 2.0 is considered as comparable to that of wild type.

Discussion

Chemoreceptor output signal control and its adaptation region. The dynamic bundle model proposes that a phase stutter arrangement between the AS2 and MH1 helices couples the structural stabilities of the HAMP and MH bundles antisymmetrically (11–13) (Fig. 3.5A). Mutational and biochemical analyses suggested that chemotactic signals are transduced by conformational changes in helix-helix packing and that packing in the methylation region and protein interaction region are also tightly coupled in an oppositional way (8, 10, 23). Taken together, the packing stability of the MH bundle (adaptation region) regulates the coupled CheA kinase activity by opposing influences of packed helices along the length of signal conversion and kinase control modules: attractant induced inward piston sliding of the TM2 stablizes the HAMP packing, forces the adaptation region to be less stable, stabilizes the protein interaction region, and thereby shifts receptor toward the kinase-off state; the sensory adaptation system cancels these ligand induced responses by adjusting the packing stability of the MH bundle: Methylation should enhance stability; demethylation and deamidation should reduce stability.

Tsr methylation sites 1 - 4 reside at the subunit interface in receptor dimers (Fig. 3.1B and 3.5B) and should influence packing stability of the MH bundle, mostly by modulating the inter-subunit packing interactions. The third adaptation site is the first site and the major site for CheR mediated methylation (7, 16–18) and also the fastest deamidation site among all five sites (7). Moreover, Tsr-Q311 is closest to the downstream kinase

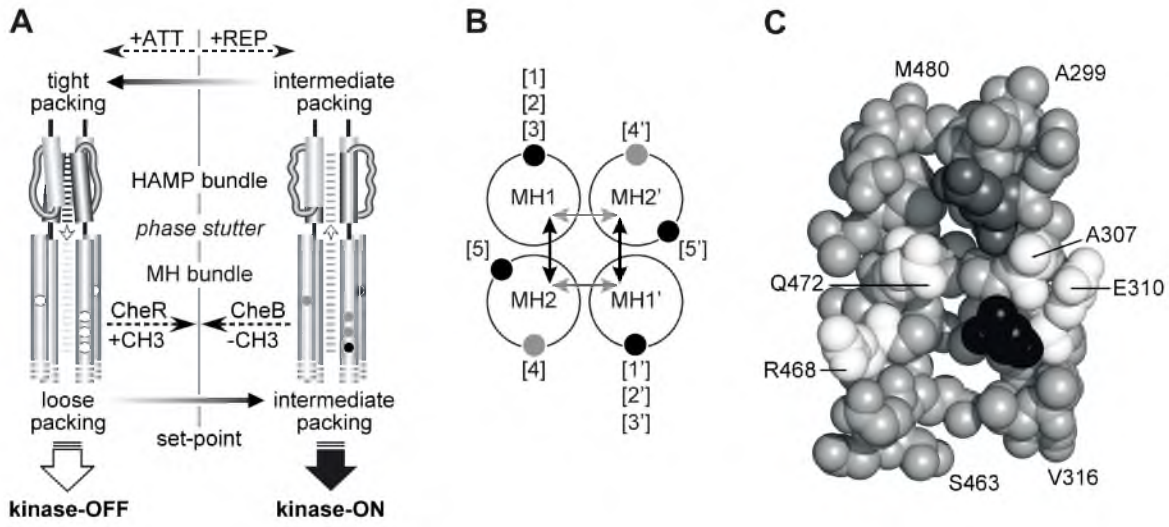

Fig. 3.5 Mechanistic interpretation of Tsr-Q311 signaling effects. A. Dynamic bundle model of Tsr signal control. A phase stutter at the HAMP-MH bundle junction is proposed to produce an oppositional stability relationship between packing of the HAMP and MH bundles. Open arrows between the bundles indicate the direction of structure-destabilizing forces: Tight packing of HAMP destabilizes MH bundle packing, leading (by an unspecified mechanism) to deactivation of CheA; tight packing of the MH bundle destabilizes HAMP, leading (by an unspecified mechanism) to CheA activation. Attractants and repellents produce stimulus responses by acting on HAMP stability; subsequent methylation (sites 1, 2, 4 [gray]; site 3, 5 [black]) and demethylation (sites 1 - 5 [white]) changes produce sensory adaptation by shifting the packing stability of the MH bundle to counterbalance HAMP input effects, driving the system back to an intermediate set-point stability. B. Structure-stabilizing effects of receptor methylation. The four helices of the MH bundle are shown in cross-section, as viewed from the membrane toward the cytoplasmic tip. Adaptation sites 1 - 4 probably modulate MH bundle stability by influencing inter-subunit interactions (gray arrows); site 5 probably modulates MH bundle stability by influencing intra-subunit interactions (black arrows). All five sites operate in similar mode by affecting overall packing stability of the MH bundle. C. Local structural environment of Tsr-Q311. Segments of the MH1 helix (A299-V316) from one subunit and MH2' helix (S463-M480) from the other subunit of the Tsr dimer are shown. All C, N, and O atoms are shown as spheres. Side chain of amino acid residue Q311 is shown in black, while main chain is not shown. E304 is shown in dark gray. Residues whose side chain may be in physical contact range with Q311 are shown in white; other residues are in gray. The A307 label line points to the carbon atom of its side chain and the E310 label line points to the oxygen atom of the side chain. The R468 label line points to the nitrogen atom of its positively charged side chain, and the Q472 label line points to the oxygen atom of the hydrophobic side chain.

control domain. I suggest that Q311 has a stabilizing effect on the local MH bundle packing and that Q311 has a more potent effect on modulating CheA kinase activity than the other sites. Tsr-E502 is closest to the HAMP domain and lies more buried between the inteface of N and C helices from the same monomer of the Tsr dimer. Therefore, I suggest that E502 regulates the overall MH bundle packing by modulating the intra-subunit packing interactions and that E502 has a more potent effect on modulating the structural interplay between HAMP and MH bundle than the other sites.

Signaling consequences of amino acid replacements at Tsr-Q311. The wild type Q311 residue of Tsr probably has a moderate stabilizing effect on the local MH bundle packing close to the kinase control domain (Fig. 3.1, 3.5C). In the modeled bundle structure extrapolated from the X ray structure of the Tsr hairpin tip (24), the uncharged side chain of Q311 resides in a relatively hydrophobic environment, openly exposed to the outer solvent. Neutralization at methylation sites stabilizes the MH bundle packing, presumably by reducing the charge density and favoring closer helix packing (10). Thus, it is most likely that residues with negatively charged side chains (D and E) at site 3 should reduce the packing of MH bundle and that the ones with uncharged side chains should increase the packing stability. A glutamine (Q) mimicks the modification and signaling properties of a glutamyl methyl-ester (Em) (25). Therefore, deamidation at Q311 should destabilize the packing stability of MH bundle and shift output toward the kinase-off state. This would account for the behavioral changes of the Tsr-Q311E receptor: lower response threshold to serine and lower kinase activity.

An aspartate (D) is the closest structure to glutamtate (E), but cannot be modified by CheR or CheB. Similar to Q311E, Tsr-Q311D also showed a lower response threshold and lower kinase activity than Tsr-wt (Q311). The slower mobility of Q311D and Q311E on SDS-PAGE relative to wild type Tsr is consistent with their signaling behaviors. Substitutions of amino acids with polar uncharged side chains (for example, S, T, and N) did not change the receptors signaling behaviors much, consistent with similar packing stability of MH bundle. Q311R probably reflects an extreme stabilization of MH packing, driving the receptor to an ON-locked state, out of the physiological operational range of CheR and CheB (Fig. 3.1 and 3.3).

Q311 is thought to be the major methylation site and also the first and the fastest site to be modified. I ascribe these properties to the large uncharged side chain of Q311 located widely exposed to the outer environment, and more importantly, its C-terminal residence on the helix compared to the other sites, which gives site 3 the prior access for adaptation enzymes (16–18). The first 3 sites Q297, E304, and Q311 localize linearly along the same helix surface, with exact one-heptad-turn spacing. It had been suggested that CheR first recognizes and catalyzes the site located in C-direction (i.e., site 3 for Tsr) and that a negatively charged residue 7 residues away in C-direction inhibits the following methylation, while a neuturally charged residue does not (16–18). Taking Tsr for example, negatively charged amino acid replacement (D, but not E, as glutamate can be methylated to Em) at Q311 should prevent the methylation (specifically methylation at E304) at other sites. The modification pattern of Q311D is clearly

consistent with this idea: Q311D did not undergo any CheR-mediated methylation, in either SDS-PAGE analysis or FRET kinase assay. Due to the destabilizing effect of Q311D replacement on the MH bundle, CheR may preferentially bind to Tsr-Q311D. Aspartate residue in site Q311 cannot be modified by CheR methylation. It is most likely that CheR is somehow in a position (presumably by side chain electrostatic interactions with receptor) that prevents it moving up and binding to any other sites.

The proximity of Q311 to the kinase control domain probably confers it a much stronger effect on the receptor-regulated kinase activity, rather than on the packing stability of MH bundle. The majority of Tsr-Q311* mutant receptors showed mobility on SDS-PAGE similar to the Tsr-wt, suggesting a limited effect of site 3 on regulating MH packing stability. All mutant receptors showed reduced intrinsic kinase activity compared to the wild type Tsr, suggesting a more potent effect of Q311 on kinase control. The disparity that the wild type Q311 residue does not assume the most stabilized packing, but does confer the highest kinase activity to receptor, may have some important implications about the sensory adaptation mechanism. Cells use methylation levels to allow continuous sensing to chemoeffector gradients, and the gradual methylation or demethylation of receptor by sensory adaptation system plays an important role in sensitive and robust signal detection. It makes a lot of sense to impose only a moderate stabilizing effect on the MH bundle for the initial methylation (Q is essentially equivalent to Em), as it is most likely reflecting low levels of chemoeffectors. However, the default state of the Tsr coupled kinase is ON, which would impose an

unavoidable demand to assume a high kinase activity to the receptor in wild type modification state (QEQEE). I attribute the more potent effect on kinase control but limited effect on MH packing of Tsr-Q311, to its proximity to the kinase control domain.

Signaling consequences of amino acid replacements at Tsr-E502. I have suggested that the wild type E502 residue of Tsr is likely to have a destabilizing effect on local MH bundle packing near the HAMP junction (Chapter 2). The negatively charged side chain of E502 resides in a moderately hydrophobic cavity lined with alanine residues from both the N and C helices in the same subunit. Tsr-E502* mutant receptors showed a variety of response thresholds to serine, and most are higher than Tsr-wt (Fig. 3.4). Tsr-E502M showed very similar signaling properties to that of Tsr-E502I: a large shift to the kinase-ON state; CheB function shifted Tsr-E502M to a responsive range, whereas CheR function alone did not (Fig. 3.4). Both isoleucine and methionine side chains at E502 might prefer the hydrophobic environment of the E502 cavity, enhancing intra-subunit methylation helices packing interactions, driving the receptor to a relatively stable state with high kinase activity.

Tsr-E502C and E502G had signaling behaviors similar to Tsr-E502Q: large shift to the kinase-on state; CheB function shifted receptor to responsive range, and so did CheR (Fig. 3.4). These mutants most likely also reflect stabilized packing interactions of MH bundle and high kinase activity. Tsr-E502K, N, S, H, and L probably also had stabilized packing interactions of MH and high kinase activity. And CheR probably drives all these mutants (Q, C, G, K, N, S, H, and L) to a less stable state of MH packing instead of more

stable (Fig. 3.4), consistent with no CheR catalytic activity on them: neither E502Q nor E502K showed measurable CheR mediated methylation (data not shown). Except E502P, the rest of Tsr-E502* mutant receptors showed similar signaling patterns to wild type Tsr, suggesting packing stability changes in near-native functional structures. These proposed structural consequences of amino acid replacements at E502 are also consistent with the interpretation of the SDS-PAGE analyses.

Structural insights from SDS-PAGE bandshifts of Tsr-Q311*. The majority of amino acid replacements at Q311 did not shift Tsr subunit mobility in denaturing gel electrophoresis (Fig. 3.2). Although the exact mechanism of mobility shift is unclear, it is possible that receptor subunits retain certain native secondary and even tertiary structures in the presence of SDS, and subsequent interactions between these structural components could influence gel migration rates. I interpreted these mobility shifts in terms of relative packing stability of the receptor methylation helices: tightly packed molecules should migrate faster than loosely packed ones. For example, Tsr-Q311D and Q311E should reduce the MH bundle packing interactions, whereas Tsr-Q311R probably enhances those interactions: Q311D and Q311E subunits had the slowest SDS-PAGE mobility, while Q311R had the fastest. Despite the complication of those unknown denatured structures, the relative mobility of other mutant subunits also reflects similar structural and signaling changes. These results are consistent with the limited stabilizing effect of Q311 on the packing stability of the MH bundle.

Differential signaling roles of methylation sites. Both methylation site 3 (Q311) and site 5 (E502) operate in a similar way as do other sites, modulating the overall packing stability of the MH bundle and thereby influencing receptor signaling. Tighter packing of the MH bundle drives the receptor to kinase-on state, while looser packing of the MH bundle shifts the receptor to kinase-off state. However, my study also supported that site 3 and site 5 may have distinct signaling consequences, rather than merely modulating packing stability of the MH bundle.

E502 is likely to have a strong effect on the MH bundle packing interactions near the HAMP junction, whereas Q311 probably has a weaker effect on local MH bundle packing interactions. The fact that E502 is localized more buried between the intra-subunit interface, and that it is closest to the oppositionally coupled HAMP module, may account for its dramatic effect on MH bundle packing stability. The unique more-buried intra-subunit location of E502 most likely also affects the helices packing much stronger than the outer-facing inter-subunit interactions. Additionally, its proximity to the HAMP may impose more effect on the structural interplay between the MH bundle and HAMP region. Tsr-E502* mutant receptors had various response thresholds to serine and probably a very broad packing stabilities. In contrast, most Q311* mutants are likely to have similar packing stability of MH to wild type Tsr, suggesting a much less significant effect of site 3 on MH bundle packing. This is most likely due to the fact that Q311 is farthest from the HAMP domain, is affecting the inter-subunit packing interactions, and is widely exposed to solvent.

Q311 probably has a more potent effect on controlling kinase activity, while E502 does not. Although Q311 does not impose much influence in the packing stability of MH bundle, it may have more effect on kinase activity. The lower kinase activities of all Tsr-Q311* mutants than that of wild type Tsr are good evidences, whereas Tsr-E502* mutants showed a much wider range of kinase activities. It had been shown that it is the inter-subunit interface conformation change within the kinase control module that affects the kinase activity (8, 9, 19). This is consistent with the inter-subunit location of Tsr-Q311.

I further conclude that it is the localization differences between these two sites that cause the distinctly different signaling roles of E502 and Q311. The inter-subunit location and proximity to the kinase control tip probably make Q311 the first and fastest site to be modified and also make it the site that imposes the most significant effect on CheA kinase control. The intra-subunit location and proximity to the HAMP probably make E502 have a huge impact on the overall packing stabilities of MH and HAMP and also make it the methylation site of last resort. The differential signaling roles of Q311 and E502 suggest that not all methylation sites are created equal, implying functional individuality.

The seemingly superfluous five methylation sites exist for good reasons. The observation that neither Q311 nor E502 alone is necessary or sufficient for the Tsr chemotaxis function suggests that chemotaxis function, specifically the sensory adaptation mechanism, requires a highly sophisticated, delicate, and accurate regulation

of the receptor methylation, which is beyond the capacity of one single site. It most likely takes at least three of the five methylation sites to support considerable chemotaxis. As the most populated and multifunctional chemoreceptor in *E.coli,* Tsr is probably the most important among the MCP-family, sensing a variety of signals with considerably wide ranges (up to 5 orders of magnitude), including amino acids, sugars, pH, and even temperature. The diverse functions and wide signal detection range of Tsr impose a higher requirement for precise and dynamic adaptation. Receptors with less than three intact adaptation sites apparently do not have such capability to accomplish the task, although they may still undergo significant modifications. It is most likely that those modifications are not sufficient for sensory adaptation, presumably due to either a sluggish transition of modification states or lack of precise control.

The unexpected signaling effect of CheR. CheR typically stabilizes the MH bundle packing interactions and shifts the receptor to the kinase-ON state by methylation reactions at adaptation sites. Most of the mutant receptors tested in this study conform to this signaling pattern. However, quite a few Tsr mutant receptors showed the opposite signaling consequence of CheR effect, shifting receptor to kinase-OFF state (lowering threshold). Mutant receptors Tsr-Q311D, G, V, Y, W, L, I, F, and M all showed the threshold-lowering signaling effect of CheR more or less (Fig. 3.3). Another group of Tsr receptors (Tsr-E502L, H, S, N, K, C, G, P, and Q) also produced certain more sensitive response to serine in presence of CheR (Fig. 3.3). This counterintuitive effect of CheR is most likely not due to the CheR-mediated methylation. For example,

Tsr-E502K cannot be modified by CheR, but still showed considerable threshold-lowering effect of CheR. It is probably that CheR can bind to receptor methylation region and somehow destabilize the packing interactions of MH bundle directly or indirectly. A follow-up study will focus on the threshold-lowering effect of CheR.

The possible source of receptors' response cooperativity. In a $R^- B^-$ host, all the receptor molecules are in an unmodified uniform state, and Tsr receptors (wild type Tsr, Hill coefficient ~15) typically showed a very cooperative response to serine stimuli. Receptors typically showed lower cooperativity in $R^+ B^-$, $R^- B^+$, and $R^+ B^+$ hosts, in which receptors typically existed as mixture of different modification states. Although it is not clear what caused their lower cooperativity in those hosts, it is most likely because receptors in different modification states had different sensitivities to serine. Thus, a fraction of receptor molecules in a lower modification state can probably respond to a low concentration of serine, while the other fraction of receptor molecules in a higher modification state may not show any response unless they encounter a fairly higher concentration of serine. This broader response range of the heterogeneous population of receptor molecules may lead to a gradual stepwise stimulation of CheA and thereby causes lower apparent cooperativity. All the mutant receptors tested in this study showed essentially the same signaling pattern to that of wild type Tsr in terms of cooperativities in different hosts, suggesting that neither residue Q311 nor E502 is critical in modulating response cooperativity to serine stimuli. The major source of extensive cooperativity comes from allosteric interactions within chemoreceptor array integrating

many signaling teams composed of trimers of dimers, CheAs, and CheWs. Although it seems unlikely, whether the presence of CheR and/or CheB affects the chemoreceptor array stability or the connection interactions within the array is not fully clear yet.

In conclusion, this study of the two important methylation sites Q311 and E502 provided important knowledge of understanding the chemoreceptor sensory adaptation mechanism and input-output signal control. As the putatively most important adaptation site and closest site to kinase control domain, wild type residue Q311 is likely to stabilize the MH bundle packing moderately, but modulate the CheA kinase activity in a more significant way. Closest to the adjacent HAMP domain and regulating intra-subunit packing interactions, the fifth adaptation site E502 probably destabilizes the MH packing and functions as the last resort of modification, allowing receptors to sense higher levels of chemical ligands.

References

1. Hazelbauer GL, Falke JJ, Parkinson JS. 2008. Bacterial chemoreceptors: high-performance signaling in networked arrays. Trends Biochem Sci **33**:9–19.

2. Sourjik V, Armitage JP. 2010. Spatial organization in bacterial chemotaxis. EMBO J **29**:2724–2733.

3. Porter SL, Wadhams GH, Armitage JP. 2011. Signal processing in complex chemotaxis pathways. Nat Rev Microbiol **9**:153–165.

4. Bibikov SI, Biran R, Rudd KE, Parkinson JS. 1997. A signal transducer for aerotaxis in *Escherichia coli*. J Bacteriol **179**:4075–4079.

5. Terwilliger TC, Wang JY, Koshland DE, Jr. 1986. Surface structure recognized for covalent modification of the aspartate receptor in chemotaxis. Proc Natl Acad Sci USA **83**:6707–6710.

6. Nowlin DM, Bollinger J, Hazelbauer GL. 1987. Sites of covalent modification in Trg, a sensory transducer of Escherichia coli. J Biol Chem **262**:6039–6045.

7. Rice MS, Dahlquist FW. 1991. Sites of deamidation and methylation in Tsr, a bacterial chemotaxis sensory transducer. J Biol Chem **266**:9746–9753.

8. Starrett DJ, Falke JJ. 2005. Adaptation mechanism of the aspartate receptor: electrostatics of the adaptation subdomain play a key role in modulating kinase activity. Biochemistry **44**:1550–1560.

9. Winston SE, Mehan R, Falke JJ. 2005. Evidence that the adaptation region of the aspartate receptor is a dynamic four-helix bundle: cysteine and disulfide scanning studies. Biochemistry **44**:12655–12666.

10. Swain KE, Gonzalez MA, Falke JJ. 2009. Engineered socket study of signaling through a four-helix bundle: evidence for a yin-yang mechanism in the kinase control module of the aspartate receptor. Biochemistry **48**:9266–9277.

11. Zhou Q, Ames P, Parkinson JS. 2009. Mutational analyses of HAMP helices suggest a dynamic bundle model of input-output signalling in chemoreceptors. Mol Microbiol **73**:801–814.

12. Zhou Q, Ames P, Parkinson JS. 2011. Biphasic control logic of HAMP domain signalling in the *Escherichia coli* serine chemoreceptor. Mol Microbiol **80**:596–611.

13. Ames P, Zhou Q, Parkinson JS. 2014. HAMP domain structural determinants for signalling and sensory adaptation in Tsr, the Escherichia coli serine chemoreceptor. Mol Microbiol **91**:875–886.

14. Airola MV, Sukomon N, Samanta D, Borbat PP, Freed JH, Watts KJ, Crane BR. 2013. HAMP domain conformers that propagate opposite signals in bacterial chemoreceptors. PLoS Biol **11**:e1001479.

15. Falke JJ, Piasta KN. 2014. Architecture and signal transduction mechanism of the bacterial chemosensory array: progress, controversies, and challenges. Curr Opin Struct Biol **29**:85–94.

16. Shapiro MJ, Chakrabarti I, Koshland DE, Jr. 1995. Contributions made by individual methylation sites of the *Escherichia coli* aspartate receptor to chemotactic behavior. Proc Natl Acad Sci USA **92**:1053–1056.

17. Shapiro MJ, Panomitros D, Koshland DE, Jr. 1995. Interactions between the methylation sites of the Escherichia coli aspartate receptor mediated by the methyltransferase. J Biol Chem **270**:751–755.

18. Shapiro MJ, Koshland DE, Jr. 1994. Mutagenic studies of the interaction between the aspartate receptor and methyltransferase from *Escherichia coli*. J Biol Chem **269**:11054–1059.

19. Bass RB, Coleman MD, Falke JJ. 1999. Signaling domain of the aspartate receptor Is a helical hairpin with a localized kinase docking surface: cysteine and disulfide scanning studies. Biochemistry **38**:9317–9327.

20. Parkinson JS, Houts SE. 1982. Isolation and behavior of *Escherichia coli* deletion mutants lacking chemotaxis functions. J Bacteriol **151**:106–113.

21. Ames P, Studdert CA, Reiser RH, Parkinson JS. 2002. Collaborative signaling by mixed chemoreceptor teams in *Escherichia coli*. Proc Natl Acad Sci USA **99**:7060–7065.

22. R.Z. L, J.S. P. 2014. Functional suppression of HAMP domain signaling defects in the E. coli serine chemoreceptor. J Mol Biol **426**:3642–3655.

23. Hazelbauer GL, Lai WC. 2010. Bacterial chemoreceptors: providing enhanced features to two-component signaling. Curr Opin Microbiol **13**:124–132.

24. Kim KK, Yokota H, Kim SH. 1999. Four-helical-bundle structure of the cytoplasmic domain of a serine chemotaxis receptor. Nature **400**:787–792.

25. Shimizu TS, Tu Y, Berg HC. 2010. A modular gradient-sensing netwo chemotaxis in *Escherichia coli* revealed by responses to time-varying stimuli. Mol Syst Biol **6**:382

CHAPTER 4

A COUNTERINTUITIVE SIGNALING ROLE FOR CHER

Abstract

Sensory adaptation of the serine receptor (Tsr) and other chemoreceptors occurs through covalent modifications of specific residues in the cytoplasmic signaling domain of receptor molecules. Methylation of Tsr increases the serine response threshold and is thought to enhance packing stability of the MH bundle. Demethylation and deamidation lower the serine response threshold and are thought to reduce MH packing stability. However, I found that CheR significantly lowered the serine response thresholds of some mutant Tsr receptors. To explore the mechanistic basis for this counterintuitive signaling effect of CheR, I first constructed different Tsr variants with or without the C-terminal tether (NWETF) and tested their signaling behaviors in different FRET host strains *in vivo*. My results showed that the threshold-lowering effect of CheR largely depended on the presence of NWETF. I also constructed FRET hosts that have wild type CheR or mutant CheR-R53E lacking catalytic activity expressed under induction and tested the effects of CheR catalytic function and CheR expression levels on its threshold-lowering action. The results showed that the threshold-lowering

effect of CheR depended on both the CheR interaction with the methylation region of Tsr and the intracellular level of CheR enzymes.

Introduction

MCPs (Methyl-accepting Chemotaxis Proteins) are homodimeric transmembrane receptors defined by highly conserved cytoplasmic signaling domains (Fig. 4.1A). *E. coli* contains four MCPs, Tsr (serine), Tar (aspartate and maltose), Trg (ribose and galactose), and Tap (dipeptides and pyrimidines). It also has a fifth MCP-like aerosensor (1), which has no periplasmic domain, but mediates aerotactic behavior through a cytoplasmic FAD-binding domain. All the four MCPs contain 4 to 6 methylation sites per subunit (2–4). Both glutamine (Q) and glutamate (E) residues can serve as sites for CheR and CheB mediated adaptational modification. Each monomer of Tsr has five methylation sites: Q297, E304, Q311, E493, and E502 (Fig. 4.1), denoted as Tsr-QEQEE (wt). Glutamines first need to be deamidated to glutamates; CheR methylates glutamates, forming glutamyl-methyl esters (Em); CheB demethylates Em sites back to glutamates. CheR-mediated methylation increases the serine response threshold and is thought to enhance packing stability of the MH bundle. CheB-mediated demethylation and deamidation lower the serine response threshold and are thought to reduce MH packing stability (5–7). CheR catalytic activity on the receptor has been shown to be largely dependent on the C-terminal NWETF (Fig. 4.1) (8–11), which serves as a binding site to increase the local concentration of CheR near the methylation sites of the receptor.

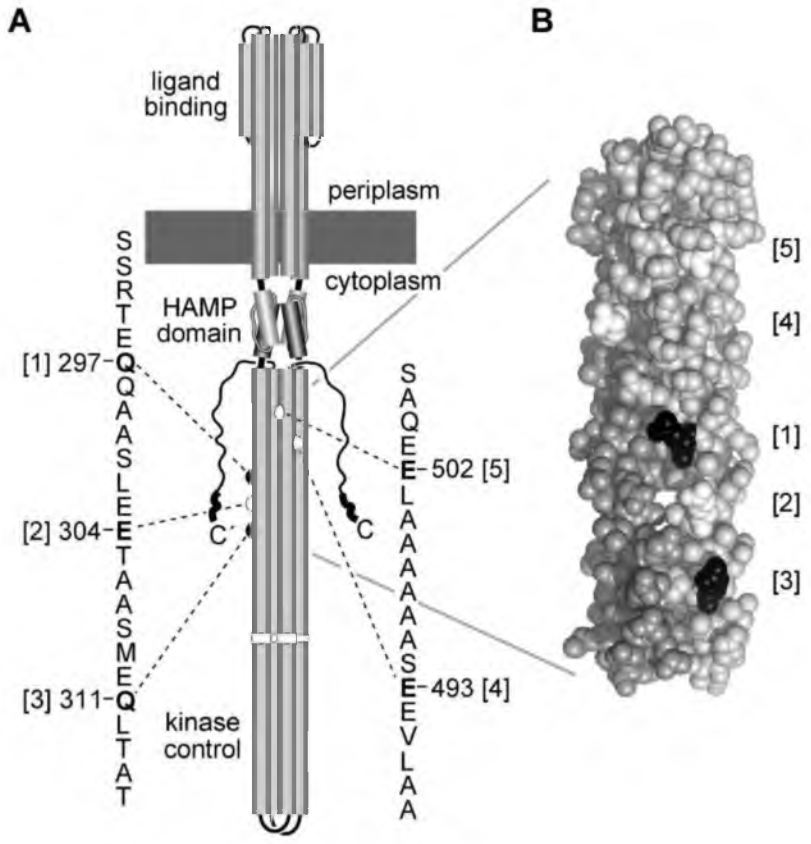

Fig. 4.1 Structural features of Tsr and its methylation sites. A. The Tsr homodimer. Cylindrical segments represent α-helices, drawn approximately to scale. Each Tsr subunit has five methylation sites (bolded residues) in the primary sequence: glutamate sites are labeled in white, and glutamine sites are labeled in black. B. Structure of the native methylation helix (MH) bundle. Shown are residues R271 - A320 and A462 - V512 in each subunit of the Tsr dimer. One subunit is shaded gray, the other light gray. Methylation sites 1 and 3 are labeled as black (glutamine) and others white (glutamate). Methylation sites 1 - 4 lie near the inter-subunit interface; methylation site 5 lies near the intra-subunit interface. The atomic coordinates were modeled and extrapolated from the crystal structure of the kinase control region of Tsr.

(The Intracellular ratio of CheR molecules to Tsr molecules is only about 1:30.) (12). CheB catalytic activity is activated by phosphorylation and is less dependent on the NWETF than CheR is. CheR likely recognizes and acts on receptors with loose MH packing interactions in a kinase-off output state. Subsequent methylations stabilize the MH bundle, shift receptor output to the kinase-on state, and elevate the serine response threshold ($K_{1/2}$). CheB probably recognizes and acts on receptors that have tight MH bundle packing interactions in a kinase-on output state. Subsequent deamidation and/or demethylation reactions destabilize the MH bundle, shift the receptor toward the kinase-off state, and lower the response threshold ($K_{1/2}$). Surprisingly, I discovered that CheR could significantly lower the serine response thresholds of some Tsr receptors, especially those with no available methylation sites (e.g., Tsr-NDNDR). Similarly, I found that CheB could increase the response thresholds of some Tsr receptors.

To explore the mechanistic basis for the counterintuitive signaling effects of CheR and CheB, I constructed different Tsr variants with or without the C-terminal tether NWETF and tested their signaling behaviors in host strains with different combinations of CheR and CheB enzymes. I found that the threshold-lowering effect of CheR largely depended on the presence of the NWETF in the receptor. The NWETF sequence also affected the response threshold of wild type Tsr in the absence of CheR or CheB, presumably by influencing receptor structure. I also constructed new FRET hosts that express the wild *cheR* gene under xylose control and tested the importance of CheR catalysis and CheR expression level to the CheR threshold-lowering effect. The results

showed that the threshold-lowering effect of CheR depended on CheR binding to the methylation region of the receptor, but not on subsequent catalyses. I also found that the CheR threshold-lowering effect depended on the intracellular level of CheR enzymes. These findings can be readily explained by a modified dynamic bundle model of Tsr signal control.

Materials and Methods

Bacterial Strains. Strains used in this study were isogenic derivatives of *E. coli* K-12 strain RP437 (13). Their designations and relevant genotypes were UU1634 [*ΔcheR*]; UU2614 [*ΔcheB*]; UU1250 [*Δaer-1 Δtsr-7028 Δ(tar-tap)5201 Δtrg-100*] (13); UU2610 [*Δaer-1 Δ(tar-cheB)4346 Δtsr-5547 Δtrg-4543*] (13); UU2611[*Δaer-1 Δ(tar-cheR)4283 Δtsr-5547 Δtrg-4543*] (13); UU2612 [*Δaer-1 Δ(tar-tap)4530 Δtsr-5547 Δtrg-4543*] (13); UU2632 [*Δaer-1 Δ(tar-tap)4530 Δ(cheB)4345 Δtsr-5547 Δtrg-4543*] (13); UU2567 [*Δ(tar-cheZ)4211 Δ(tsr)-5547 Δ(aer)-1 Δtrg-4543*] (13); UU2697 [*Δ(cheY-cheZ)1215 Δ(cheB)4345 Δ(tar-tap)4530 Δtsr-5547 Δaer-1 Δtrg-4543*] (13); UU2699 [*Δ(cheY-cheZ)1215 Δ(tar-cheR)4283 Δtsr-5547 Δaer-1 Δtrg-4543*] (13); UU2700 [*Δ(cheY-cheZ)1215 Δ(tar-tap)4530 Δtsr-5547 Δaer-1 Δtrg-4543*] (13); XH05 [*xylAB::cheR-wt Δ(tar-cheZ)4211 Δ(tsr)-5547 Δ(aer)-1 Δtrg-4543*] (This work); XH01 [*xylAB::cheR-R53E Δ(tar-cheZ)4211 Δ(tsr)-5547 Δ(aer)-1 Δtrg-4543*] (This work).

CheR/CheB phenotype notation. A shorthand notation is used throughout to indicate strain phenotypes with respect to the CheR (R^-, R^+) and CheB (B^-, B^+) proteins.

Plasmids. Plasmids used in the study were pKG116, a derivative of pACYC184 (14) that confers chloramphenicol resistance and has a sodium salicylate-inducible expression/cloning site (15); pPA114, a relative of pKG116 that carries wild-type *tsr* under salicylate control (16); pPA810, a derivative of pKG116 that carries wild-type *cheR* under salicylate control; pPA827, a derivative of pKG116 that carries wild-type *cheB* under salicylate control; pRZ30, a derivative of pKG116 that carries *cheY-YFP* and *cheZ-CFP* fusions under salicylate control (17); pRR48, a derivative of pBR322 (18) that confers ampicillin resistance and has an expression/cloning site with a *tac* promoter and an ideal (perfectly palindromic) *lac* operator under the control of a plasmid-encoded *lacI* repressor, inducible by IPTG (19); pRR53, a derivative of pRR48 that carries wild-type *tsr* under IPTG control (19); and pVS88, a plasmid that carries *cheY-YFP* and *cheZ-CFP* fusions under IPTG control (20).

Chemotaxis assays. Host strains carrying *tsr* plasmids were assessed for chemotactic ability on tryptone or minimal glycerol plus serine soft agar plates (21) containing the appropriate antibiotics (ampicillin [50 μg/ml] or chloramphenicol [12.5 μg/ml]) and inducers (100 μM IPTG or 0.6 μM sodium salicylate). Tryptone plates were incubated at 30 - 32.5 °C for 7 - 10 h or at 24 °C for 15 - 20 h. Minimal plates were incubated at 30 - 32.5 °C for 15 - 20 h. Host strains carrying *cheR* or *cheB* expression plasmids were also tested for chemotactic ability on tryptone soft agar plates by similar methods.

Mutant construction. Mutations in the *tsr* gene of plasmids pPA114 or pRR53 were generated by QuikChange PCR mutagenesis, using either degenerate-codon or site-specific primers, as previously described (16). QuikChange products were introduced into UU1250 by $CaCl_2$ transformation and tested for the ability to support Tsr function on tryptone and minimal serine soft agar plates. Candidate plasmids were verified by sequencing the entire *tsr* coding region. Mutations in the *cheR* gene of plasmid pPA810 were generated by similar method and introduced into UU1634 to test for chemotaxis. Mutation of the *cheB* gene of plasmid pPA827 was generated by similar methods and introduced into UU2614 to test for chemotaxis.

Expression levels and modification patterns of proteins. Cells harboring pRR53 derivatives were grown in tryptone broth containing 50 μg/ml ampicillin and 100 μM IPTG; cells harboring pPA114 derivatives were grown in tryptone broth containing 12.5 μg/ml chloramphenicol and 0.6 μM sodium salicylate. Strain UU2610 (R^- B^-) was used for measuring expression levels of mutant proteins to avoid receptor molecules in multiple modification states. Strains UU2611 (R^- B^+), UU2632 (R^+ B^-), and UU2612 (R^+ B^+) were used to assess the CheR and CheB substrate properties of mutant Tsr proteins. Cells were grown at 30 °C to midexponential phase, and 1-ml samples were pelleted by centrifugation, washed twice with KEP (10 mM K-PO_4, 0.1 mM K-EDTA, pH 7.0), and lysed by boiling in sample buffer (22). Tsr bands were resolved by electrophoresis in 11% polyacrylamide gels containing sodium dodecyl sulfate and visualized by immunoblotting with a polyclonal rabbit antiserum raised against Tsr residues 290 - 470 (23). For CheR

or CheB proteins, different concentrations of D-Xylose were applied to cell culture, and the gels were immnoblotted with a polyclonal goat antiserum raised against CheR or CheB (Gifts from Stock Lab). Gel band intensities were quantified with ImageJ software (*http://imagej.nih.gov/ij*).

***In vivo* FRET CheA kinase assay.** The experimental system, cell sample chamber, stimulus protocol, and data analysis closely followed the hardware, software, and methods described by Lai and Parkinson (20). Cells containing a FRET reporter plasmid (pRZ30 or pVS88) and a compatible *tsr* expression plasmid (pRR53 or pPA114 derivative) were grown to midexponential phase in tryptone broth, washed, attached to a round coverslip with polylysine, and mounted in a flow cell (24). The flow cell and all motility buffer test solutions [KEP containing 10 mM Na lactate, 100 µM methionine, and various concentrations of serine] were maintained at 30 °C throughout each experiment. Cells were illuminated at the CFP excitation wavelength and light emission detected at the CFP (FRET donor) and YFP (FRET acceptor) wavelengths with photomultipliers. The ratio of YFP to CFP photon counts accurately reflects CheA kinase activity and changes in response to serine stimuli (25, 26). Fractional changes in kinase activity versus applied serine concentrations were fitted to a multisite Hill equation, yielding two parameter values: $K_{1/2}$, the attractant concentration that inhibits 50% of the kinase activity, and the Hill coefficient, reflecting the extent of cooperativity of the response (20, 27). The maximum amount of the receptor-regulated kinase activity was also obtained by using either saturating serine stimuli or 3 mM KCN, or both.

Protein modeling and structural display. Structure images were prepared with MacPyMOL software (*http://www.pymol.org*). Atomic coordinates for the modeled Tsr methylation helix bundle were obtained from Professor Sung-Hou Kim (UC-Berkeley).

Results

***In vivo* FRET kinase assays of Tsr [NDND-X] variants.** The signaling properties of Tsr-wt (QEQEE) were tested by FRET kinase assay in different host strains having various combinations of the CheR and CheB adaptation enzymes. In an $R^- B^-$ host strain lacking both enzymes, Tsr-wt showed a sensitive, highly cooperative response to serine ($K_{1/2}$, ~17 μM; Hill coefficient, ~15), whereas in an $R^+ B^-$ host strain containing only the CheR enzyme, the serine threshold of Tsr-wt was shifted higher ($K_{1/2}$ ~49 μM; Hill coefficient ~8.5) (Fig. 4.2; Table 4.1). This CheR effect on Tsr-wt is due to its catalytic activity at the receptor methylation sites. In an $R^- B^+$ host strain containing only the CheB enzyme, Tsr-wt failed to respond even to 10 mM serine, whereas in an $R^+ B^+$ strain containing both adaptation enzymes, Tsr-wt showed sensitive but low cooperativity responses ($K_{1/2}$ ~0.4 μM; Hill coefficient ~2.4) (Fig. 4.2; Table 4.1). All these behaviors of Tsr-WT are consistent with the known catalytic activities of CheR and CheB. CheB-mediated deamidation drives the receptor to a very low modification state (i.e., Tsr-EEEEE), which elicits little or no kinase activity. CheR-mediated methylation restores kinase activity and brings the receptor to a serine-responsive state.

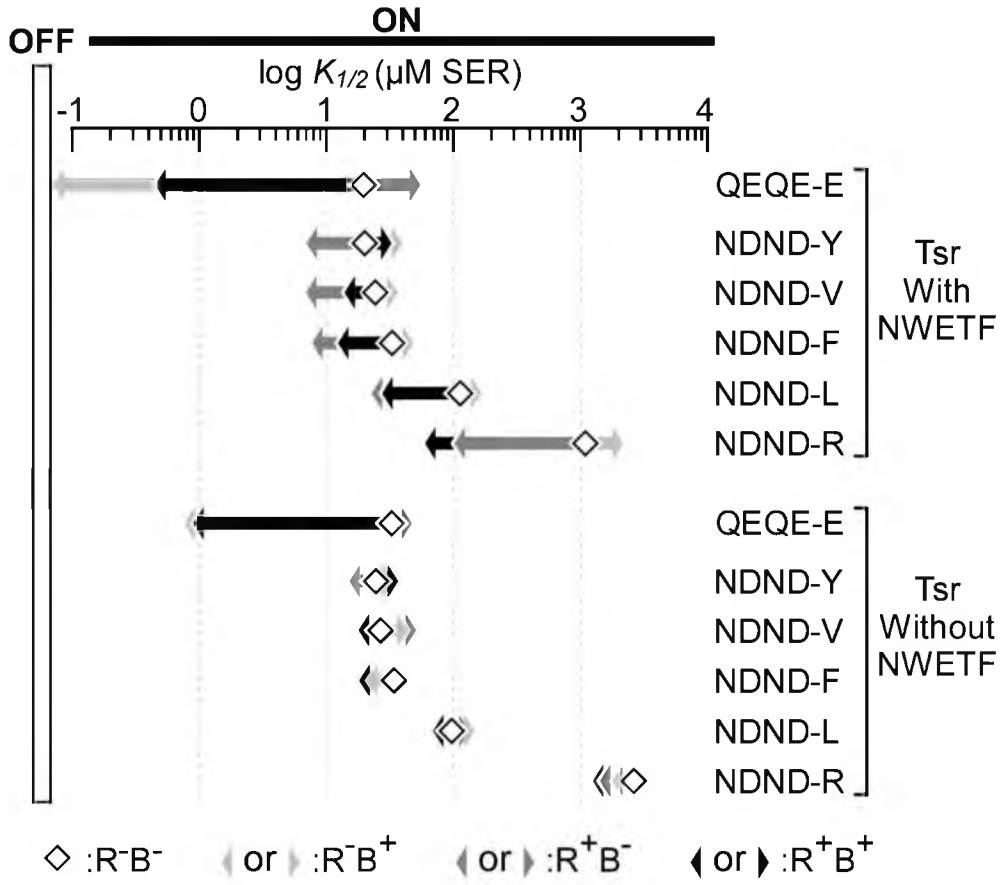

Fig. 4.2 The threshold-lowering effect of CheR on Tsr receptors. Shown is a summary of average $K_{1/2}$ values for Tsr wild type and some variants (see Table 4.1 and Table 4.2). Plasmid pRR53 derivatives encoding Tsr wild type or variants were tested for serine responses in different host strains. Diamond, host strain UU2567 (R^- B^-); light gray arrow, host strain UU2699 (R^- B^+); gray arrow, host strain UU2697 (R^+ B^-); black arrow, host strain UU2700 (R^+ B^+). The upper portion showed Tsr wild type and variants with the presence of C-terminal tether end NWETF; the lower portion showed Tsr wild type and variants without NWETF.

Table 4.1 Serine dose-response parameters for Tsr NDNDX variants.

Tsr mutant [a]	FRET host strain [b]	$K_{1/2}$ (μM) [c]	Hill coefficient [c]	number of experiments
QEQEE	UU2567	17 ± 1.1	15 ± 7.5	2
	UU2699	NR	NR	3
	UU2697	49 ± 6.6	8.5 ± 4.8	3
	UU2700	0.4 ± 0.1	2.4 ± 0.2	2
NDNDF	UU2567	34 ± 5.5	9.5 ± 5.5	3
	UU2699	38 ± 2.5	6.3 ± 0.2	3
	UU2697	9.0 ± 3.5	8.2 ± 3.8	3
	UU2700	18 ± 2.4	6.7 ± 0.2	2
NDNDL	UU2567	111 ± 12	10 ± 2	3
	UU2699	112 ± 28	1.9 ± 0.3	2
	UU2697	34 ± 15	3.3 ± 1.0	2
	UU2700	31	5.2	1
NDNDR	UU2567	1150 ± 20	11 ± 1.1	2
	UU2699	2090	2.2	1
	UU2697	118	8.4	1
	UU2700	73 ± 10	5.1 ± 3.0	2
NDNDV	UU2567	24 ± 13	9.5 ± 3.0	3
	UU2699	28 ± 8.3	5.3 ± 1.6	2
	UU2697	7.4 ± 0.8	3.6	2
	UU2700	18	6.6	1
NDNDY	UU2567	24 ± 6	8.1 ± 1.0	4
	UU2699	32 ± 18	1.8 ± 0.5	2
	UU2697	7.6	10	1
	UU2700	32	2.4	1

[a] Derivatives of plasmid pRR53 were transferred to FRET host strains; induction with 100 μM IPTG. [b] Strains also carried the FRET reporter pRZ30; induction with 2 μM sodium salicylate. [c] For multiple experiments, means and standard errors were determined from the best fit parameter values for each independent experiment.

Tsr variants (i.e., NDNDF, NDNDL, NDNDR, NDNDV, and NDNDY) with no accessible methylation site could not mediate serine chemotaxis on soft agar plates.However, these receptors all showed sensitive responses to serine in the R^- B^- host (Fig. 4.2; Table 4.1). Surprisingly, the physiological level of CheR enzyme (in an R^+ B^- host) shifted these receptors to lower serine thresholds than they had in the R^- B^- host: for Tsr-NDNDR, $K_{1/2}$ was reduced ~10-fold, from ~1100 μM to ~110 μM; for Tsr-NDNDL, $K_{1/2}$ was reduced ~4-fold, from ~110 μM to ~30 μM; for Tsr-NDNDF, $K_{1/2}$ was reduced ~4-fold, from ~34 μM to ~9 μM; for Tsr-NDNDV, $K_{1/2}$ was reduced ~3-fold, from ~24 μM to ~7 μM; for Tsr-NDNDY, $K_{1/2}$ was reduced ~3-fold, from ~24 μM to ~8 μM (Fig. 4.2; Table 4.1). This counterintuitive effect of CheR (enhancing response sensitivity) turned out to be opposite to its effect on Tsr-wt. Moreover, the higher the response threshold of the mutant receptor in the R^- B^- host, the larger the CheR-induced threshold decrease was. As these mutant receptors cannot be modified by CheR nor CheB (data not shown), the CheR effect observed here cannot be the result of CheR catalytic activity. All these Tsr [NDND-X] variants also had lower response thresholds in the R^+ B^+ host than they did in the R^- B^+ host (Fig. 4.2; Table 4.1), consistent with the CheR threshold-lowering effect.

These Tsr [NDND-X] variants also showed slightly higher response thresholds to serine in R^- B^+ host than they did in the R^- B^- host (Fig. 4.2; Table 4.1), suggesting an unexpected signaling action of CheB: shifting receptors to a higher threshold, presumably by stabilizing the MH bundle packing interactions. Given that CheB cannot modify these

Tsr [NDND-X] variants, the threshold-increasing effect of CheB cannot be due to its catalytic activity. Tsr variants NDNDF, NDNDL, NDNDV, and NDNDY had somewhat higher thresholds in the $R^+ B^+$ host than they did in the $R^+ B^-$ host, but Tsr-NDNDR did not (Fig. 4.2; Table 4.1). It seemed that the lower the response threshold of a mutant receptor in the $R^- B^-$ host, the larger the CheB-induced threshold increase was. Surprisingly, all these Tsr [NDND-X] mutant receptors generated considerable kinase activities (data not shown) and a near-wild-type Hill coefficient to serine stimuli in $R^- B^-$, $R^- B^+$, $R^- B^+$, and $R^+ B^+$ hosts (Fig. 4.2; Table 4.1).

The threshold-lowering effect of CheR is dependent on the NWETF tether. To explore the possible mechanism of this novel effect of CheR, I asked the following questions: Does this CheR threshold-lowering effect depend on the C-terminal pentapeptide? Does it depend on CheR catalytic activity? Does an increased level of CheR amplify the threshold-lowering effect? Does this effect only occur with certain Tsr mutants and what are their important attributes?

CheR catalytic activity at the methylation sites of Tsr is largely dependent on the presence of NWETF at the C-terminus of receptor subunits. CheR binds to the tether end NWETF with ~3 μM affinity, thereby increasing the local concentration of CheR around the methylation sites (28). To answer whether the threshold-lowering effect of CheR on Tsr variants also depends on NWETF, I constructed NWETF deletions of Tsr-wt and Tsr-NDNDX variants (NDNDF, NDNDL, NDNDR, NDNDV, and NDNDY) and then tested their serine response behaviors in FRET host strains with different combinations of

CheR and CheB enzymes (Fig. 4.2; Table 4.2). For Tsr-wt-ΔNWETF, it produced a higher serine threshold than the Tsr-wt did in R^- B^- host strain (Tsr-wt, $K_{1/2}$ ~ 17 μM; Tsr-wt-ΔNWETF, $K_{1/2}$ ~ 32 μM), and the presence of CheR did not change its $K_{1/2}$ (Tsr-wt-ΔNWETF, R^+ B^-, $K_{1/2}$ ~ 34 μM). In both R^- B^+ and R^+ B^+ hosts, Tsr-wt-ΔNWETF also produced similar signaling behaviors (R^- B^+, $K_{1/2}$ ~ 0.9 μM; R^+ B^+, $K_{1/2}$ ~ 1 μM) (Fig. 4.2; Table 4.2), suggesting no CheR effect or CheR catalytic activity on Tsr-wt-ΔNWETF. These results are consistent with the previous study that CheR catalytic activity depends on the C-terminal pentapeptide tether end NWETF. Also, the observation that CheB drove Tsr-wt-ΔNWETF to a much lower serine threshold suggests that CheB might still remain some residual catalytic activity on the receptor even without NWETF.

All Tsr-NDNDX-ΔNWETF mutants produced responses to serine in the R^- B^- host, but did not exhibit large CheR- or CheB-dependent threshold-shift effects (Fig. 4.2; Table 4.2). For example, Tsr-NDNDR-ΔNWETF had $K_{1/2}$ ~2700 μM in the R^- B^- host and $K_{1/2}$ ~1600 μM in the R^+ B^- host; Tsr-NDNDF-ΔNWETF showed $K_{1/2}$ ~32 μM in the R^- B^- host and $K_{1/2}$ ~23 μM in the R^+ B^- host (Fig. 4.2; Table 4.2). Combining all these results (Fig. 4.2; Table 4.1), I conclude that the threshold-lowering effect of CheR is dependent on the C-terminal pentapeptide tether end NWETF.

In an R^- B^- host, receptor molecules remain unmodified, undergoing neither methylation nor demethylation/deamidation reactions. The observation that Tsr-wt-ΔNWETF had a higher serine threshold than did Tsr-wt in the R^- B^- host suggests that the pentapeptide NWETF alone may somehow affect the signaling behavior of Tsr in

Table 4.2 Serine dose-response parameters for Tsr-NDNDX-ΔNWETF variants.

Tsr mutant [a]	FRET host strain [b]	$K_{1/2}$ (μM) [c]	Hill coefficient [c]	number of experiments
WT-ΔNWETF	UU2567	32	11	1
	UU2699	0.9	4.2	1
	UU2697	35	14	1
	UU2700	1.0	3.3	1
NDNDF-ΔNWETF	UU2567	32	16	1
	UU2699	25	9.2	1
	UU2697	23	8.6	1
	UU2700	24	12	1
NDNDL-ΔNWETF	UU2567	97	6.8	1
	UU2699	129	7	1
	UU2697	108	5.6	1
	UU2700	94	13	1
NDNDR-ΔNWETF	UU2567	2780	2.7	1
	UU2699	1966	5.5	1
	UU2697	1566	2.9	1
	UU2700	1510	3.5	1
NDNDV-ΔNWETF	UU2567	23 ± 1.2	8.9 ± 2.4	2
	UU2699	35 ± 6.1	20 ± 1.5	2
	UU2697	38 ± 4.3	17 ± 2.6	2
	UU2700	20 ± 8.4	8.3 ± 1.7	2
NDNDY-ΔNWETF	UU2567	22	7.6	1
	UU2699	22	15.2	1
	UU2697	17	6.2	1
	UU2700	23	5.8	1

[a] Derivatives of plasmid pRR53 were transferred to FRET host strains; induction with 100 μM IPTG. [b] Strains also carried the FRET reporter pRZ30; induction with 2 μM sodium salicylate. [c] For multiple experiments, means and standard errors were determined from the best fit parameter values for each independent experiment.

absence of adaptation enzymes. But Tsr-NDNDX-ΔNWETF receptors did not show corresponding threshold differences. These findings suggest that the NWETF may somehow interact with the methylation region of receptor. Moreover, all Tsr-NDNDX-ΔNWETF receptors generated considerable kinase activities (data not shown) and a Hill coefficient near wild type range to serine stimuli in $R^- B^-$, $R^- B^+$, $R^- B^+$, and $R^+ B^+$ hosts (Fig. 4.2; Table 4.2).

Some important structural features of CheR. The crystal structure of CheR provides important insights into its mechanism of CheR function (9, 29). CheR is a mixed α/β two-domain protein (9). A methylation reaction product and methylation reaction inhibitor, SAH (S-adenosylhomocysteine) binds to the fairly conserved central β1-loop-αA region of CheR, the putative Ado-Met binding sites (Fig. 4.3). The C-terminal NWETF of Tsr binds to the β-subdomain of CheR (Fig. 4.3). Binding of the methylation helix of the Tsr receptor may occur within the wide opening of CheR flanked by the β-subdomain and the N-terminal helical domain (Fig. 4.3). It had been suggested that α2 of CheR (residues 44–61) is very important for interaction with the receptor methylation region (30).

To test whether the CheR threshold-lowering effect depends on its catalytic activity, I constructed CheR-R53E, which has significantly reduced catalytic activity and might impair binding to the methylation helices of the receptor. Residue R53 has been suggested to be critical for CheR catalytic activity, presumably due to its positively

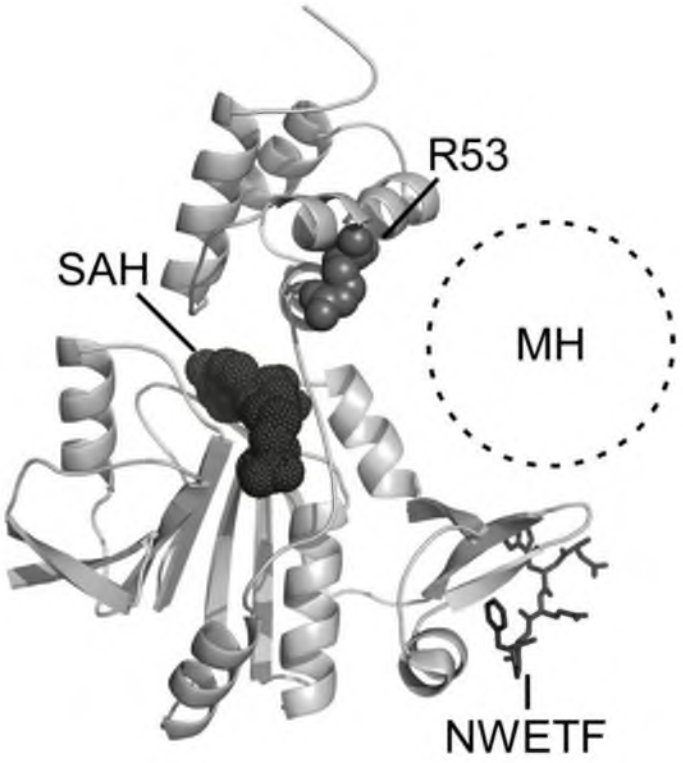

Fig. 4.3 Structural features of CheR. CheR is colored in light gray ribbon, and SAH, S-adenosylhomocysteine dark gray dots. Pentapeptide NWETF, in gray sticks, binds to the β-subdomain of CheR. The methylation helix, shown in cross section and dotted circle, is proposed to interact with the major grove of CheR. CheR-R53 residue in α2 helix, in gray sphere, is proposed to be critical for binding to MH region and for CheR catalytic activity, mainly due to its large positively charged side chain.

charged side chain, which could form ionic pairs with negatively charged glutamyl residues in receptor methylation helices. CheR-R53E is defective in CheR function in chemotaxis assays (30), modification assays (data not shown), and FRET assays (data not shown). To test the signaling effects of CheR-WT and CheR-R53E on Tsr receptors, I first constructed new FRET strains that had the genes for these proteins expressed under xylose control (Fig. 4.4A).

Construction and properties of CheR expression FRET strains. I inserted the *cheR-wt* or *cheR-R53E* coding sequences into the xylose operon, replacing the *xylAB* coding sequences (Fig. 4.4A). The *cheR-wt* or *cheR-R53E* coding region was immediately preceded by a *xylA* start codon and followed immediately by a *xylB* stop codon (Fig. 4.4B). The two newly constructed FRET strains were named XH05 and XH01, respectively: XH05 ($[R^{+}]$ B^{-}) is primarily host strain UU2567 with *cheR-wt* under xylose induction, and XH01 ($[R^{*}]$ B^{-}) is primarily host strain UU2567 with *cheR-R53E* under xylose induction. I first used SDS-PAGE analysis to quantify the expression level of CheR protein at different concentrations. Both CheR-WT and CheR-R53E proteins had essentially the same expression levels and patterns (Fig. 4.4C), indicating the near-native structure and intracellular stability of mutant CheR-R53E. The expression pattern of CheR proteins under xylose induction showed that at low concentrations of D-xylose (<20 μM), very little CheR protein was expressed; at intermediate concentrations of D-xylose (between 20 μM and 100 μM), CheR expression increased with increased D-xylose level; at high concentrations of D-xylose (>100 μM), CheR

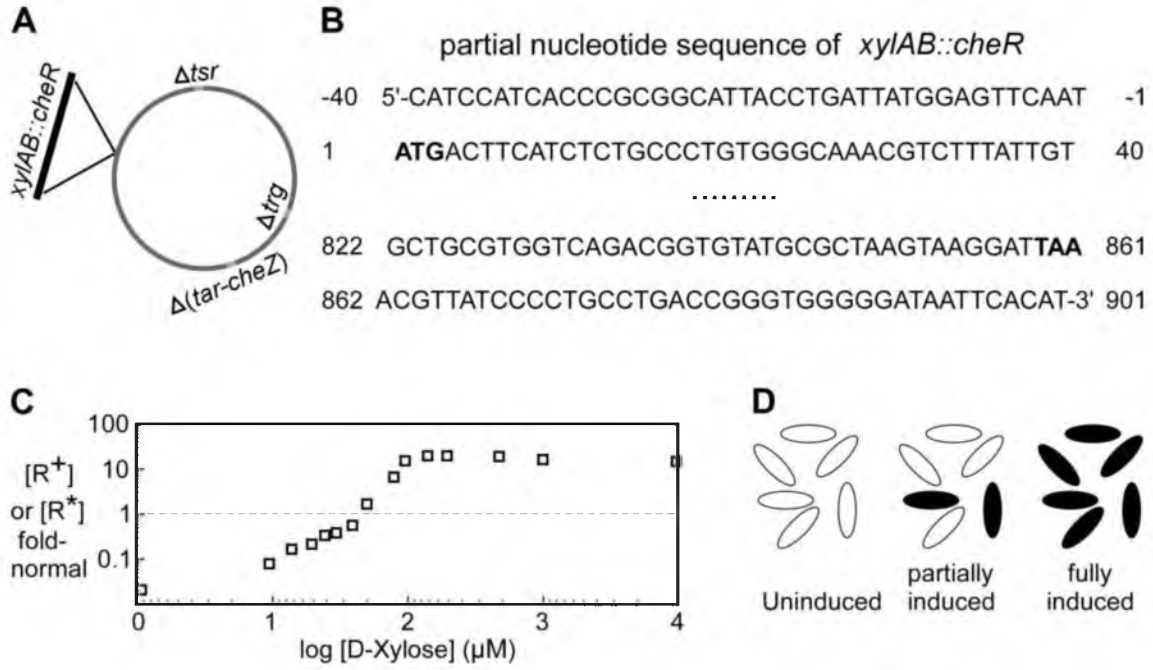

Fig. 4.4 Construction of CheR expression strains for FRET. The gene coding for CheR-WT or CheR-R53E was transferred into the xylose operon. A. Schematic chromosomal diagram of the constructed FRET strain. Both strains carry ΔMCPs, Δ*xylAB,* Δ*cheRB,* and Δ*cheYZ*. XH05 has *cheR-wt* under D-xylose control and XH01 has *cheR-R53E* under D-xylose control. B. Partial nucleotide sequence (5'–3') of the *xylAB::cheR* region, showing the promoter region and partial gene sequence. The start codon and stop codon are in bold, and between them is the coding sequence for CheR. C. CheR expression levels at different induction levels of D-xylose were determined by SDS-PAGE analyses and normalized to the physiological expression level of strain UU2697 (R^+ B^-). D. All-or-none induction of CheR genes under control of the *xylAB* promoter.

expression reached plateau level (about 20-fold higher). The D-xylose utilization pathway exhibited "all-or-none" responses wherein the sugar concentration only affected the relative fraction of cells in the uninduced or fully induced states (31). At low concentrations of D-xylose (<20 μM), all cells are uninduced; at intermediate concentration of D-xylose (between 20 μM and 100 μM), some of the cells are fully induced and some are uninduced. Thus the fraction of cells in the fully induced state increases with D-xylose in the population. All the cells become fully induced at >100 μM D-xylose.

Is the threshold-lowering effect of CheR dependent on its catalytic activity? For Tsr-wt (QEQEE) in the XH05 ($[R^+]$ B^-) host, the serine response $K_{1/2}$ was ~20 μM at low xylose concentrations and ~200 μM at high inducer levels (Fig. 4.5A). For Tsr-wt (QEQEE) in the XH01 ($[R^*]$ B^-) host, the serine response was ~20 μM at all inducer levels (Fig. 4.5A). These observations indicate that CheR catalytic activity is responsible for the threshold-raising effect of CheR on Tsr-wt (QEQEE) and that overexpression of CheR-R53E cannot compensate its defect in catalytic activity. The $K_{1/2}$ value (~200 μM) at full induction of Tsr-wt (QEQEE) in XH05 ($[R^+]$ B^-) host strain is much higher than that of Tsr-wt in an R^+ B^- host strain (~49 μM), indicating that elevated levels of CheR further enhance its methylation effects.

Among all the Tsr variants tested, Tsr-NDNDR showed the largest shift in serine threshold in response to a physiological level of CheR ($K_{1/2}$ reduced, from ~1100 μM to ~110 μM) (Fig. 4.2; Table 4.1). Thus, I used Tsr-NDNDR and Tsr-NDNDR-ΔNWETF

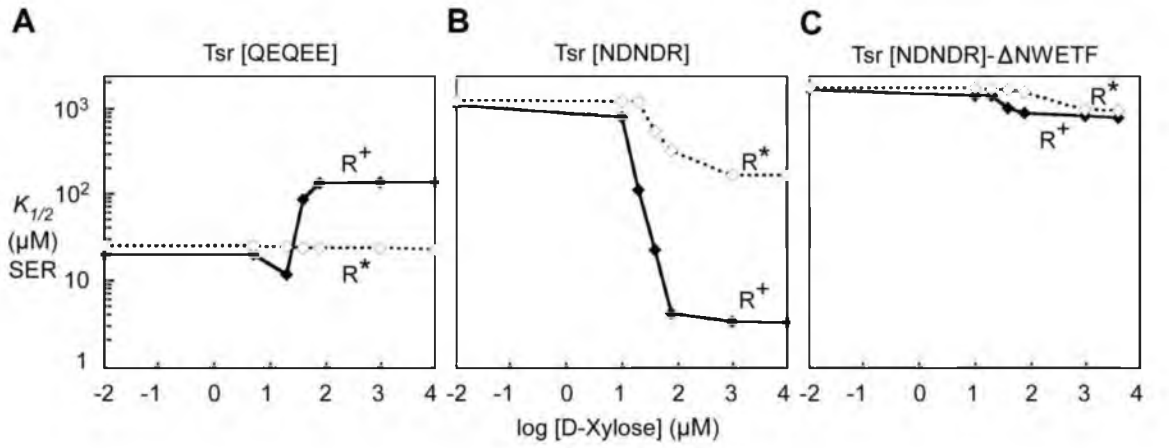

Fig. 4.5 The effects of D-xylose levels on $K_{1/2}$ of Tsr receptors. Plasmid pRR53 derivatives encoding Tsr-QEQEE (wt), Tsr-NDNDR, or Tsr-NDNDR-ΔNWETF were tested for serine responses in host strains XH05 or XH01 at various concentrations of D-xylose. Filled diamonds and solid lines indicate XH05 behaviors, which have *cheR-wt* under D-xylose control; Blank diamonds and dotted lines indicate XH01 responses, which have *cheR-R53E* under D-xylose control.

mutant receptors for the following experiments. I first tested the dose-response behaviors of Tsr-NDNDR in host XH05 ([R^+] B^-) with differential concentrations of D-xylose. For Tsr-NDNDR in XH05 ([R^+] B^-), very low levels of CheR-wt enzyme produced a serine response threshold $K_{1/2}$ ~1200 μM, whereas very high levels of CheR-wt enzyme produced a much lower serine threshold $K_{1/2}$ ~4 μM (Fig. 4.5B). These results demonstrated that increased levels of CheR enzymes can augment the threshold-lowering effect of CheR (in [R^+] B^- host) on the NDNDR receptor up to 30-fold. I then tested the signaling behaviors of Tsr-NDNDR in XH01 ([R^*] B^-). A high expression of CheR-R53E produced only a small drop in response threshold ($K_{1/2}$ ~ 1600 μM to ~ 200 μM) (Fig. 4.5B). These combined results indicate that the CheR threshold-lowering effect largely depends on the CheR activity impaired by the R53E lesion. The residual signaling effect of overexpressed CheR-R53E protein shows that its functional defects, either in substrate helix binding or subsequent catalysis, are not absolute (Fig. 4.5A).

I also tested the signaling properties of Tsr-NDNDR-ΔNWETF in XH05 ([R^+] B^-) and XH01 ([R^*] B^-). Its response threshold remained high at all expression levels of CheR-WT and CheR-R53D proteins (Fig. 4.5C). These results further confirmed that the threshold-lowering signaling effect of CheR depends on the C-terminal NWETF of the receptor.

The threshold-lowering effect of CheR on Tsr receptors with intact adaptation sites. Besides Tsr receptors lacking adaptation sites, I also tested the *in vivo* FRET

behaviors of some Tsr receptors with intact adaptation sites. This group of Tsr variants were previously classified showing an "inverted response" to adaptational modification: lower time in CW flagellar rotation in an $R^+ B^-$ host than in an $R^- B^-$ host. This "inverted response" behavior could be another example of the threshold-lowering effect of CheR. To test this idea, I examined the FRET responses of seven inverted mutants (Table 4.3). Tsr-I232W, A233E, and E248D showed slight decreases of response thresholds in the presence of CheR; the other mutant receptors showed large threshold reductions in the presence of CheR (Table 4.3). Tsr-L225S had a relatively sensitive response to serine in the $R^- B^-$ host ($K_{1/2}$ ~38 μM) and a much more sensitive response to serine in the $R^+ B^-$ host ($K_{1/2}$ ~6 μM). Tsr-L263F showed a $K_{1/2}$ value ~640 μM in $R^- B^-$ host and a much lower $K_{1/2}$ value ~100 μM in $R^+ B^-$ host. Tsr-I229T and L252F failed to respond even to 10 mM serine in the $R^- B^-$ host, but both responded to serine in the $R^+ B^-$ host (I229T, $K_{1/2}$ ~9000 μM; L252F, $K_{1/2}$ ~1000 μM). These findings, consistent with the previous studies (Chapter 2), indicated that the threshold-lowering action of CheR can occur on receptors with intact adaptation sties. Beside all these mutants tested in this study, quite a few other Tsr mutant receptors also showed an obvious threshold-lowering effect of CheR (Chapter 3).

Table 4.3 Serine dose-response parameters for Tsr variants with "inverted response"

Tsr mutant	FRET host strain	$K_{1/2}$ (μM)	Hill coefficient	Tsr plasmid
L225S	UU2567	38	8.1	pPA114
	UU2699	NR	NR	pPA114
	UU2697	6.0	9.7	pPA114
	UU2700	0.2	0.8	pPA114
L263F	UU2567	644	6.3	pPA114
	UU2699	4.0	8.0	pPA114
	UU2697	100	12	pPA114
I229T	UU2567	NR	NR	pPA114
	UU2697	9195	4.4	pPA114
L252F	UU2567	NR	NR	pPA114
	UU2697	1097	2.8	pPA114
I232W	UU2567	367	8.5	pPA114
	UU2697	305	2.0	pPA114
A233E	UU2567	73	16	pRR53
	UU2697	57	3.7	pRR53
E248D	UU2567	48	3.6	pRR53
	UU2697	38	3.3	pRR53

Tsr variants were expressed from plasmid pRR53 or pPA114 derivatives in strains containing the pRZ30 or pVS88 FRET reporter plasmid, with appropriate induction.

NR: no response even to 10 mM serine.

Discussion

Structural interplay of the HAMP and MH bundles modulates Tsr input-output signal control. HAMP domains mediate input-output signal transductions in many bacterial signaling proteins. The dynamic bundle model proposes that overall HAMP packing stability, defined by ensembles of iso-energetic conformations, rather than a few discrete conformations of HAMP (32), regulates receptor signal output (33). It also proposes that the structural stabilities of the HAMP and MH bundles are coupled in opposition (Fig. 4.6A). Therefore, tighter packing of the helices in the HAMP bundle destabilizes packing arrangement in the MH bundle, leading to kinase-off output. Conversely, tighter packing of the MH bundle destabilizes the HAMP bundle and favors kinase-on output. This model predicts that chemoeffector stimuli produce signaling responses by modulating HAMP stability and that the sensory adaptation enzymes cancel those responses by modulating the opposed packing stability of the MH bundle: CheR-mediated methylation enhances stability; CheB-mediated demethylation and deamidation reduce stability.

Methylation bundle function and packing stability have been intensively investigated in MCP-family chemoreceptors. Extensive studies of methylation sites 1 - 4 in the aspartate receptor Tar, which are structurally analogous to Tsr sites 1 - 4, suggest that adaptational modifications regulate receptor output by controlling the packing stability of the four-helix methylation bundle (5–7). Unmethylated adaptation sites that contain negatively charged glutamic acid (E) residues could destabilize the MH bundle through

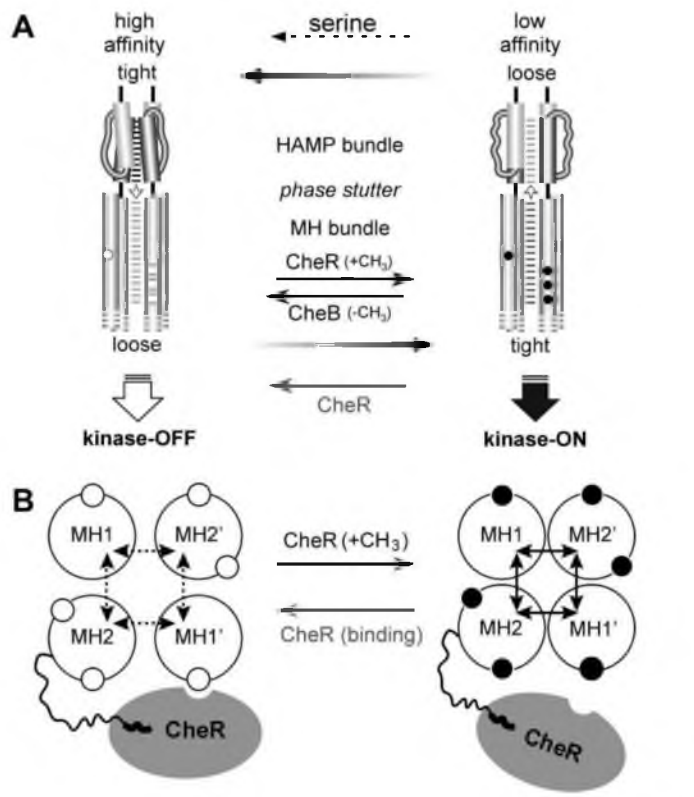

Fig. 4.6 Mechanistic interpretation of CheR signaling effects on Tsr receptors. A. Dynamic bundle model of Tsr signal control. A phase stutter at the HAMP-MH bundle junction is proposed to produce an oppositional stability relationship between packing of the HAMP and MH bundles. Open arrows between the bundles indicate the direction of structure destabilizing forces: tight packing of HAMP destabilizes MH bundle packing, leading (by an unspecified mechanism) to deactivation of CheA; tight packing of the MH bundle destabilizes HAMP, leading (by an unspecified mechanism) to CheA activation. Attractants promote HAMP stability; high modification states promote MH bundle stability. CheR prefers to catalyze loosely packed methylation helices (Black fonted CheR), while CheB prefers to catalyze tightly packed methylation helices (Black fonted CheB). CheR (gray) can also somehow shift the receptor to the kinase-OFF state. B. On-shifting effect of CheR via receptor methylation and Off-shifting effect of CheR via binding interactions with MH bundle. Unmethylated, negatively charged E residues should lower MH bundle stability; methylation (or uncharged amino acid replacements, such as Q), should stabilize MH bundle packing interactions. CheR-mediated methylation reactions stabilize the packing stability of the MH bundle. Methylated MH bundle becomes much less accessible for CheR catalysis putatively due to tight packing, whereas the ongoing presence of CheR can still somehow shift the receptor toward OFF state, probably by binding interactions with methylation helices. The Tsr output is affected by the combination of these two different forces of CheR: On-shifting effect of CheR mediated methylation and Off-shifting effect of CheR binding interactions with the MH bundle.

localized electrostatic effects on helix structure and coiled-coil packing interactions. Methylation of E residues forms glutamyl methyl-esters (Em), which are uncharged and should enhance MH packing. All adaptation sites regulate the overall packing stability of the MH bundle in a similar way (Chapter 2).

Orthodox signaling roles of CheR and CheB for chemoreceptors. The orthodox signaling effects of CheR and CheB on Tsr receptors are attributed to their catalytic acitivities on the adaptation sites: CheR enhances MH bundle packing stability through its methylation reactions, shifts Tsr output to the kinase-on state, and thereby increases serine response threshold; CheB reduces packing interactions of the MH bundle through its deamidation and demethylation reactions, shifts Tsr output to the kinase-off state, and thereby decreases response threshold.

In an R^- B^- strain lacking both adaptation enzymes, Tsr-wt has a uniform modification state (QEQEE) and produces a relatively sensitive, highly cooperative response to serine ($K_{1/2}$ ~17 μM; Hill coefficient ~15). In an R^+ B^- strain containing only the CheR enzyme, wild type Tsr molecules underwent CheR-mediated methylation (at sites 1 - 4, modification state similar to Tsr-QEmQEmE), shifting Tsr output toward the kinase-on state and accordingly driving serine response threshold to a higher level ($K_{1/2}$ ~49 μM; Hill coefficient ~8.5) (Fig. 4.2; Table 4.1). In an R^- B^+ host strain containing only the CheB enzyme, wild type Tsr molecules underwent CheB-mediated deamidation (at sites 1 and 3, modification state similar to Tsr-EEEEE), driving Tsr output toward the kinase-off state. Therefore, Tsr-wt in an R^- B^+ host did not have enough kinase activity to detect a

signaling response even to 10 mM serine. In an R^+ B^+ host strain containing both adaptation enzymes, Tsr-wt showed a much more sensitive but less cooperative signaling behavior ($K_{1/2}$ ~0.4 μM, Hill coefficient ~2.4) (Fig. 4.2; Table 4.1) than it did in an R^- B^- host, due to the combined catalytic activities of both CheB and CheR. The competing activities of CheR and CheB most likely brought the wild type Tsr to a modification state overall approximating 1 Q or Em site per subunit: probably a mixture of Tsr receptors with different modification states.

Given the small number of CheR molecules present in the normal chemoreceptor signaling array (12), the orthodox signaling role of CheR can be magnified by overexpression of CheR: overexpressed CheR enzyme produced a $K_{1/2}$ ~200 μM for Tsr-wt, much higher than the $K_{1/2}$ ~49 μM, seen at a physiological level of CheR (Fig. 4.2; 4.5A). Overexpressed CheR most likely brought the receptor to a modification state approximating 5 Q or Em sites per subunit, meaning full methylation at all sites including the fifth unorthodox site (Chapter 2). The fact that overexpressed catalysis-defective CheR-R53E did not change the threshold of Tsr-wt (Fig. 4.5A) further confirmed that it is the CheR catalytic activity that causes the orthodox threshold-increasing effect of CheR.

The new signaling roles of CheR and CheB. My study has provided the first direct evidence of such a counterintuitive CheR effect. In an R^- B^- host, mutant receptors with no accessible adaptation site (Tsr-NDNDF, NDNDL, NDNDV, NDNDY, and NDNDR) showed various response sensitivities to serine ($K_{1/2}$ ranges from ~24 to ~1100 μM) (Fig. 4.2; Table 4.1). These receptors all produced more sensitive responses (at least 3-fold

more sensitive) to serine in an $R^+ B^-$ host than they did in an $R^- B^-$ host, demonstrating the threshold-lowering effect of CheR. This CheR effect seems to counteract its orthodox effect, which is accomplished by CheR catalytic activity on adaptation sites. The fact that none of these mutant Tsr receptors could be methylated by CheR indicated that the CheR threshold-lowering effect cannot be due to its methylation reactions. Although the exact mechanism of the CheR threshold-lowering effect is not yet known, it is most likely that CheR binding to the receptor somehow destabilizes the methylation bundle, thereby shifting the receptor toward the kinase-off state.

This study also provided the first direct evidence that CheB can increase the response thresholds of Tsr receptors: all Tsr-NDNDX mutant receptors had higher response thresholds in an $R^- B^+$ host than they did in an $R^- B^-$ host (Fig. 4.2; Table 4.1). As none of these receptors could be modified by CheB, this signaling effect cannot be due to CheB's catalytic activity. Although the exact mechanism of the CheB effect still is unclear, it is most likely that CheB binding to the receptor methylation regions somehow stabilizes the packing stability of the methylation bundle, thereby shifting the receptor to the kinase-on state.

Possible mechanisms of CheR signaling effect. My study indicated that the threshold-lowering effect of CheR depends on the presence of the NWETF pentapeptide in the receptor: Tsr-NDNDX mutant receptors lacking NWETF did not show this CheR effect (Fig. 4.2; Table 4.1). Indeed, none of the Tsr-NDNDX mutant receptors lacking NWETF showed any obvious signaling change in host strains with different combinations

of adaptation enzymes (R^- B^+, R^- B^+, and R^+ B^+) (Fig. 4.2; Table 4.2). Neither overexpressed CheR-wt nor CheR-R53E had much effect on the serine response threshold of Tsr-NDNDR-ΔNWETF much (Fig. 4.5C). This provided further solid evidence that the CheR effect is largely dependent on the NWETF tether. However, due to the complication of CheR's binding interactions with both the methylation region and NWETF of the receptor, it is hard to know whether the CheR effect depends on NWETF itself or on less direct consequences of NWETF, for example, CheR's binding interactions with the methylation helices or its catalytic reactions. It is possible that the two seemingly counteracting effects of CheR depend on the NWETF tether in the same way, i.e., through the increase in local concentration of CheR around methylation regions.

I conclude that it is more likely that CheR binding to the methylation regions of the receptor rather than its catalytic activity contributes to the threshold-lowering action. The observation that overexpressed CheR-R53E did not change the FRET behaviors of wild type Tsr, whereas overexpressed wild type CheR increased its serine threshold up to about 10-fold (much higher than the normal level of CheR did), indicated that the elevated level of CheR-R53E did not compensate the defect in its catalytic activity. For Tsr-NDNDR, overexpressed CheR-R53E lowered its threshold about 8-fold, whereas overexpressed wild type CheR lowered its threshold about 300-fold, which is much more significant than the shift caused by a physiological level of wild type CheR (lowered about 10-fold). Seemingly, CheR catalytic activity plays an important role in lowering serine threshold, but a second thought invalidated this idea. Although overexpressed

CheR-R53E did not confer much of the catalytic activity on Tsr-WT, it recovered considerable threshold-lowering effect on Tsr-NDNDX (reduced ~8-fold, similar to what the normal level of wild type CheR did). This observation suggested that it is probably not the catalytic activity of CheR that caused the threshold-lowering effect. It is more likely that the substitution R53E in CheR not only ruined its catalytic activity, but also affected CheR's binding interactions with the methylation regions of the Tsr receptor, which are responsible for the threshold-lowering effect.

Does the threshold-lowering effect of CheR only operate on certain Tsr receptors? Lai and Parkinson suggested that the counterintuitive CheR effect may only operate on receptors that retain kinase-ON output at low modification states: for all the ON-shifted Tsr mutant receptors they tested, at least 10-fold lower thresholds were observed in an $R^+ B^+$ host than in $R^- B^+$ or $R^- B^-$ hosts, but the threshold-lowering effect was not obvious in an $R^+ B^-$ host (17). My study provided the first direct evidence of the threshold-lowering effect in $R^+ B^-$ host with mutant receptors that don't have any adaptation site. These mutant receptors precluded the complication of CheR modifications to the receptor. In conclusion, the threshold-lowering action of CheR can occur on receptors without modification sites, if retaining some kinase-ON output.

CheR's threshold-lowering effect can also work on Tsr receptors with intact adaptation sites (Fig. 4.6). Receptors with "inverted response" behaviors showed the significant threshold-lowering effects of CheR. CheR's ability t shift receptors to the kinase-OFF state may compete with its catalytic activity, which shifts receptors to the

kinase-ON state (Chapter 2). For Tsr receptors that responded to the threshold-lowering action of CheR, the CheR structural effects on MH packing interactions must be more significant than the structural consequences of CheR catalytic activity: Tsr-L225S, L263F, I229T, and L252F all showed much lower response thresholds in the presence of CheR. For Tsr receptors that did not show a CheR threshold-lowering effect, the CheR catalytic activity may have the dominant structural consequences. Tsr-I232W, A233E, E248D, and Tsr-wt showed this pattern. In other words, for Tsr receptors with adaptation sites, it is more likely that both the catalytic activity and the threshold lowering action of CheR can operate on their methylation regions, in a dynamic mode. Whether the threshold-lowering effect of CheR eventually showed up or not depended on the relative strength or amplitude of these two different forces.

Important implications about CheR and CheB signaling roles. The dynamic-bundle model proposes that loose packing of the MH bundle leads to kinase-off output, while tighter packing produces kinase-on output (Fig. 4.6A; Fig. 4.7). Modifications at adaptation sites affect the overall packing stability of MH bundle and thus control the Tsr output. CheB prefers to recognize and act on tightly packed on-state receptors; CheR prefers to recognize and act on loosely packed, off-state receptors (Fig. 4.6A; Fig. 4.7). CheB-mediated deamidation and demethylation reactions destabilize the MH bundle and shift the receptor to the kinase-OFF state, whereas CheR-mediated methylation enhances MH stability and shifts the receptor to the kinase-ON state.

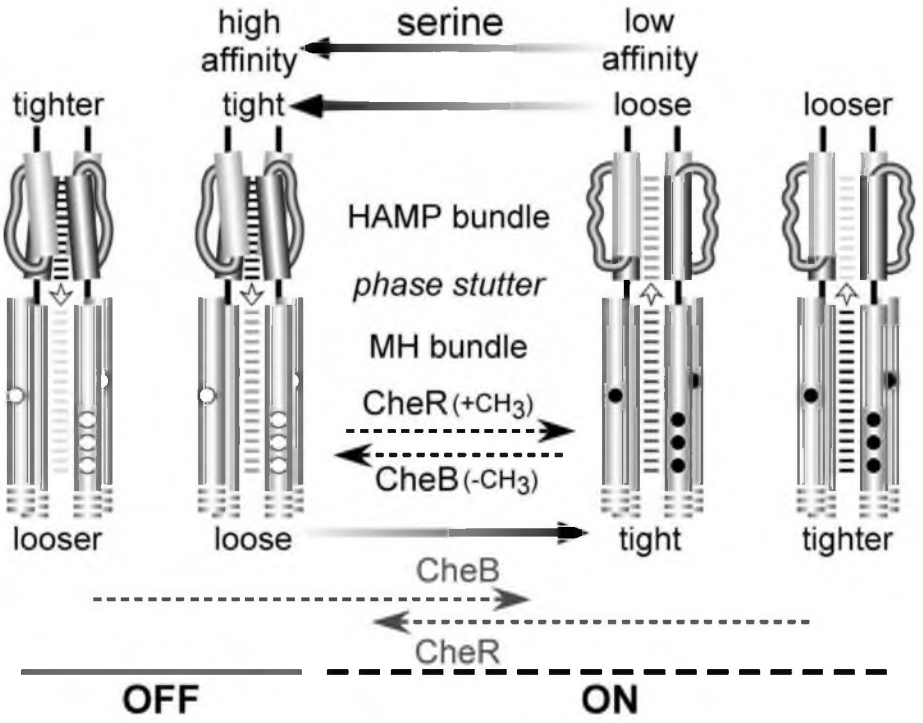

Fig. 4.7 A modified dynamic bundle model of Tsr signal control. This model proposes that the OFF-shifting effect of CheR may have a broader operational range than the ON-shifting effect of CheR-mediated methylation reactions. The OFF-shifting effect of CheR can also favor the CheR catalytic activity on the methylation sites by shifting receptor toward a better substrate state. The ON-shifting effect of CheB may also have a broader operational range than the OFF-shifting effect of CheB mediated deamidation or demethylation reactions. The ON-shifting effect of CheB may also favor the CheB catalytic activity by shifting receptor toward a better substrate state. This model further proposes that the existence of the opposing signaling effects of CheR and CheB may eventually allow a wider and more dynamic operational range for CheR and CheB and a wider signal detection range for Tsr receptor.

This study suggested that the counterintuitive OFF-shifting signaling effect of CheR is accomplished by destabilizing the packing of the MH bundle, probably due to binding interactions between CheR and the methylation regions, not its subsequent catalytic activity. The CheR signaling effect may only work on receptors with a particular level of kinase activity in an R^- B^- host, given that the receptors must respond to CheR's structure-destabilizing effects (Fig. 4.7). For receptors with no available adaptation sites (for example, Tsr-NDNDR), because CheR cannot act on them catalytically, the only structural influence of CheR comes through its binding to the methylation helices. It is reasonable to predict that the higher starting intrinsic threshold (more stable MH packing) the receptor has in an R^- B^- host, the more significant the CheR threshold-lowering effect in an R^+ B^- host might be. My study provided support for this prediction: for Tsr-NDNDR, $K_{1/2}$ was reduced ~10-fold, from ~1100 μM to ~110 μM; for Tsr-NDNDL, $K_{1/2}$ was reduced ~4-fold, from ~110 μM to ~30 μM; for Tsr-NDNDF, $K_{1/2}$ was reduced ~4-fold, from ~34 μM to ~9 μM; for Tsr-NDNDV, $K_{1/2}$ was reduced ~3-fold, from ~24 μM to ~7 μM; for Tsr-NDNDY, $K_{1/2}$ was reduced ~3-fold, from ~24 μM to ~8 μM (Fig. 4.2; Table 4.1).

For receptors with available adaptation sites, CheR-methylated MH bundle becomes tightly packed and a good substrate for CheB, but not readily accessible for CheR catalytic activity any longer. But the ongoing presence of CheR can still somehow interact with the methylation helices and thus shift the receptor toward off state (Fig. 4.6B). That is to say, the ultimate Tsr output is the combined consequence of these two different forces: CheR-mediated methylation (stabilizing, on-shifting) versus CheR binding

interactions with methylation regions (destabilizing, off-shiting) (Fig. 4.6B). The CheB signaling effect may work in a similar but opposite way.

The CheR and CheB signaling effects have some interesting and important implications for the sensory adaptation process and the chemoreceptor signal control mechanism. Sensory adaptation, the accurate resetting of chemotaxis components and behaviors to their prestimulus state, requires sophisticated, delicate, and dynamic control of the methylation level. Gradual, stepwise methylation at different methylation sites provides an elegant way to fulfill this requirement. However, the discrepancy between the differential methylation rates at differerent adaptation sites and the constant apparent adaptation rate of overall signal output seems to require more than gradual methylation. The counterintuitive signaling roles of CheR and CheB may fill in this gap. On one hand, each methylation reaction adds one methyl group to the receptor and its subsequent consequence. The CheR threshold-lowering effect can offset this consequence caused by one methylation to a state less than one-methylation-progress, producing an even smaller “step” for methylation process. On the other hand, the ongoing off-shifting effect of CheR may also help CheR recognition and catalysis as CheR catalytic activity prefers destabilized methylation helices. In other words, the two opposing effects of CheR can work in a collaborative way in a more subtle and dynamic manner even without CheB activity. Tsr-WT (QEQEE) in an R^+ B^- host should mimic the modification state of Tsr-QQQQE in an R^- B^- host, but the response thresholds of these receptor did not conform to their modification states. Tsr-WT (QEQEE) in an R^+ B^- host had a $K_{1/2}$~49

μM (Fig. 4.2), whereas Tsr-QQQQE in an R^- B^- host had a much higher $K_{1/2}$ (~200 μM) (Chapter 2), roughly what overexpressed CheR did for Tsr-WT (Fig. 4.5A). I ascribe this difference to CheR's destabilizing effect (threshold-lowering or OFF-shifting) on the MH bundle packing interactions. The observation that overexpressed CheR-R53E did not change the threshold of Tsr-WT might be due to that the compensated catalytic activity by overexpression is cancelled by the off-shifting effect of CheR, resulting in a net zero effect.

I conclude that the destabilizing effect of CheR on the MH bundle may operate constantly on the methylation regions of the receptor, fine-tuning the methylation steps in a more delicate and subtle way and thereby enabling a more precise and dynamic adaptation. I further concluded that the operational range of this CheR destabilizing effect may be even broader than that of CheR catalytic activity. This allows CheR to act on receptors with relatively tighter packing of MH bundle, broadening the possible functional range of CheR (Fig. 4.7). All these principles of CheR should apply to the CheB signaling roles as well, but in a reversed direction (Fig. 4.7).

In summary, this study provided the first direct evidence for novel signaling effects of CheR and CheB and provided significant insights into understanding the sensory adaptation mechanism and the Tsr signal control mechanism. This study demonstrated that the CheR threshold-lowering effect is dependent on the NWETF tether site in the receptor molecule. It is most likely CheR binding interactions with methylation regions of the receptor, rather than its catalytic activity, that contribute to the threshold-lowering

action of CheR. This study further confirmed that the overall packing stability of MH bundle rather than the discrete conformational packing arrangement determines the Tsr output.

References

1. Bibikov SI, Biran R, Rudd KE, Parkinson JS. 1997. A signal transducer for aerotaxis in *Escherichia coli*. J Bacteriol **179**:4075–4079.

2. Terwilliger TC, Wang JY, Koshland DE, Jr. 1986. Surface structure recognized for covalent modification of the aspartate receptor in chemotaxis. Proc Natl Acad Sci USA **83**:6707–6710.

3. Nowlin DM, Bollinger J, Hazelbauer GL. 1987. Sites of covalent modification in Trg, a sensory transducer of Escherichia coli. J Biol Chem **262**:6039–6045.

4. Rice MS, Dahlquist FW. 1991. Sites of deamidation and methylation in Tsr, a bacterial chemotaxis sensory transducer. J Biol Chem **266**:9746–9753.

5. Starrett DJ, Falke JJ. 2005. Adaptation mechanism of the aspartate receptor: electrostatics of the adaptation subdomain play a key role in modulating kinase activity. Biochemistry **44**:1550–1560.

6. Winston SE, Mehan R, Falke JJ. 2005. Evidence that the adaptation region of the aspartate receptor is a dynamic four-helix bundle: cysteine and disulfide scanning studies. Biochemistry **44**:12655–12666.

7. Swain KE, Gonzalez MA, Falke JJ. 2009. Engineered socket study of signaling through a four-helix bundle: evidence for a yin-yang mechanism in the kinase control module of the aspartate receptor. Biochemistry **48**:9266–9277.

8. Wu J, Li J, Li G, Long DG, Weis RM. 1996. The receptor binding site for the methyltransferase of bacterial chemotaxis is distinct from the sites of methylation. Biochemistry **35**:4984–4993.

9. Djordjevic S, Stock AM. 1998. Chemotaxis receptor recognition by protein methyltransferase CheR. Nat Struct Biol **5**:446–450.

10. Barnakov AN, Barnakova LA, Hazelbauer GL. 1999. Efficient adaptational demethylation of chemoreceptors requires the same enzyme-docking site as efficient methylation. Proc Natl Acad Sci USA **96**:10667–0672.

11. Okumura H, Nishiyama S, Sasaki A, Homma M, Kawagishi I. 1998. Chemotactic adaptation is altered by changes in the carboxy-terminal sequence conserved among the major methyl-accepting chemoreceptors. J Bacteriol **180**:1862–1868.

12. Li M, Hazelbauer GL. 2004. Cellular stoichiometry of the components of the chemotaxis signaling complex. J Bacteriol **186**:3687–3694.

13. Parkinson JS, Houts SE. 1982. Isolation and behavior of *Escherichia coli* deletion mutants lacking chemotaxis functions. J Bacteriol **151**:106–113.

14. Chang ACY, Cohen SN. 1978. Construction and characterization of amplifiable multicopy DNA cloning vehicles derived from the p15A cryptic miniplasmid. J Bacteriol **134**:1141–1156.

15. Gosink KK, Buron-Barral M, Parkinson JS. 2006. Signaling interactions between the aerotaxis transducer Aer and heterologous chemoreceptors in *Escherichia coli*. J Bacteriol **188**:3487–3493.

16. Ames P, Studdert CA, Reiser RH, Parkinson JS. 2002. Collaborative signaling by mixed chemoreceptor teams in *Escherichia coli*. Proc Natl Acad Sci USA **99**:7060–7065.

17. R.Z. L, J.S. P. 2014. Functional suppression of HAMP domain signaling defects in the E. coli serine chemoreceptor. J Mol Biol **426**:3642–3655.

18. Bolivar F, Rodriguez R, Greene PJ, Betlach MC, Heyneker HL, Boyer HW. 1977. Construction and characterization of new cloning vehicles. Gene **2**:95–113.

19. Studdert CA, Parkinson JS. 2005. Insights into the organization and dynamics of bacterial chemoreceptor clusters through *in vivo* crosslinking studies. Proc Natl Acad Sci USA **102**:15623–15628.

20. Sourjik V, Vaknin A, Shimizu TS, Berg HC. 2007. In vivo measurement by FRET of pathway activity in bacterial chemotaxis. Methods Enzymol **423**:363–391.

21. Parkinson JS. 1976. *cheA*, *cheB*, and *cheC* genes of *Escherichia coli* and their role in chemotaxis. J Bacteriol **126**:758–770.

22. Laemmli UK. 1970. Cleavage of structural proteins during assembly of the head of bacteriophage T4. Nature **227**:680–685.

23. Ames P, Parkinson JS. 1994. Constitutively signaling fragments of Tsr, the *Escherichia coli* serine chemoreceptor. J Bacteriol **176**:6340–6348.

24. Berg HC, Block SM. 1984. A miniature flow cell designed for rapid exchange of media under high-power microscope objectives. J Gen Microbiol **130**:2915–2920.

25. Sourjik V, Berg HC. 2002. Receptor sensitivity in bacterial chemotaxis. Proc Natl Acad Sci USA **99**:123–127.

26. Shimizu TS, Tu Y, Berg HC. 2010. A modular gradient-sensing network for chemotaxis in *Escherichia coli* revealed by responses to time-varying stimuli. Mol Syst Biol **6**:382.

27. Sourjik V, Berg HC. 2004. Functional interactions between receptors in bacterial chemotaxis. Nature **428**:437–441.

28. Li M, Hazelbauer GL. 2005. Adaptational assistance in clusters of bacterial chemoreceptors. Mol Microbiol **56**:1617–1626.

29. Djordjevic S, Stock AM. 1997. Crystal structure of the chemotaxis receptor methyltransferase CheR suggests a conserved structural motif for binding S-adenosylmethionine. Structure **5**:545–558.

30. Perez E, West AH, Stock AM, Djordjevic S. 2004. Discrimination between Different Methylation States of Chemotaxis Receptor Tar by Receptor Methyltransferase CheR. Biochemistry **43**:953–961.

31. Afroz T, Biliouris K, Kaznessis Y, Beisel CL. 2014. Bacterial sugar utilization gives rise to distinct single-cell behaviours. Mol Microbiol **93**:1093–1103.

32. Hulko M, Berndt F, Gruber M, Linder JU, Truffault V, Schultz A, Martin J, Schultz JE, Lupas AN, Coles M. 2006. The HAMP domain structure implies helix rotation in transmembrane signaling. Cell **126**:929–940.

33. Zhou Q, Ames P, Parkinson JS. 2009. Mutational analyses of HAMP helices suggest a dynamic bundle model of input-output signalling in chemoreceptors. Mol Microbiol **73**:801–814.

CHAPTER 5

CONCLUSION

Tsr-E502 is an Adaptational Modification of Last Resort

The study of the unorthodox sensory adaptation site, Tsr-E502, showed that the fifth site alone is not critical for chemotaxis because most mutant receptors with an amino acid replacement at E502 mediated normal chemotactic behavior on tryptone soft agar (Fig. 2.2) and showed sensitive responses to serine in FRET kinase assays (Fig. 3.3). A few changes caused considerably reduced detection sensitivity, but even so, the remaining sensory adaptation sites compensated effectively for the on-shifted outputs of these mutant receptors.

Tsr residue E502 is not sufficient for chemotaxis: it failed to support Tsr function when adaptation sites 1 - 4 were rendered nonfunctional. The disparity in CheR and CheB modification rates at site 5 probably contributes to this functional defect. CheR-mediated methylation occurs more readily at E502 than does CheB-mediated deamidation or demethylation. Considering the small number of CheB molecules that operate in a normal receptor array, methylation at E502 might be effectively irreversible. Probably methylation of Tsr-E502 is an adaptational modification of last resort that only

comes into play at very high serine levels. Perhaps other *E. coli* MCPs lack a corresponding adaptation site because the cells seldom encounter, or prefer to ignore, high levels of their cognate ligands.

The FRET assays of Tsr-E502* mutants also showed that, adaptation site 5 regulates receptor signaling in the same way as do sites 1 to 4, but it has a much more significant effect on packing stability of the MH bundle and on response sensitivity, most likely due to its proximity to the adjacent HAMP domain. In summary, my study of Tsr-E502 has provided new insights into how the structural interplay between HAMP and adjoining sensory adaptation elements controls the signaling behavior of a chemoreceptor.

Tsr-Q311 Has a More Potent Effect on

Kinase Control Than Other Sites

This study showed that site Q311 alone is not critical for chemotaxis, as most mutant receptors with Q311 amino acid replacement mediated normal chemotactic behavior on tryptone soft agar (Fig. 3.2) and showed sensitive responses to serine in FRET kinase assays (Fig. 4.3). My results also indicated that Tsr-Q311 alone is not sufficient for chemotaxis function. It probably takes at least three adaptation sites for Tsr to support decent function.

The wild type Q311 residue conferred the highest kinase activity to the Tsr receptor, suggesting a more important role of Q311 than other sites in kinase control. The signaling behaviors of Tsr-Q311E and Q311D clearly reflect local destabilization of the

MH bundle. Consistent with the SDS-PAGE analyses that CheR cannot modify Tsr-Q311D, Tsr-Q311D did not show an increased response threshold in the presence of CheR. It is likely that nonmodification of Q311D residue locks CheR in a position (CheR prefers to bind to MH in loose packing) that prevents CheR binding to other adaptation sites. In other words, the Q311D receptor blocked the CheR catalysis at other site in methylation helices.

The study of Tsr-Q311 further confirmed that all the adaptation sites work in a similar way, modulating the overall packing stability of the MH bundle. However, the Q311 site seems to have a more significant effect on regulating kinase activity than do other sites, most likely owing to its priority in adaptational modification and its proximity to the kinase control domain. In conclusion, this study provided additional knowledge of the sensory adaptation system and the mechanism of Tsr output signal control.

The Signaling Roles of CheR and CheB

My study provided the first direct evidence for counterintuitive signaling roles of CheR and CheB, i.e., a threshold-lowering effect of CheR and a threshold-increasing effect of CheB. This study further showed that the CheR threshold-lowering action is dependent on the presence of the C-terminal tether NWETF in receptor molecules (Fig. 4.2). The CheR effect was largely abolished by a CheR mutant lacking catalytic activity. However, the mutant protein could also be defective in binding to methylation region rather than loss of catalytic activity, and this defect could be responsible for the threshold-lowering

action. I also showed that an increased level of CheR can amplify the CheR effect significantly (Fig. 4.5).

I further tested some other receptor mutants for unusual signaling behaviors in the presence of a physiological level of CheR. The results showed that the threshold-lowering effect of CheR is more likely to show up on Tsr receptors that have relatively high kinase activity but are in a fairly low modification state. For Tsr receptors with adaptation sites, it is likely that both the catalytic activity and the threshold lowering action of CheR can operate on their methylation regions, in a dynamic mode. Whether the threshold-lowering effect of CheR eventually showed up or not depended on the relative strength of these two different forces: the catalytic activity mediated on-shifting effect versus the off-shifting effect caused by CheR molecule binding interactions with the methylation region. The signaling roles of CheR and CheB can be readily explained by a modified dynamic bundle model of Tsr input-output signal control. This study provides a new layer of understanding for the signaling roles of CheR and CheB on modulating Tsr signal output.

APPENDIX

RESPONSE PARAMETERS OF TSR-E391* VARIANTS

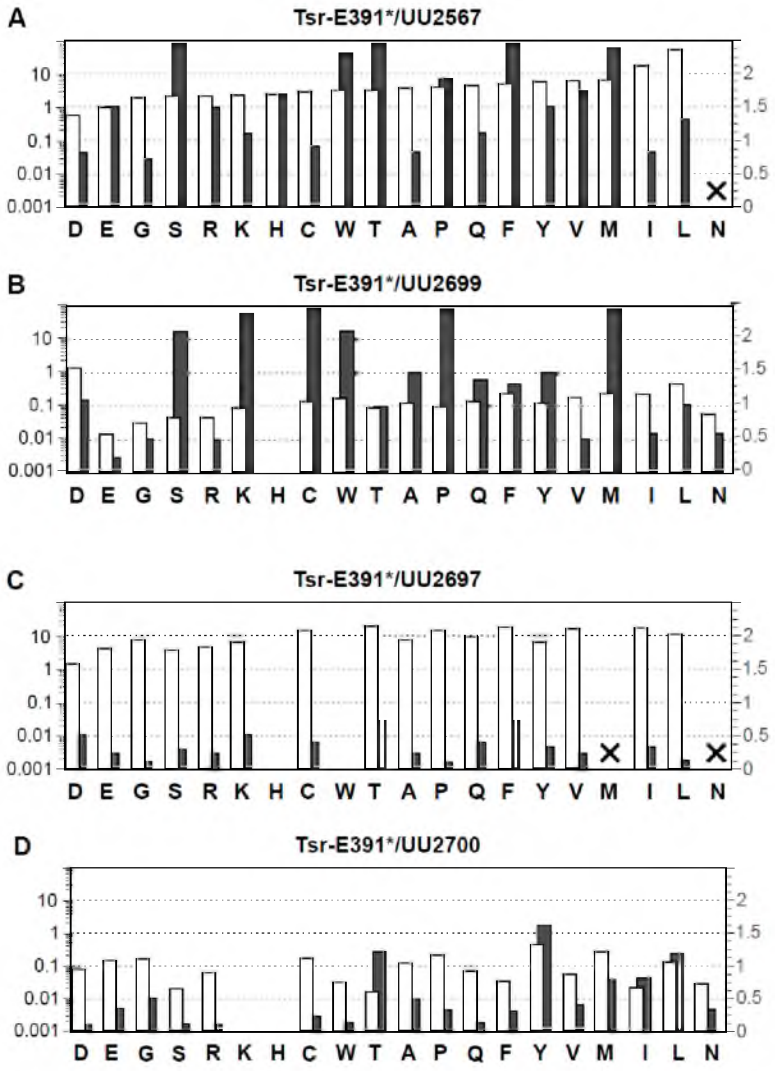

Fig. A.1 Serine dose-response parameters of Tsr-E391* variants. Bold letters below the histogram indicate the amino acid at residue E391 of Tsr (E = Tsr wild type). White bars denote the relative fold of $K_{1/2}$ of indicated mutant receptor in that host, compared to that of wild type in host UU2567 ($R^- B^-$). White bars were measured by the left Y-axis in log scale. Gray bars denote the relative fold of *Hill coefficient* indicated mutant receptor in that host, compared to that of wild type in host UU2567 ($R^- B^-$). Gray bars were measured by the gray-font right Y-axis in linear scale. No response means the receptor failed to respond even to 10mM serine. A, UU2567 (R^-B^-); B, UU2699 (R^-B^+); C, UU2697 (R^+B^-); D, UU2700 (R^+B^+).